Development and Analysis of a New Direct Steam Generation-Based Parabolic Trough Collector Power Plant Hybridized with a Biomass Boiler

By

BASHAR ALHAYEK

A Thesis Submitted in Partial Fulfilment of

the Requirements for the degree of

Master of Applied Science

in

Mechanical Engineering

Faculty of Engineering and Applied Science

University of Ontario Institute of Technology

Oshawa, Ontario, Canada

Abstract

Direct steam generation (DSG) is the process by which steam is directly produced in parabolic trough fields and supplied to a power block. This process simplifies parabolic trough plants and improves cost effectiveness by increasing the permissible temperature of the working fluid. In the present work, an innovative DSG plant hybridized with a biomass boiler is proposed and analyzed in detail. Two additional configurations comprising indirect steam generation in parabolic trough collector (PTC) plants were also analyzed in order to compare their energy and exergy performance. In addition, energy and exergy analyses of DSG are conducted and compared to an existing indirect steam generation PTC power plants such as the Andasol. To further understand the biomass subsystem, multiple fuels were presented and analyzed in detail. The obtained results indicate that the proposed DSG-based PTC plant is able to increase the overall system efficiency by 3% in comparison to indirect steam generation when linked to a biomass boiler that supplies 50% of the energy.

Acknowledgment

First and foremost, I thank God for His abundant love, compassion and His endless blessings. Unto Him is due all grace and glory for standing with me every step of the way.

Furthermore, I would like to assert my nethermost gratitude to my supervisor, Prof. Martin Aglein-Chaab and my co-supervisor Dr. Bale Reddy for their continuous support, patience, motivation and guidance. Their doors were never closed whenever I had any concerns and questions regarding my research work. They consistently steered me in the right direction through their immense knowledge and their encouragement. This thesis would have remained a dream had it not been for their constructive criticism and persistent assistance.

To my parents and grandparents, I owe my absolute profound acknowledgement and appreciation. Majdi and Fatena Alhayek, anything good that has come to my life has been because of your example, your guidance, and utmost love. Your selfless affection and dedication has nourished me and raised me to be who I am today, and for that I am thankful.

I am also indebted to my many colleagues of lab ACE 3030B at UOIT for allowing a growing and positive environment to work in. Their academic related advice offered me many insights on my research and the positive environment they provided, supported me in completing my thesis. Through their hard work and strive for success I was motivated and was able to excel at whatever I did, as they were a great influence.

Table of Contents

List of Tables

List of Figures

Nomenclature

A	Area (m^2)
C_p	Specific heat capacity (kJ/kgK)
ex	Specific exergy (kJ/kg)
$\dot{Ex}$	Exergy rate (kW)
f	Dilution factor
h	Specific enthalpy (kJ/kg)
M	Molar mass of species (kg/mole)
m	Total mass (kg)
$\dot{m}$	Mass flow rate (kg/s)
Nu	Nusslet number
P	Pressure (bar)
Q	Total heat supplied (kJ)
$\dot{Q}$	Heat transfer rate (kW)
s	Specific entropy (kJ/kgK)
T	Temperature (°C or K)
w	Moisture content on mass basis
$\dot{W}$	Rate of work output (kW)
X	Mass fraction of species

Greek Letters

$\boldsymbol{\eta}$	Efficiency
θ	Incidence angle
ρ	Reflectance

τ	Transmittance
α	Absorptance
Υ	Intercept factor
K	Angle modifier
λ	Stoichiometric constant in biomass combustion reaction (moles)
ε	Emittance
σ	Stefan-Boltzman constant
γ	Air to fuel ratio
θ	Incidence angle

Subscripts

a, b, c	Number of moles of CO_2, H_2O, and N_2 in biomass combustion gasses mixture
amb	Ambient conditions
conv	Convective heat
f	Fluid circulating in the solar field
m	Collector mirror
rad	Radiative heat
x, y, z	Number of atoms of carbon, hydrogen, and nitrogen in biomass (atoms/molecule)

Acronyms

BB	Biomass boiler
BP	Boiler pump

CB	Contaminated biomass
COND	Condenser
CP	Condenser pump
DEA	Deaerator
DNI	Direct normal irradiance (W/m^2)
DSG	Direct steam generation
HAB	Herbaceous and agricultural biomass
HAG	Herbaceous and agricultural biomass (grasses)
HAR	Herbaceous and agricultural biomass (residues)
HAS	Herbaceous and agricultural biomass (straws)
HHV	Higher heating value (kJ/kg)
HPT	High pressure turbine
HRSG	Heat recovery steam generator
HTF	Heat transfer fluid
LHV	Lower heating value (kJ/kg)
LPT	Low pressure turbine
NREL	National Renewable Energy Laboratory
PTC	Parabolic trough collector
SF	Solar field
TES	Thermal energy storage
WWB	Wood and woody biomass
WH	Water heater

Chapter 1: Introduction

In this chapter, energy security issues and their relation to the environment are introduced. Renewable energy sources are identified as one of the most promising solutions for sustainability. Additionally, solar and biomass energies are introduced in detail in this chapter as they are the main focus of this thesis.

1.1 Energy Security and the Environment

The definition of energy security varies in each part of the world depending on the advancement of a given country. In developing countries, energy security can be defined as the substantial access to energy in order to supply basic living needs which consist of clean water, lighting and public transportation, whereas in the developed parts of the world, energy security is more concerned with the reliability of power supply, affordability and energy resources in adequate amounts [1]. The lack of a reliable source of energy can cause both negative social and economic impacts. The lack of energy security can result in multiple other issues, such as; the reliance on alternate foreign energy sources, geopolitics, and environmental issues including climate change, oil depletion and energy needs for the less developed countries [2].

In multiple attempts to solve energy security issues, cheaper energy alternatives were sought and non-renewable sources won the day. As the world population keeps rising, the global demand for power is increasing, and to address this increasing demand, once again, cheaper energy alternatives remain the most accessible and affordable. However, the exaggerated depletion of such non-renewable sources imposes their extinction, and the conversion of such resources for the use of power generation and other commodities

compromises the environment and deteriorates the planet. Fossil fuels, though they may currently offer considerable power, they are finite and over time, their reserves decrease. According to [3], in the next few decades, the world's oil production will decline. As Fossil fuels are the most dominant source of power, where they contribute to a cumulative value of 85% of total global power supply [4], further increase in the consumption of fossil fuels leads to proliferation of carbon dioxide (CO_2) and other emissions as unwanted secondary products.

Through the years, the emission of CO_2 has increased drastically. CO_2 is noted to account for 70-75% of emission from burning of fossil fuels, making it the main greenhouse gas emitted during fossil fuel combustion [5]. Different fossil fuel resources emit different percentages of CO_2. According to Figure 1.1 [6], the global CO_2 emissions increased by 101% from the year 1973 to the year 2013. From Figure 1.1, it can also be concluded that although the percentage CO_2 emissions increased from the burning of coal by 28%, it also increased from natural gas by 37.5%. However, CO_2 emissions decreased from oil sources by 32.4%. In 2013, there are CO_2 emissions from other sources which include industrial wastes as well as non-renewable municipal wastes. It should also be noted that the CO_2 emissions percentages attained from the combustion of fossil fuels for Figure 1.1 are based on the energy balances of IEA, and also excludes any emissions from non-energy sources. The percentage of CO_2 emission from peat and oil shale are accounted for within the total CO_2 emitted by coal.

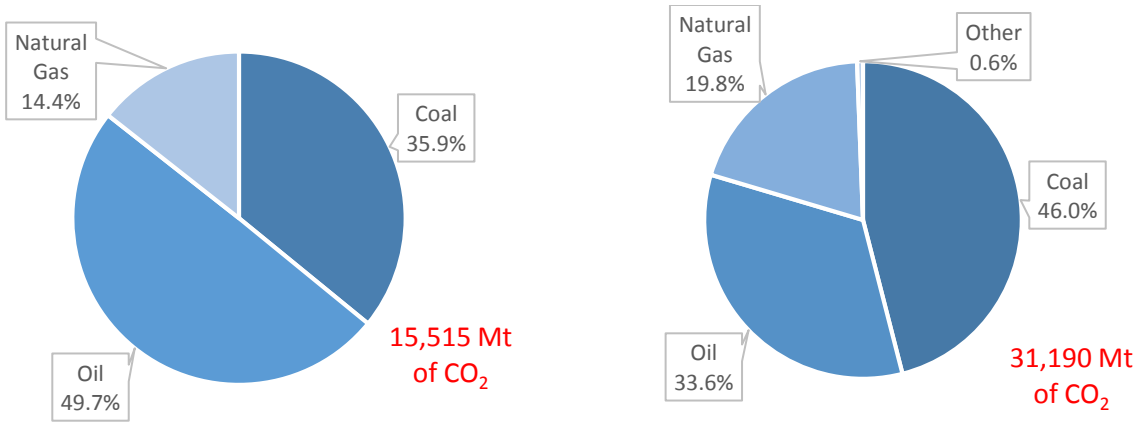

(a) *(b)*

Figure 1.1: Fuel shares of CO_2 emissions from fuel combustion in (a) year 1973 and (b) year 2013 [6]

The burning of fossil fuels suggests a much larger issue than their depletion. It has been established that acid precipitation, stratospheric ozone depletion, and global climate change are the three large-scale international environmental issues [7]. The burning of fossil fuels is essentially dangerous to the environment and life forms on earth.

Furthermore, the use of fossil fuels harms both aquatic and terrestrial ecosystems. Environmental hazards that arise from the use of fossil fuels include acid rain, oil spills and release of environmental pollutants such as CO_2 and NO_2. Lethal acid rainfall and the accumulation of CO_2 in the earth's system of natural resources provokes irreversible outcomes. A myriad of inevitable results include but are not limited to the absorption of the emissions by the ocean and organisms inhabiting such areas [8], as well as land ecosystems, particularly the growth of tissue-cultured plants [9]. Oil spills can affect fish and larvae development [10]. It is utterly perceptible that the chronic consumption of fossil fuels devalues various life forms to better enhance the lifestyle of human beings in a given

community. Existing evidence suggests that the future will be negatively influenced as long as degradation of the environment continues [11].

Energy security concerns can alter the industry of world energy in many positive ways, such as create a movement towards energy conservation and increase the use of a cleaner source of energy, that is, renewable energy [3]. Since the world is so heavily dependent on fossil fuels, it would be progressive to use a cleaner energy alternative. An alternative method that would allow for the production of energy and be environmentally benign is the employment of renewable energy sources. It has been established that climate change is one of the largest concerns for humankind in the 21st century [12]. However, if renewable energy is used in exchange of non-renewables, a 30% reduction of greenhouse gas emissions is estimated by the year 2020 [13].

1.2 Renewable Energy

Renewable energy is obtained from resources that can naturally be replenished. Sources of renewable energy include a vast array of solar, wind, biomass, and hydropower, geothermal and marine energies [14]. The use of such resources for the production of power provides zero to little air pollutants and greenhouse gasses [15]. This is necessary to affect the environment positively, and this is why the use of energy obtained from renewable sources is ideal.

The use of renewable energy would allow for a resolution of many encountered problems such as: enhancing energy supply reliability and organic fuel economy, resolving issues related to local energy and water supply, increasing the standard of living as well as the level of employment of a given local population, ensuring sustainable development of the remote regions in the desert and mountain zones, and implementation of the obligations

of countries with regards to fulfilling the international agreements related to environmental protection [15, 16] . Since renewable energy sources are a reliable, and sustainable source of practice found to be at reasonable cost, and their use does not impose harmful effects [11], considerable work has covered the assessment of renewable energy sources and their potential to replace conventional fuels.

Throughout recent years, there has been an incremental implementation of renewable energy sources leading to a significant increase in the renewable energy market. The market for heating, transportation and electricity have sharply increased over the last five years, and the arrangement of renewable technology including hydro, solar photovoltaic and wind has increased rapidly leading to a boost in the confidence of these technologies and a reduction in their cost [17]. It is projected that by the year 2035 global electricity generation is expected to grow by roughly 170% from the year 2010 [17, 18]. According to Figure 1.2 [19-24], it is evident that the share of renewables in global electricity production continues its rapid growth over the years, with the year 2015 having the greatest electricity production from renewables. This percentage is expected to grow as the replacement of non-renewables to renewables takes place, and renewables are used as a primary source of power.

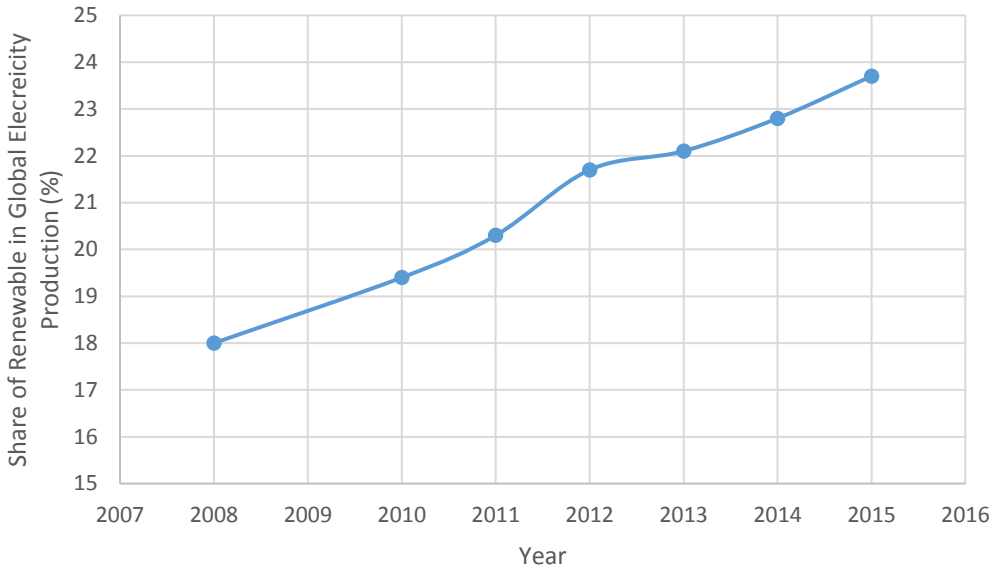

Figure 1.2: Share of renewables in global electricity production [19-24]

1.2.1 Solar

Solar energy presented in the form of inexhaustible irradiance striking the earth's surface presents a renewable energy source that can ultimately supply humanity's energy demands in a clean and sustainable manner. On average, the amount of sunlight striking the earth's surface for 90 minutes is enough to provide the earth's energy needs for one year [25]. Solar energy can be utilized through two main approaches; passive and active. Passive technologies relate to building design and material developments such as window size and orientation; aiming to maximize the utilized/captured solar irradiance. A comprehensive review available in the literature considered the development of passive solar technologies for space heating and cooling and pointed out some research needs in that area [26]. Active technologies are simply the employment of solar collectors to harvest sun irradiance and use it for various applications. Mainly, active technologies are divided into two main categories; photovoltaic (PV) and concentrated/thermal Solar Power (CSP).

Photovoltaics is the process of directly converting sunlight into electricity at an atomic level [27]. The development of PV systems have evolved over time, reaching a total installed capacity of 197 GWe based on the countries involved in the Photovoltaic Power Systems Programme commenced by International Energy Agency (IEA). Another 30 GWe are produced by countries which are not part of the program to raise the total to 227 GWe which makes up only about 1.3% of total world's electricity demand [28]. In an attempt to measure the environmental impacts of solar PV-based electricity generation systems, a review of life cycle assessment of these systems has been completed for the full process of manufacturing these panels; starting from silica extraction to the last assembly [29]. In another study, the research and development of PV/Thermal technologies have been considered with the main aim of identifying the challenges in those systems and pointing out future research/development areas needed to further enhance their performance [30].

Concentrated solar power is the process of focusing sunlight through the use of specially designed reflectors to obtain elevated temperature/thermal levels, which is later used to heat up a heat transfer fluid (HTF) that can be utilized in various applications such as, power production, heating and cooling. Although the market for CSP was stagnant in the period of 1990-2004, a 70% increase of CSP has been witnessed in the period of 2005-2009 as shown in Figure 1.3 [19-24]. Various panels' technologies are available in the market depending on the required temperature and application. Due to CSP systems' high potential for power production, a considerable amount of work has been done by institutions and corporations to further develop a greater understanding of the behavior of these systems and develop more efficient methods to improve the performance of CSP-based plants. Many comprehensive reviews outlining the latest innovations and

development in the field of CSP are presented in the literature. A study has reviewed the various collectors' technologies available and discussed the latest advancements for each collector along with progress in thermal energy storage (TES) options for CSP [31]. The study has concluded that over the past few years, an impressive advancement has been accomplished in every aspect of CSP. Another review has covered CSP technologies and focused on solar tower power plants and compared them to other CSP technologies [32]. In this study, the variation of solar beam irradiance was considered and provided preliminary recommendations for a chosen plant configuration based on the projected irradiance data .

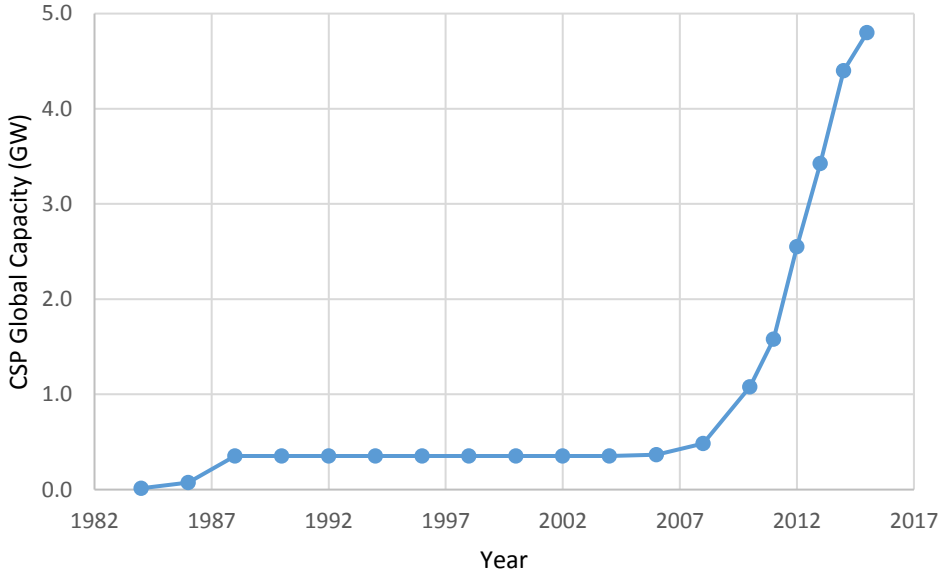

Figure 1.3: Growth of global concentrated power capacity [19-24]

Parabolic trough collector (PTC) is a CSP technology that has proved its maturity through the installation of multiple power plants. When integrated with the appropriate auxiliary equipment such as backup boilers and TES, PTC-based plants represent a stable and reliable supply of power. In fact, it was estimated that PTCs accounted for more than 90% of the total installed CSP capacity up to the year 2000 [33]. Current PTC plants deployed around the world utilize an indirect steam generation technique, where a HTF is

heated up in the absorber tube of the collector, the heat in the HTF is then transferred to the main working fluid of the power block in a heat recovery steam generator (HRSG)[34]. A considerable amount of work has been reported in the literature covering various areas of designing and optimizing PTC-based power plants [35-37]. One of the most comprehensive reviews on PTCs and their application can be found in Jebasingh [38] and will not be repeated here.

A recent study [39] presented an extensive energy and economic analysis of PTC-based power plants, where the effects of operating parameters such as; turbine inlet pressure and temperature and design irradiance on the system's performance were investigated. The study found that the overall plant efficiency increases and the levelized cost of energy decreases as the turbine inlet temperature increases. The plant considered in that study has a capacity of 1 MWe, and TES was not considered. In another study [40], the feasibility of solar PTC power plants for a specific location was conducted, where optimization of PTC power plants utilizing two different working fluids in the absorber tubes was carried out. The fluids considered for the analysis were Therminol VP-1 and molten salt. The results of the study showed that molten salt is the best economic option in PTC-based plants, as it has the lowest cost of energy. On the economic aspect of PTC-based plants, a simulation-based optimization methodology was proposed to improve the thermo-economic performance of a PTC-based plants [41]. The Andasol power station in Spain represents an example of a successful PTC-based power plant that uses an indirect steam generation technique and has shown impressive operation and stability, demonstrated through the high efficiency and stable supply of electricity [42, 43].

Although solar energy is being implemented as a viable option to replace conventional fuels for power production, solar-based energy systems still undergo a number of challenges. These challenges can be divided into two main categories; technical and economic. In the technical aspect, the solar energy supply is limited due to the intermittent nature of solar irradiance, and also, the maximum temperature available at the inlet of the power block is dependent on the collector technology used. On the other hand, the economics of solar energy systems is not yet competitive with conventional energy systems due to the high initial investment cost [44].

To ensure a reliable and continuous power supply, TES represents a feasible solution that will ultimately help to overcome the inconsistency of solar irradiance and boost the performance of solar-based power plants. Multiple studies have been conducted covering the performance and economics of solar power plants when integrated with TES [45-48]. These studies cover the design and integration of TES within solar-based plants; they also consider multiple plant arrangements where several HTF are considered. To improve the cost-effectiveness of PTC-based power plants, a number of studies have attempted several techniques to improve the efficiency of the systems which directly enhances the economics of the PTC system. One technique being the process of direct steam generation (DSG) in solar PTC [49]. This process is based on utilizing water/steam in the absorber tube instead of another HTF. By implementing this technique, the intermediate heat exchanger linking the solar field with the power block in the existing systems can be avoided, which in turn decreases thermal losses and investment costs [34]. The results presented by the European direct solar steam (DISS) project shows a positive experience with DSG plant testing, as the project has shown the potential of DSG and

explained the operation of such systems [50, 51]. Analyses available in the literature have shown that live steam at the exit of DSG fields can reach a temperature of 500 °C and a pressure of 120 bar, which leads to a direct increment in system's overall efficiency, ultimately leading to a low cost of energy [47, 52]. The economic potential of DSG-based PTC plants compared to indirect steam generation PTC plants, which mainly use synthetic oil as HTF, has been reported in the literature [51, 53]. These studies have concluded that DSG-based PTC has the potential to reduce the levelized cost of energy up to 11%. However, all the cost-effectiveness of DSG over indirect steam generation demonstrated in the literature was shown for DSG systems without TES. Several previous studies have evaluated different aspects of DSG plants such as the solar multiples [34], TES [51], and the economics [54], in order to develop a greater understanding of those systems as they present a reasonable solution to enhance PTC plant performance. In another study [51], the cost of DSG-based PTC plants and synthetic oil PTC plants integrated TES was evaluated, and it was concluded that the cost of DSG-based PTC plants is higher than oil plants as the cost of storage in DSG system is still not competitive.

Furthermore, another essential component in solar-based power plants to ensure a stable supply of energy is back up boilers [45, 55-58]. These boilers ensure the stability of energy input supply to the system by compensating the supply shortage in cases of low/no solar input to the system. However, the same alarming issue of greenhouse gasses exists in the use of boilers as they are usually fired by fossil fuels. To overcome this issue, many studies have suggested the replacement of fossil fuels used in boilers with biomass, as they are identified as a renewable carbon-based energy source [59].

1.2.2 Biomass

Biomass is defined as fuel derived from organic matter such as agricultural crops and organic waste. Biomass is considered a renewable energy source as it is carbon neutral [60]. When burned, biomass releases carbon dioxide that is largely balanced by the carbon dioxide captured during its own development and growth. Biomass can be utilized in various ways as a flexible fuel with similar characteristics to those of coal. It can be directly fired, co-fired with coal, or gasified to produce syngas.

The process of coal-biomass co-firing has received a lot of attention in the last decade as it is easy to implement and requires minimal adjustments to the current coal-based power plants. It can be defined as the process of instant mixing and combustion of biomass with other fuels such as coal or natural gas [60]. A recent review covering the latest development of biomass-coal co-firing in North America has been conducted [60]. The review also covered the different co-firing technologies available and compared the process in North America and around the world. In the review, it is demonstrated that up to 10% of the coal can be substituted by biomass with zero to minimal drop in the combustion efficiency. On the technical side, a recent study considered computational fluid dynamics (CFD) models for coal-biomass co-firing. It covers the current approaches utilized to predict the combustion characteristics of co-firing taking in consideration turbulence and gas phase combustion and many other factors [61]. The review concluded that current CFD models for coal and biomass co-firing are capable of solving complex processes such as heat transfer, flow turbulence and chemical reactions.

Biomass gasification is the process of converting solid/liquid biomass fuels to higher calorific value producer gas. The characteristics of the producer gas depend on

gasification parameters, such as gasification temperature and agent [62]. A recent review has covered the state of the art of the current biomass gasification technologies, the study viewed and evaluated the advantages and disadvantages of the process, along with outlining the potential of utilizing the produced syngas [63].

In spite all the advantages associated with using biomass as a primary fuel to run energy systems, the energy density of biomass is less than fossil fuel, requiring more storage space or preprocessing techniques such as pelleting to further enhance the energy density. Also, the feed of biomass can be inconsistent at times, due to cost fluctuations and logistic difficulties. Moreover, further development in biomass combustors/boilers is still needed as biomass fuels have not been used on a commercial scale for a long time.

1.3 Motivation

In spite of all the advantages and environmental savings associated with renewable-based energy systems, the employment of those systems is still limited, and fossil fuels are the dominant source of energy supply. This scenario is a result of several challenges that arise with renewable sources. Solar energy is one of the most vital solutions to replace conventional fuels for power production because it is available everywhere. In addition the current technologies represented in PV and CSP are at a mature stage, which makes them reliable to implement. However, solar energy is intermittent in nature, which leads to an unstable energy supply, making it difficult to be fully independent. The inconsistency of solar irradiance is not only due to day/night cycles but also due to rainy or cloudy periods. Intensive research that aims to identify reasonable solutions for this issue has been conducted. TES comes as the first option to be integrated with solar-based energy systems. During high solar irradiance periods, energy can be stored in various mediums. Energy

stored can be later utilized as needed during low/no irradiance periods or peak demand time. The main disadvantage of TES is the high capital cost, which adds a heavier burden on solar systems which are already expensive. Another option is the employment of backup heaters/boilers that can supply the system with energy input as required. However, those boilers still impose the issue of generating emissions when fossil fuels are used as the energy input. Biomass fuels are another renewable source that has been extensively reviewed as a potential source to replace fossil fuels in backup boilers. The main advantage of utilizing biomass is that it has similar characteristics to fossil fuels, leading to minimal adjustments to the current technologies. However, the energy density of biomass is lower than fossil fuels and, the feed of biomass can be inconsistent at times. Thus, the challenges associated with utilizing solar and biomass systems as standalone systems are the motivation for the present work. The combination of solar and biomass in a hybrid system has the potential to overcome the individual drawbacks of each system and lead to a more stable energy supply. Solar irradiance can be collected using various collector types, and biomass fuels can be utilized in a boiler or a gasifier. This hybridization would complement each source as it helps achieve more sustainable power production by eliminating the use of fossil fuels and reducing the feedstock of biomass needed while avoiding the use of TES.

1.4 Thesis Structure

The thesis is divided into six chapters including the current chapter. Chapter 2 presents an extensive literature review that has been conducted, covering the area of solar and biomass hybridization. The literature review is divided into two main categories; solar and biomass hybridization for power production, and multi-generation. In Chapter 3 the proposed systems in this research work are presented. In particular, four systems consisting of simplified arrangements combining solar and biomass energies are reported. Chapter 4 presents the methodology followed to analyze the proposed systems, where mass, energy, entropy, and exergy balance equations are presented for all systems. In Chapter 5, the results of the analyses are discussed in detail, including exergy destruction rates. Finally, the summary of the results, concluding remarks, and recommendations for future work are reported in Chapter 6.

Chapter 2: Literature Review

The focus of this research is the hybridization of solar and biomass as an alternative approach to run energy systems in a sustainable manner. An extensive literature review has been conducted in the present work which covers various areas of designing and developing solar-biomass energy systems. The review is organized as follows; solar-biomass hybridization, solar-biomass energy systems for power production, and solar-biomass energy systems for multi-generation.

2.1 Solar-Biomass Hybridization

Various configurations combining solar energy and biomass fuels to produce electrical power and other commodities have been introduced in the literature. The sole purpose of these arrangements is to provide a source of clean, reliable and affordable energy supply that would ultimately replace the conventional use of fossil fuels. Thirty years ago, a system was proposed in which solar parabolic dish technology was combined with a Brayton cycle to run on multiple types of fuels; biomass being one of them [64]. The system was designed to run in a combined heat and power mode, providing a small community with a continuous energy supply. Although the proposed system was well designed and discussed, no physical plants were deployed for almost 3 decades, owing to the high initial cost at that time as well as the abundant fossil fuels availability. In 2012, the first power plant called *Termosolar Borges* combining solar technologies and biomass fuels was commissioned in Les Borges Blanques, Spain. Termosolar Borges produces 22.5 MW and utilizes PTC with biomass boilers. The construction cost of the facility is around 153 million euros, which results in direct CO_2 savings of 24500 tons a year [65].

2.1.1 Solar-Biomass Energy Systems for Power Production

Recently, researchers are concentrating on combining solar and biomass energies for power generation. Various systems were designed, evaluated, and optimized in order to achieve the highest efficiency possible along with minimizing the cost of the plants, for the exclusive purpose of ensuring competitiveness with conventional energy systems. This section intends to provide a comprehensive review of the latest development of advanced energy systems combining solar energy and biomass fuels for power production. The two energy sources can be arranged in diverse ways depending on an array of factors such as; technology used, space available, location, power output required, etc.

A comprehensive study has investigated the technical, economic and environmental performance of 17 concentrated solar power and biomass-fueled power plant configurations. Moreover, the feasibility of coupling TES and its effect on systems' performance was also evaluated. To ensure that the results of the assessment are realistic and reliable, only mature technologies with a power rating of at least of 5 MWe were considered in this study. The technologies considered in the solar field are PTC, Fresnel, and solar tower. For biomass, the technologies evaluated are grate, fluidized bed and gasification with producer gas in a boiler. This study was simulated using "Thermoflex 23.0." Technical results show that a maximum energy efficiency of 32.9% can be obtained when solar towers and gasification are utilized. However, from an economic point of view, the most feasible option would be the hybridization of Fresnel and fluidized bed. Similarly, the hybridization of solar and biomass is shown to be more viable than standalone CSP with a 69% lower investment cost. The utilization of TES increased the production by 17%.

However, the cost of such technologies is still expensive which makes it not feasible to be integrated yet [66].

The execution of the combination of solar and biomass fuels is contingent on location due to varying solar intensities, along with biomass/biogas fuel availability in those regions. In a subsequent matter, several assessments have been conducted in diverse locations, in order to examine the feasibility of the hybridization in these locations. In 2012, a study assessed the feasibility of utilizing solar energy and biomass fuels for electricity production, heat or tri-generation in India. The work has focused on optimizing "solar multiple" values for those hybrid plants and the simulations were carried in TRNSYS. TRNSYS is a special software used to simulate transient thermal and electrical processes. Results concluded that the levelized cost of such arrangements exceeds the cost of conventional energy sources. However, energy prices from CSP-biomass for all the configurations were found to be less in cost than photovoltaic in addition to competition with wind turbines systems. In such case where there is an increment in the cost of biomass fuel feed by 1.2-3.2 times, the CSP-biomass hybridization would be depicted as a competitive option for standalone biomass power plants [67].

A strategic approach is considered for CSP deployment in Brazil by hybridizing CSP with biomass in semiarid regions. Similar to the work done in India, the study has assessed the feasibility of combining CSP and biomass for Brazil's semiarid northeast. Extensive factors such as the high direct normal irradiance (DNI) along with the availability of low-cost biomass feed from the forests in the "Fazendauniao" area pose a great advantage to such regions, allowing for the implementation of the specified systems. These arrangements were described and simulated in a manner such that their operation

will not hinder the sustainability of the forests. Results showed an optimized hybridized system can generate electricity at the cost of 11 cents USD/kWh when the utilization of a solar multiple (SM) of 1.2 and a biomass fill fraction of 30% are employed [68].

Moreover, a recent study aiming to show the advantageous process of integrating biogas within existing CSP plants rather than using molten salt thermal storage for better operation time and stable production has been completed. The potential of such system has been evaluated through a feasibility study considering multiple factors such as the location of plants with hybridization potential, biomass feed potential in that region, biogas demand, and waste availability evaluation for biogas production required for the process. The study has also analyzed the latest technologies in organic waste bio-digestion and considered the best cases for integration. The data analyzed shows that a continuous feed of Argo-livestock and industrial waste is available in the areas where CSP plants are present, which allows the steady operation of a hybridized system combining biogas and CSP rather than the use of TES [69].

In addition to evaluating the hybridization process based on location, substantial analysis has been devoted to evaluating several arrangements in which the two sources are linked in various manners depending on available technology and required production. A study has examined the potential of utilizing biomass fuels to superheat the working fluid in a solar PTC plant, aiming to increase the overall efficiency of the system. The analysis evaluated 7 different scenarios with molten salt thermal storage for the production of 50 MWe. Both water and air cooling were considered for the evaluation as well. Steam parameters ranging from 380ºC at a pressure of 100 bar to 540ºC at 130 bar were modeled using Thermoflex 23.0. The results demonstrated that the usage of biomass to externally

superheat steam advances the performance of the system; where solar to net electricity efficiency has increased by 30% to reach a value of 10.5%. Moreover, the integration directly leads to a reduction of CSP standalone cost by up to 23% [70].

In addition, supplementary assessment that considered the combination of CSP and biomass was conducted, where solar tower technology was employed with biomass boilers along with a 3-hour molten salt thermal storage. The location considered for the evaluation is Griffith, in Australia. The objective of the study was to compare the suggested arrangement with a standalone solar tower power plant with 15-hour TES and to report the benefits associated with the hybridization. The process was simulated using Thermoflex 23.0 for a 30 MWe production. The two sources were arranged in such manner where both steam generators can supply a feed at 525ºC and 120 bar separately. The results of the technical and economic assessments have showed considerable benefits, as the arrangement was able to achieve 43% reduction in plant investment when compared to a standalone CSP plant with 15 hours of thermal storage with an electricity cost of AU$155/MWh [71].

An alternative approach was sought in which many researchers took into consideration is the integration by utilizing solar energy through the use of parabolic troughs for preheating the feed water before its entrance into the biomass boiler. In such approach, the stage at which steam is extracted from the turbine to preheat feed water is avoided. In a study done for 12 MW biomass plant in Lhasa, China, where PTCs were used to heat up a HTF which was in turn used to preheat the water before entering the steam generator. The results showed that for the same power output, the proposed arrangement was able to reduce the consumption rate of biomass fuels. It was also shown that the

arrangement has increased the net solar to electricity efficiency and concluded that both thermal and economic performance of the system are improved with a higher grade of the replaced extraction steam[72]. A similar study was conducted on a smaller capacity plant of 2 MW. The focus of the study was to optimize the arrangement through a parametric study varying steam pressure and regeneration parameters [73].

The hybridization of a solar-biomass power plant without the use of TES has been discussed and further elaborated in the literature. A system considered the arrangement of biomass and solar PTCs for the objective of electrical power production [74]. Despite that the system does not utilize TES, a controlled feed of biomass fuel and variable solar supply are presented for the continuous production. The study suggested a limitation of the solar share to a maximum value of 50% of the total supply while the biomass feed would contribute to a minimum of 50%. Since there is no TES employed in the system, the biomass boiler would have to operate as the only source of energy during the night when no solar contribution is present. At a boiler pressure of 20 bar, the analysis conducted shown that as the solar participation increased from 10% to 50%, the plant fuel energy efficiency also increased from 16% to 29% which directly leads to high savings in biomass fuel.

In an attempt to assess the potential of employing anaerobic digestion of animal manure for energy production, a study evaluated the integration of anaerobic digesters with CSP to generate electricity. Biogas produced from digestion process contains about 65% methane. This biogas is then utilized in a gas turbine where it directly produces electricity, and heat is cogenerated. The heat is to be utilized in the energy storage medium of the solar loop where it will enhance the thermal quality of the HTF of the PTCs. Matlab software

was used to simulate the process. The location considered for the assessment is Lodwar in Kenya. Although this study presents the potential for a successful system, many assumptions were considered where the reliability of the evaluation might presumably be hindered and thus the need for further research on this is required [75].

2.1.2 Solar-Biomass Energy Systems for Multi-generation

The combination of solar technologies and biomass fuels has the potential for the generation of multiple useful products. Consistent with the research and development work performed for the production of electrical power from renewables, substantial work has been conducted to further improve the efficiency of the hybridization in order to respond to the rapid growth in demands for various commodities. The products available from such configurations can range from electrical power, heating, and cooling to the production of chemicals.

A recent study has appraised the potential of multi-generation systems, where the two sources were integrated in such manner; through the utilization of a simple Rankine cycle, "Vapor Absorption Refrigeration" (VAR) cooling, and "Multi Effect Dehumidification" MED for fresh water desalination [76]. The solar energy is collected through a PTC field and integrated with the cycle through a heat exchanger. The flow then passes through the biomass boiler where additional heat is supplied to the working fluid. In cases where low solar irradiance is present or during the night, heat input from the biomass boiler is adjusted to compensate for the reduction of energy input, allowing a maximum of 100% energy input to be attained, solely from the biomass boiler. This arrangement does not require the deployment of TES due to the fact that the continuous supply is guaranteed by the biomass boiler. The steam leaving the biomass boiler is then

sent to a steam turbine to produce electrical power. At a high-pressure stage in the turbine, some steam is extracted and sent to a heat exchanger where heat is transferred to VAR ($LiBr-H_2O$) cycle for cooling purposes. Lastly, a limited amount of heat is recovered from VAR cycle's refrigerant (water) to run the dehumidification process for fresh water production. The configuration discussed here presents a feasible solution to overcome solar intermittent nature while maintaining a competitive cost and efficiency. It also provides a 15.3 % primary energy savings when compared to a simple power plant.

In a novel approach, a microscale system was designed to run on solar and biomass and provide heat for the purpose of water heating and power in the winter, in addition to cooling in the summer. The system utilizes an Organic Rankine Cycle (ORC) running on R245fa, linked with a Vapor Compression Cycle (VCC) that runs only in the summer for cooling purposes. The expander of the ORC and the compressor of the VCC are assumed to share the same shaft, so no external work is required to run the compressor. Also, the condensation of both cycles would occur at the same pressure, which allows for the utilization of the same condenser to further decrease the cost of the system. A thermodynamic analysis carried out based on the size of a typical apartment block on a Greek island concluded that a maximized thermal efficiency of 5.5% is obtained at an evaporation temperature of 90ºC, and an exergetic efficiency of 7% when the biomass boiler is operating at full load capacity. Further analysis showed that the superheater and the recuperator did not result in a major increase in the cycle's efficiency but added extra costs for the required expansion [77]. In the same research area of tri-generation (production of power, heating, and cooling), ORC and VCC were combined to run on solar and biomass. The main distinguishable factor is that solar energy is harnessed through a

flat plate instead of PTC. Biomass is burned in the boiler where the heat is transferred to water, which is utilized to heat up the organic medium before it is sent to the turbine. The analysis evaluated the effect of various parameters on cycle's performance including evaporator temperature, and pump and turbine operating conditions. Results were displayed in terms of energy and exergy efficiency, and electrical to heat ratio [78].

The production of power and other commodities through the hybridization of solar energy and biomass fuels is not constrained by the use of a specific thermodynamic cycle or arrangement, as viewed in a recent study. Such study examined the combination of the two sources to produce power, cooling, hot water, and heated air through the integration of 2 gas turbine cycles, 2 Rankine cycles, a VAR cycle, and multiple heat exchangers. Biomass fuel considered is olive bits and no specific location was considered for the analysis. To further understand the behavior of the system, parametric studies were carried out in order to assess the cycle's performance, where various operating conditions are varied. Parameters considered for the evaluation include ambient temperature, combustion temperature, and DNI. The analysis concluded that the energy and exergy efficiencies of the proposed renewable energy-based multi-generation system were found to be 66.5% and 39.7%, respectively, compared to only 27.3% and 44.3% when solar system is the only source [79]. Although the proposed system describes a novel approach that would provide considerable feed of useful commodities along with a competitive efficiency rating, more work in terms of economic aspects should be considered to further analyze the feasibility of deploying such arrangements in the near future. Also, considering an exact location for those systems is a crucial factor as both DNI values and biomass fuels availability highly depends on location.

The development of combined heat and power (CHP) systems running on various types of fuels has been an area of interest for researchers as such systems provide higher efficiencies when compared to only power systems. Extensive work has been conducted and documented in the literature, highlighting the potential of such systems to provide communities with basic needs of heat and power in addition to decreasing the total cost of energy. Solar and biomass have been also examined as a potential fuel to run those configurations. At an early stage of the research and development of solar-biomass power plants, a study was conducted in 2006, in an attempt to evaluate the behavior of the hybridization to run a combined heat and power system. The main objective of the study was to appoint the foremost accessible solar collector to run combined heat and power applications. With a focus on PTC technology, a comparison of three different types; Euro Trough ET, Luz Solar collector LS3, and Duke Solar collectors was recommended. A plant with an electrical capacity of 2.5 MW and thermal capacity equivalent to 18 MW was simulated [80].The temperature range of the HTF running in the collectors' loop is constrained to match the economizer and the boiler operational characteristics, with a minimum temperature of 160ºC required by the economizer and a max temperature of 210ºC to not exceed boiler's flash point. Maximum and minimum biogas energy inputs available for the process were assumed to be 20MW and 11MW, respectively. The results strongly indicated that the number of approximate loops required to compensate the biomass feed constraint for LS3 collectors is 18 loops, compared to only 10 loops by Euro trough. At that early stage of development, the analysis revealed the potential of such arrangements to efficiently produce heat and power. However, with the current advances in both solar and biomass technologies, additional work regarding the evaluation of latest

collector models and HTFs is long overdue. Likewise, the development of special control systems to make the most effective use of the biomass feed and solar energy flow is required. Energy flows should be optimized depending on the availability of both sources. The optimal control would enhance the performance of those arrangements and lead to higher efficiency. Another system consisting of a PTC field and a biomass furnace for the production of combined heat and power for a small scale application has been proposed in the literature [81]. The system utilizes a simple Rankine cycle along with TES to ensure continuous production. The end user considered for the evaluation is a typical European hotel, due to the observed high thermal to electric consumption ratio. Also, for a more challenging and realistic assessment, the study was simulated on a winter day to account for worst possible circumstance for the solar system. Transient simulation was adopted using TRNSYS with an hourly distribution to account for the time-dependent behavior of such applications. Both biomass and PTC systems work in parallel and supply a feed of 300ºC to the Rankine cycle. Performance assessment of the system shows that the proposed system is capable of matching both thermal and electrical needs of a typical hotel. This, in turn, saves energy when compared to 2 separate plants supplying the same commodities. Moreover, the system presents a clean solution, eliminating about 6,300 tons of CO_2 annually. Although the proposed configuration shows a positive potential in terms of load matching and emissions reduction, such systems are costly and not up to the economic standards of the conventional systems. Thus, more work regarding the development of inexpensive solar collectors would allow for the competition of such systems against the alternate conventional systems. For small scale applications, a system running on ORC and fueled by the combination of solar and biomass for the production of heat and electrical

power was modeled and experimentally tested with the end user being residential and building applications [82]. The main objective of the work was the development of the ORC expander (turbine). This is based on the fact that most of the commercial expanders available in the market for ORC systems are for large scale applications and endure technical issues, such as low efficiency and excessive working fluid leakage, which could ultimately be catastrophic. Due to the cost effectiveness and high expansion ratio of scroll expanders, the specified arrangement was chosen for the proposed system that used HFE7100, an environmentally friendly organic fluid as the working fluid, and wood pellets as the boiler fuel. The simulation results concluded that 86.8% combined heat and power efficiency when only biomass was used, compared to only 69.7% efficiency when running on only solar collectors. These results showed that the overall efficiency of the system is increased with the biomass share is expanding. An experimental setup has been also utilized to further explore the behavior of the cycle and monitor the performance of the expander used. The results show that maximum electrical power produced by the cycle is around 500W, along with 9.85 kW thermal energy from the condenser side. The efficiency of the utilized expander was found to be around 74% with smooth and steady operation showing the viability of such device [82]. The efficiency of the cycle is directly proportional to the biomass share in the total input whilst having an inversely proportional relationship with the solar input share that is evidently enforced due to low efficiencies of solar collection devices. This presents a motivation for the development of solar collectors with higher efficiencies to further increase the potential of solar energy in various applications.

In a similar study that rather focused on supplying heat and power to regions with low DNI values, an existing combined heat and power system was modified and assessed. This arrangement was to resort to the usage of biomass fuels. Located in Salzburg, Austria, the alteration comprised of retrofitting the system with CSP through the integration of a PTC to further enhance the energy supply and reduce biomass fuel consumption. A transient simulation model was utilized using IPSEpro software to theoretically evaluate the process. The analysis conducted considered DNI for Salzburg, along with 2 supplementary locations retaining different DNI data sets to assess the dependency of system's behavior on solar irradiance in the particular locations. The results showed that for the city of Salzburg with a DNI of 806 kWh/m^2 the integration of solar collectors with a total aperture area of 9810 m^2 dropped the consumption of biomass by almost 3% [83]. For other locations considered in Austria where DNI is about 1345 kWh/m^2 the reduction is almost 5.3%. Due to low DNI in Salzburg along with high initial costs, the dynamic investment calculation conducted has shown that the retrofitting of a PTC with the biomass system is scarcely feasible. However, for other locations in Austria where DNI is higher than Salzburg, the process is feasible and can result in considerable profit. Moreover, the integration approach followed by this assessment could be expanded to cover more options regarding the placement of the solar subsystem within the ORC. Furthermore, the development of more efficient and cost-effective solar collectors, would most definitely increase the feasibility of the retrofit of biomass-based energy systems.

In a novel approach to employ solar and biomass for heat and power production, a study has described and modeled a means of simulating the technical feasibility of an innovating combined heat and power system running on a "Stirling" engine cycle and co-

powered by solar and biomass. With the main application of the system being residential (both single and multi-family houses) and light commercial sectors, the design objective of the device has considered the optimization of the main components' configuration in terms of technical and dimensional characteristics to ensure it matches the utilization by the respective end user [84]. The proposed system utilized a fluidized bed combustion process as it offers a high range of temperature of around 850ºC; which is suitable for Stirling engine operation and leads to higher coefficients of heat exchange, in addition to low nitrogen oxide emission at that temperature. The fluidized bed would act as an absorber (receiver) for the solar mirror and a heat exchanger with the head of the Stirling engine, in addition to its main duty as a biomass combustor. Simple mathematical models were suggested for various system components in order to monitor the behavior of the arrangement. The mirror utilized had an area of 12.5 m^2, and DNI variations of 1000, 500 and zero W/m2 to respectively respond to sunny daytime, cloudy day time, and total absence of sun irradiation (night time) were considered along with global efficiency of 75% for solar energy capture. The results revealed that at max CSP suggested, the system was able to produce 1.25 kW of electrical power from the engine. In this scenario, the addition of biomass was found to increase the power produced, however, increasing the feeding rate of biomass dropped the increase of power production and leads to asymptotic behavior at a rate of approximately 4 kg/h. When irradiation drops to levels around 500 W/m^2, biomass combustion helps overcome low temperature in the combustor, with an electrical power output of about 4kW when biomass is at a feed rate of 2 kg/h. In cases where no solar irradiation is available, a minimum mass flow rate of biomass of 2.5 kg/h is required to reach temperature high enough to maintain steady and clean combustion.

Although the system described has shown its technical feasibility to supply single houses with heat and power, more work in terms and experiments and component optimization should be carried out to gain more understanding of those systems. In addition, the cost of such systems should be explored to further understand its competitiveness with conventional systems.

2.2 Summary of Literature Review

The review of studies covering the research and development of combining solar and biomass energies in one system for the production of one or more commodities has been summarized in this chapter. The main observation of this review is that; solar energy and biomass fuels can be integrated into one system through multiple arrangements. Those arrangements utilize different technologies depending on the required application. Generally, the objective of the hybridized systems is to provide a sustainable supply of energy at a competitive cost relative to conventional fuels and single source renewable energy systems, such as standalone solar power plants. Multiple studies have shown the potential of the hybridization and demonstrated the associated savings. Most of the work available utilizes PTC to run the solar subsystem, as those collectors have proven their maturity. In those PTC, indirect steam generation is used, where an intermediate heat exchanger is used to transfer the heat from the solar field to the power block. At the end of the review, it has been identified that, in the open literature, all systems combining PTC and biomass fuels utilize indirect steam generation. This limits the maximum allowable temperature in the power block, as the synthetic oils used as a HTF in the solar field are thermally instable beyond 400 °C. Thus, the present work is being conducted to increase the efficiency of the PTC plants by increasing the maximum allowable temperature in the system.

2.3 Objectives

As stated in Section 2.4 above, all the systems proposed in the open literature that combined biomass and PTC are based on indirect steam generation techniques, which limit the maximum permissible temperature in the power block. In an attempt to overcome the limitations of the indirect steam generation PTC fields and due to the high technical and economic potential of DSG-based PTC plants, the present work considers the hybridization of DSG in PTC plants with a biomass boiler. The goal of this thesis is to achieve a higher efficiency and avoid using TES, which in return will enhance the performance of the systems. This is the first of its kind in the open literature according to the best of the author's knowledge. The detailed objectives of this thesis are as follows:

- Propose an innovative DSG-based PTC power plant integrated with a biomass-fired boiler.
- Conduct full energetic and exergetic analyses of the proposed system and compare it to exiting indirect steam generation plants.
- Provide full combustion and flue gas analyses of multiple biomass fuels that can be combusted in the boiler.

Chapter 3: Proposed Solar-Biomass Systems' Description

CSP and biomass fuels can be arranged in various configurations for the production of power and other commodities. Multiple arrangements are available in the literature, where solar energy and biomass fuels are combined [70-73]. Figures 3.1-3.4 show the various potential arrangements of the two sources. The arrows represent the flow of the working fluid, which in this study is steam. Figure 3.1 is the integration of the two sources in a parallel approach, where both systems deliver the same stream characteristics to the power block. The power block refers to a thermodynamic cycle which would receive this energy and produce an end product, mainly, electricity. Each system would work independently of the other system and deliver the required energy input to the power block. The main advantage of this approach is that, in any scenario where one of the subsystems cannot supply its required share, the other subsystem can be adjusted to compensate for the shortage. Figures 3.2 and 3.3 represent the process of boosting the quality of the supply stream. The stream gets heated in the first system and then flows into the next system where more energy is supplied to further improve the quality of the stream. Figure 3.4 represents the utilization of a combined cycle approach. In this arrangement, biomass is gasified in a biomass gasifier, and the syngas is utilized in a gas turbine cycle where electricity is generated. Gas exhaust leaving the gas turbine is fed into a HRSG with energy supplied from a CSP subsystem; water is then heated in the HRSG and sent to a steam turbine for electricity production.

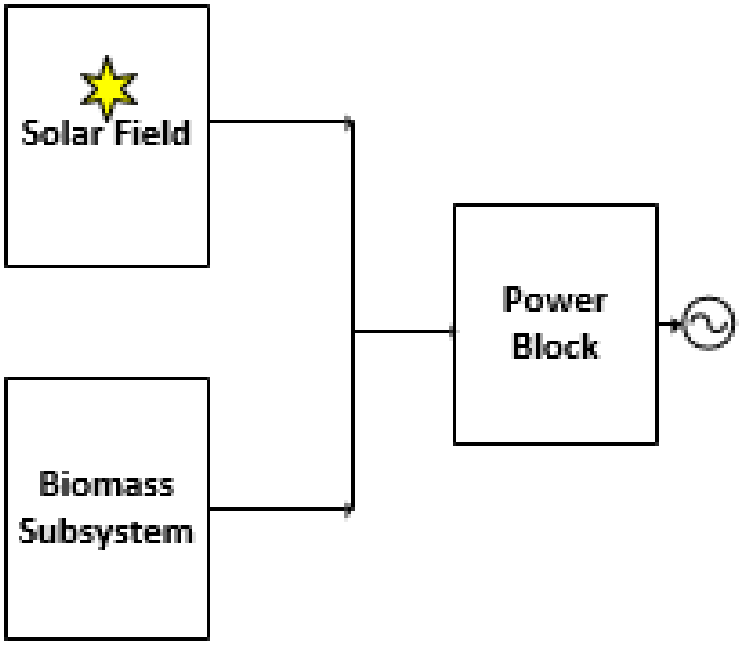

Figure 3.1: Biomass and solar in parallel

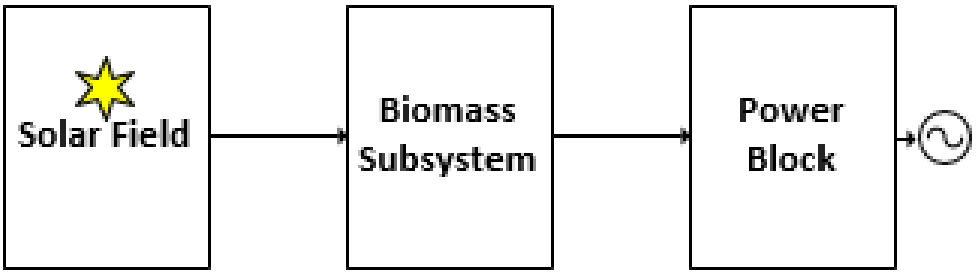

Figure 3.2: Biomass and solar in series

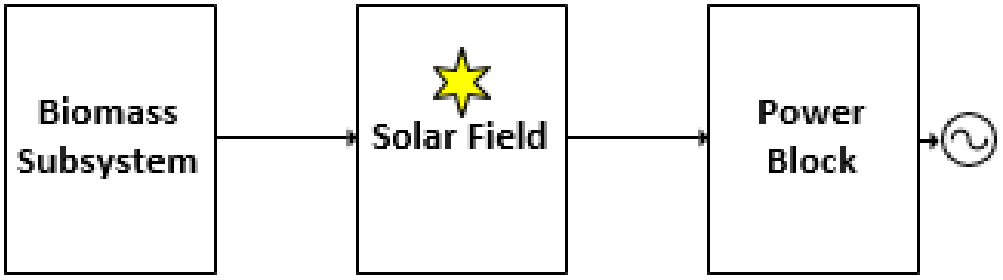

Figure 3.3: Biomass and solar in series

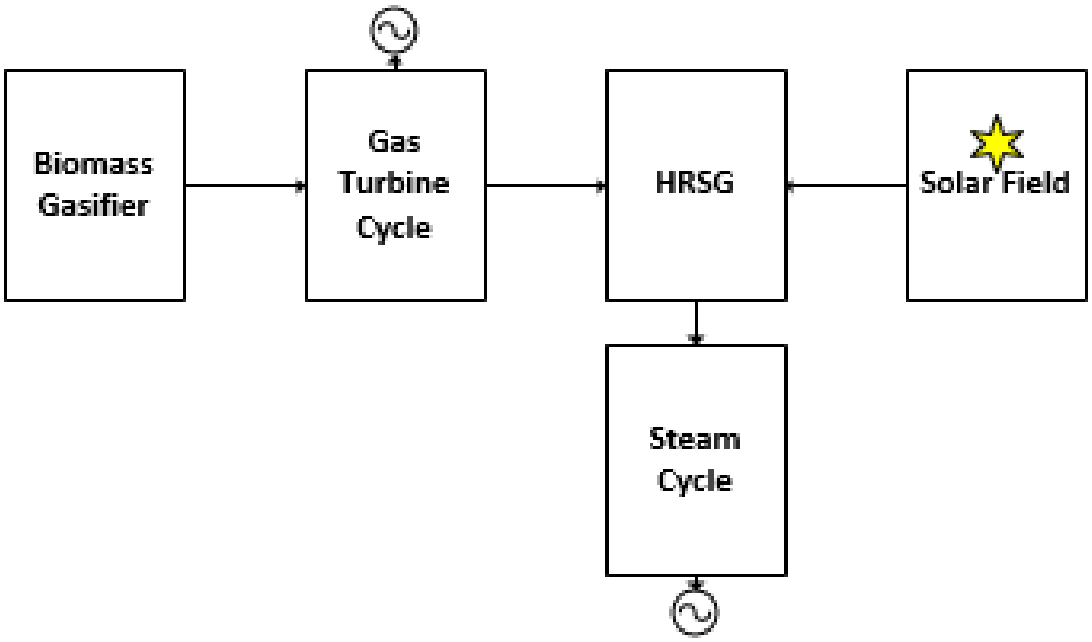

Figure 3.4: Biomass and solar in a combined cycle

3.1 Solar Field

According to the previously mentioned reasons, the collector type selected for the work presented in this thesis is a PTC. A PTC utilizes a parabola shaped mirror to reflect the sun's direct radiation on a receiver tube (absorber), which is located at the focal line of the parabola. The PTC is a single-axis tracking technology, in which a motor is used to track the sun to maximize the energy absorbed. In an indirect steam generation arrangement, the HTF flows through the absorber and gets heated to the desired temperature. The HTF can then be used in a heat exchanger where the energy is transferred to the working fluid of the power block and the HTF is cooled down and returned to the solar field. Figure 3.5 shows the basic structure of a PTC. In a direct steam generation (DSG) arrangement, the steam is directly produced in the collectors and supplied to the power block. To ensure reliable characteristics and data of the collectors, the PTC considered in this work is adopted from the Andasol 1-3 power plants in Spain. Each station has a capacity of 50 MW, and the last one was commissioned in 2011 [85]. The collector used in the Andasol project is the scaled Eurotrough (Skal-ET) collector [51]. The length and width of each collector are 150 m and 5.76 m respectively, and it is composed of RP-3 reflective mirrors produced and supplied by Flabeg Group, located in Furth-im-Wald, Germany and has a reflectivity of around 94% as reported by the manufacturer [43]. The absorber tube used in the Andasol plants is PTR70 produced by Schott Solar AG in Mainz, Germany and Solel Solar Systems Ltd. of Israel [43]. The absorber tube has a thermal emittance of 9.5 %, the absorptance of about 95.5% and to reduce convective heat losses; the tube is placed in a glass vacuum envelope with a transmittance of 95% [86]. When used with PTR70, the optical efficiency of the Skal-ET collector is about 78%. As mentioned

earlier, the Andasol was chosen as a benchmark for PTC power plants due to the reported success that is shown through the high efficiency and stable performance

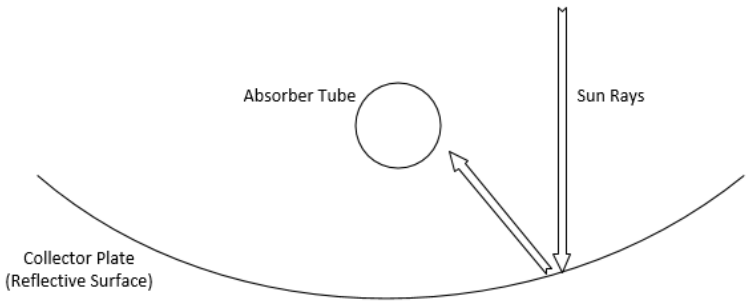

Figure 3.5: Schematic diagram of a parabolic trough collector with labels of the main components

3.2 Biomass Subsystem

As presented earlier, biomass fuels can be utilized in various configurations. For this study, biomass is directly combusted with atmospheric air and the flue gas produced is utilized in a heat exchanger/boiler to heat up the working fluid. For this work, various biomass fuels are analyzed. A combustion analysis is presented, heating value calculations and validation for the calculations are summarized as well. Table 3.1 shows one of the biomass fuels collected from the literature and considered for the study, along with their ultimate composition analysis [87]. Additional biomass fuels considered in the present work are listed in Appendix A. Each group listed consists of several types of fuels. The average of elemental contents of Carbon (C), Oxygen (O), Hydrogen (H), Nitrogen (N), and Sulphur (S) for each fuel group are summarized below.

Table 3.1: Wood and woody biomass fuels and their ultimate elemental content [87]

Biomass mixture/fuel	C	O	H	N	S
Wood and woody biomass (WWB)					
Alder-fir sawdust	53.2	40.2	6.1	0.5	0.04
Balsam bark	54	39.5	6.2	0.2	0.1
Beech bark	51.4	41.8	6	0.7	0.11
Birch bark	57	35.7	6.7	0.5	0.1
Christmas trees	54.5	38.7	5.9	0.5	0.42
Elm bark	50.9	42.5	5.8	0.7	0.11
Eucalyptus bark	48.7	45.3	5.7	0.3	0.05
Fir mill residue	51.4	42.5	6	0.1	0.03
Forest Residue	52.7	41.1	5.4	0.7	0.1
Hemlock bark	55	38.8	5.9	0.2	0.1
Land clearing wood	50.7	42.8	6	0.4	0.07
Maple bark	52	41.3	6.2	0.4	0.11
Oak sawdust	50.1	43.9	5.9	0.1	0.01
Oak wood	50.6	42.9	6.1	0.3	0.1
Olive wood	49	44.9	5.4	0.7	0.03
Pine bark	53.8	39.9	5.9	0.3	0.07
Pine chips	52.8	40.5	6.1	0.5	0.09
Pine pruning	51.9	41.3	6.3	0.5	0.01
Pine sawdust	51	42.9	6	0.1	0.01
Poplar	51.6	41.7	6.1	0.6	0.02
Poplar bark	53.6	39.3	6.7	0.3	0.1
sawdust	49.8	43.7	6	0.5	0.02
Spruce bark	53.6	40	6.2	0.1	0.1
Spruce wood	52.3	41.2	6.1	0.3	0.1
Tamarack bark	57	32	10.2	0.7	0.11
Willow	49.8	43.4	6.1	0.6	0.06
Wood	49.6	44.1	6.1	0.1	0.06
Wood residue	51.4	41.9	6.1	0.5	0.08
Mean	52.1	41.2	6.2	0.4	0.08
Minimum	48.7	32	5.4	0.1	0.01
Maximum	57	45.3	10.2	0.7	0.42

3.3 System 1: Basic Arrangement of Indirect Steam Generation in PTC Hybridized with a Biomass Boiler

In this thesis, a simple solar-biomass cycle that follows the arrangement shown in Figure 3.1 is proposed and analyzed and shown in Figure 3.6. This configuration is capable of the constant production of electricity without TES, where the subsystems complement each other. In an indirect steam generation PTC power plant, there are three major subsystems. The first subsystem is the solar field, where the HTF passes through the receiver/absorber tubes of the collectors and gets heated to a high temperature. The second subsystem is the HRSG that connects the solar field to the third subsystem which is the power block. In the HRSG, the HTF of the solar field enters with high heat content and exchanges it with the working fluid of the power block. A considerable amount of research and development is available in the literature covering various areas of PTC power plants including their performance, optimization, and economics [88-93]. In the proposed system, the power block considered is a simple Rankine cycle, where two-thirds of the turbine capacity are supplied by the biomass boiler, and the remaining third is supplied by the solar field. The solar field is assumed to have solar to thermal efficiency at a peak value of 70% and annual as low as 50% as reported by Andasol plants [43]. The biomass fuel group considered for the cycle is the herbaceous and agricultural biomass group, and its composition is shown in Appendix A. The exhaust gas from the biomass combustor is utilized to heat up the feed water before passing through to the solar field. The steam is assumed to enter the turbine at 370°C and 100 bar, and leaves the turbine to the condenser at 0.5 bar. The working fluid considered for the solar field is Therminol VP-1, as it has the necessary temperature range to operate this cycle[94]. It was also assumed that there are no changes in kinetic and potential energies, no pressure drops in the pipes, and the turbine

and the pumps are adiabatic. The efficiency of the turbine and the pumps are 87% and 80% respectively and the direct normal irradiance considered is 800 W/m^2. The objective of this system is to show the potential of combining solar thermal technologies and biomass fuels for sustainable power production through the presentation of a new configuration and to identify and provide a simple analysis of both subsystems.

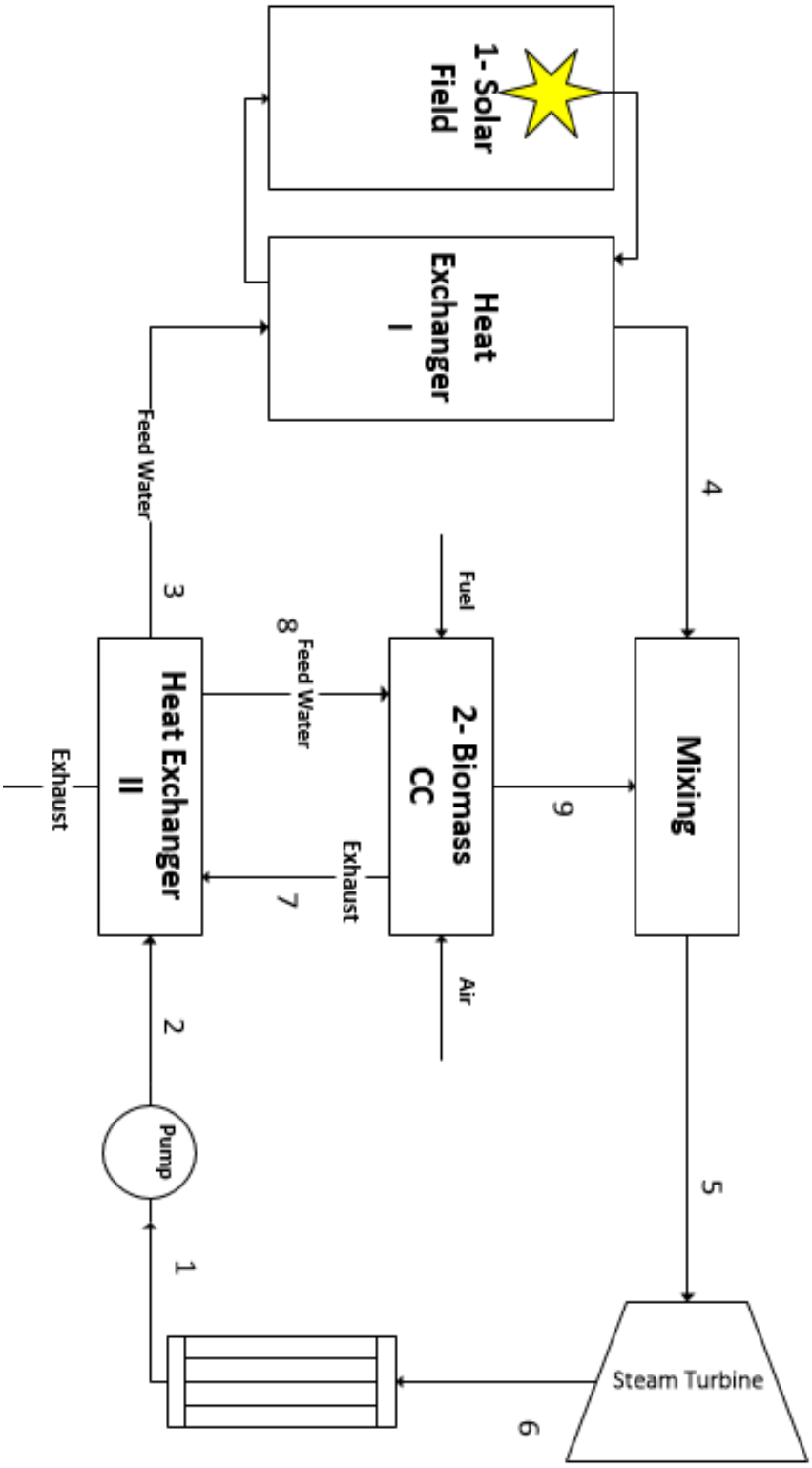

Figure 3.6: Solar-assisted biomass power generation system

3.4 System 2: Indirect Steam Generation in PTC Power Plant

The system shown in Figure 3.7 presents the indirect steam generation PTC power generation plant used for the comparison that will be drawn between DSG and indirect steam generation. The layout of the system is the same as the Andasol power plant. In the solar field, the oil enters at 295 °C and leaves at 393 °C [51]. The oil is then sent to the HRSG to heat up the working fluid of the power block. The steam produced in the HRSG can be supplied to any power block depending on the required application. The power block considered in this study is a reheat regenerative 50 MWe Rankine cycle, to ensure highest achievable efficiency. The feedwater will be heated in two closed feedwater heaters (CFWH) from the high-pressure turbine and three CFWHs from the low-pressure turbine. Feedwater heater-extraction points from the turbines are arranged in a way to increase the enthalpy of the flow in roughly the same magnitude [56]. The state points are labeled to be referred to later in the analysis. Systems 2-4 analyzed in this thesis have the same power block layout and parameters as described. Common parameters for the Rankine cycle analyzed are shown in Table 3.2.

Table 3.2: Parameters for the 50 MWe Rankine Cycle [44, 56, 95]

High-Pressure Turbine Efficiency (%)	89.5
Low-Pressure Turbine Efficiency (%)	85.5
Pumps Isentropic Efficiency (%)	75.0
Terminal Temperature Difference (°C)	3.0
Drain Cooling Approach (°C)	5.0
Heat Exchangers Effectiveness (%)	85.0
Condenser Pressure (bar)	8.0

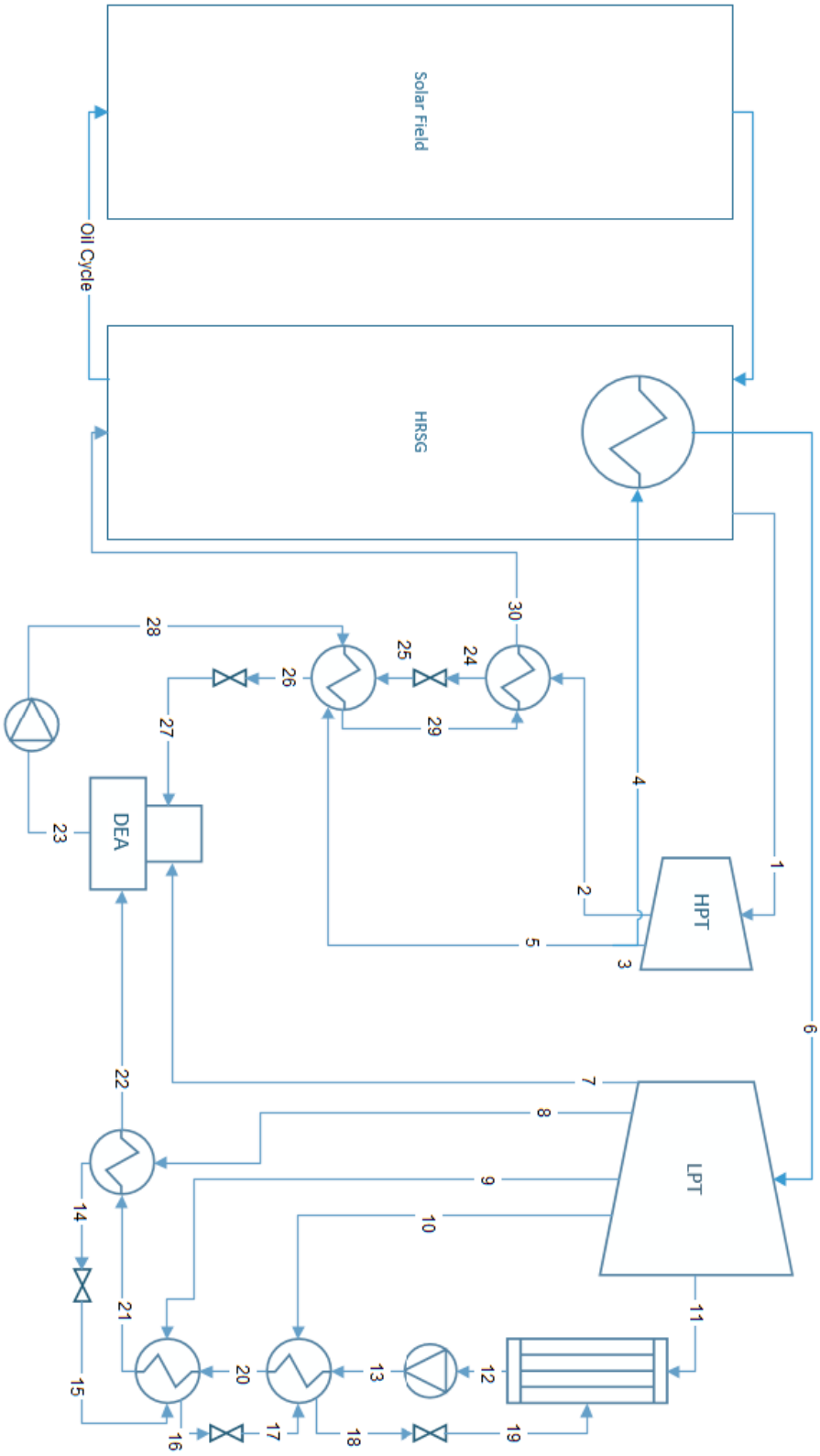

Figure 3.7: Indirect Steam Generation in Parabolic Trough Power Plant

3.5 System 3: Indirect Steam Generation in PTC Power Plant Hybridized with a Biomass Boiler

The third system shown in Figure 3.8 is an attempt to enhance the dispatchability of the solar-only system in Figure 3.7. A biomass- fired boiler is added to the system, where it will provide an energy input to the cycle in conjunction with the solar field. Another advantage of the added boiler is in situations when the solar field cannot provide the necessary energy such as night/cloudy times; the boiler can be adjusted to run the system fully. Similar to System 2, the HTF circulating in the solar field is Therminol VP-1. Both streams coming out of the solar field HRSG and the biomass boiler have the same characteristics and are fed to the power block. In this study, multiple types of biomass fuels will be presented and analyzed to understand the system's performance further. In this system, the share of each energy input can be varied depending on their supply. For instance, the biomass share can be increased to overcome sun’s absence during night time, and similarly, during high insolation periods, the solar share can be increased to reduce the fuels burned in the boiler.

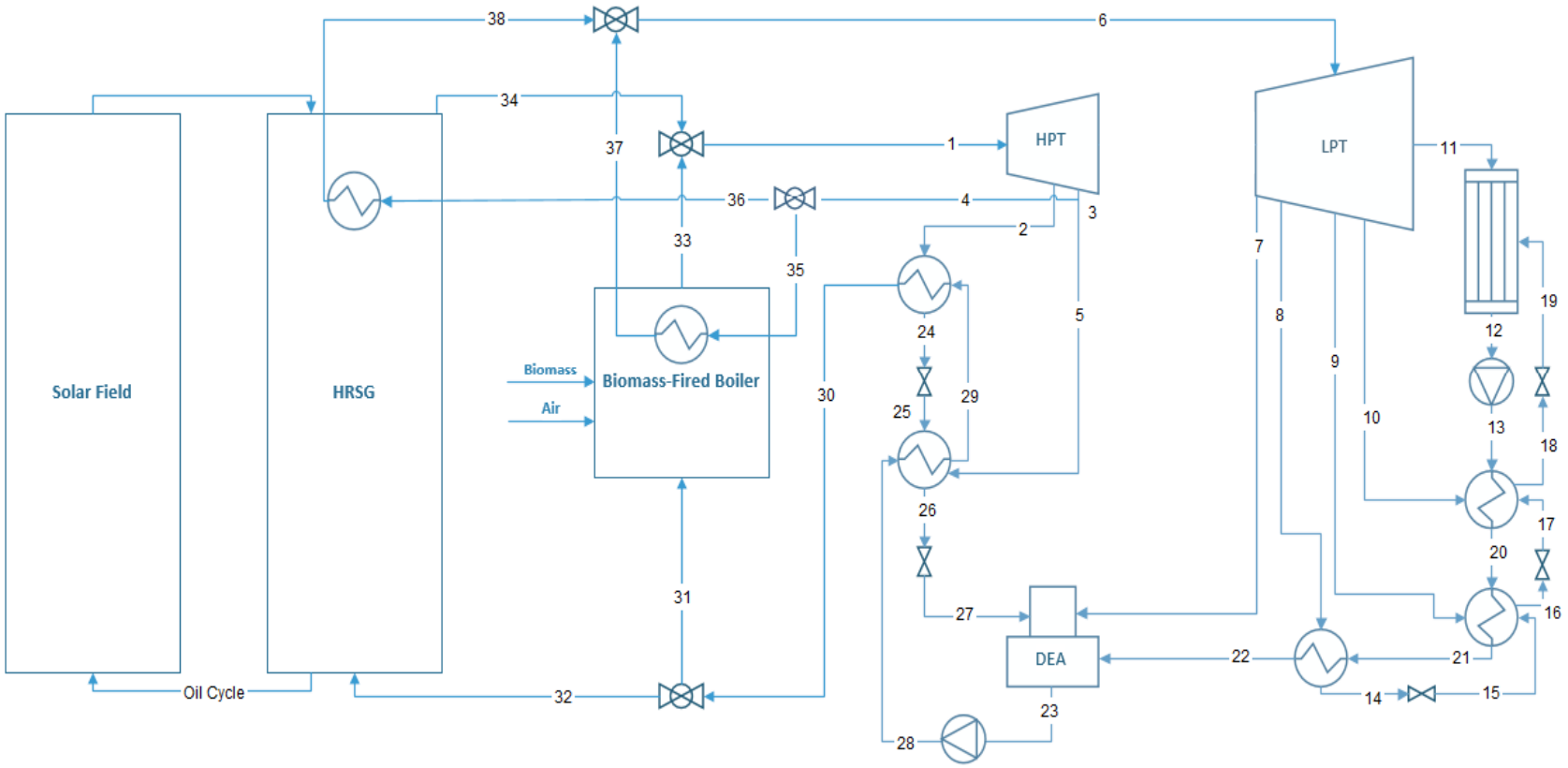

Figure 3.8: Indirect Steam Generation in Parabolic Trough Power Plant Hybridized with a biomass boiler

3.6 System 4: Direct Steam Generation in PTC Power Plant Hybridized with a Biomass Boiler

A schematic diagram of the DSG-based PTC plant proposed in the research work is shown in Figure 3.9. In a DSG-based PTC plant, the HRSG that is usually used to link the solar field and the power block in a conventional PTC plant is not needed, as the water is directly heated in the solar field. The recirculation mode is adopted in this study, which means that the solar field is divided into two sections; the evaporation section and the superheating section with a separator between the two sections [51]. In this arrangement, each evaporation loop will have six collectors in series, and the superheating loop will have three collectors in series. This allows the fluid to fully evaporate before exiting the solar field. In a previous analysis, a live steam temperature of 500 °C was identified as a viable option within DSG plants [53]. To match the pressure of the indirect steam generation plant considered, the same pressure of 100 bar is considered for the DSG plant. However, the PTR70 absorber tube used in the indirect steam plant cannot withstand the high-pressure steam. As a result, the same manufacturer (Schott) who made the PTR70 came up with PTR80-DSG, a new absorber tube that is able to withstand a pressure of up to 150 bar including an allowance for pressure vibrations [96]. The main difference between the two absorbers is the wall thickness, as the DSG absorber needs to be thicker than the oil absorber to withstand high pressure in the loops. In addition to the DSG field, a biomass-fired boiler similar to the one considered in System 3 is integrated with the DSG power plant. The ultimate goal of this hybridization is to ensure a stable supply of power without using TES and achieve higher levels of efficiency by increasing the permissible temperature in the power block compared to indirect steam generation plants.

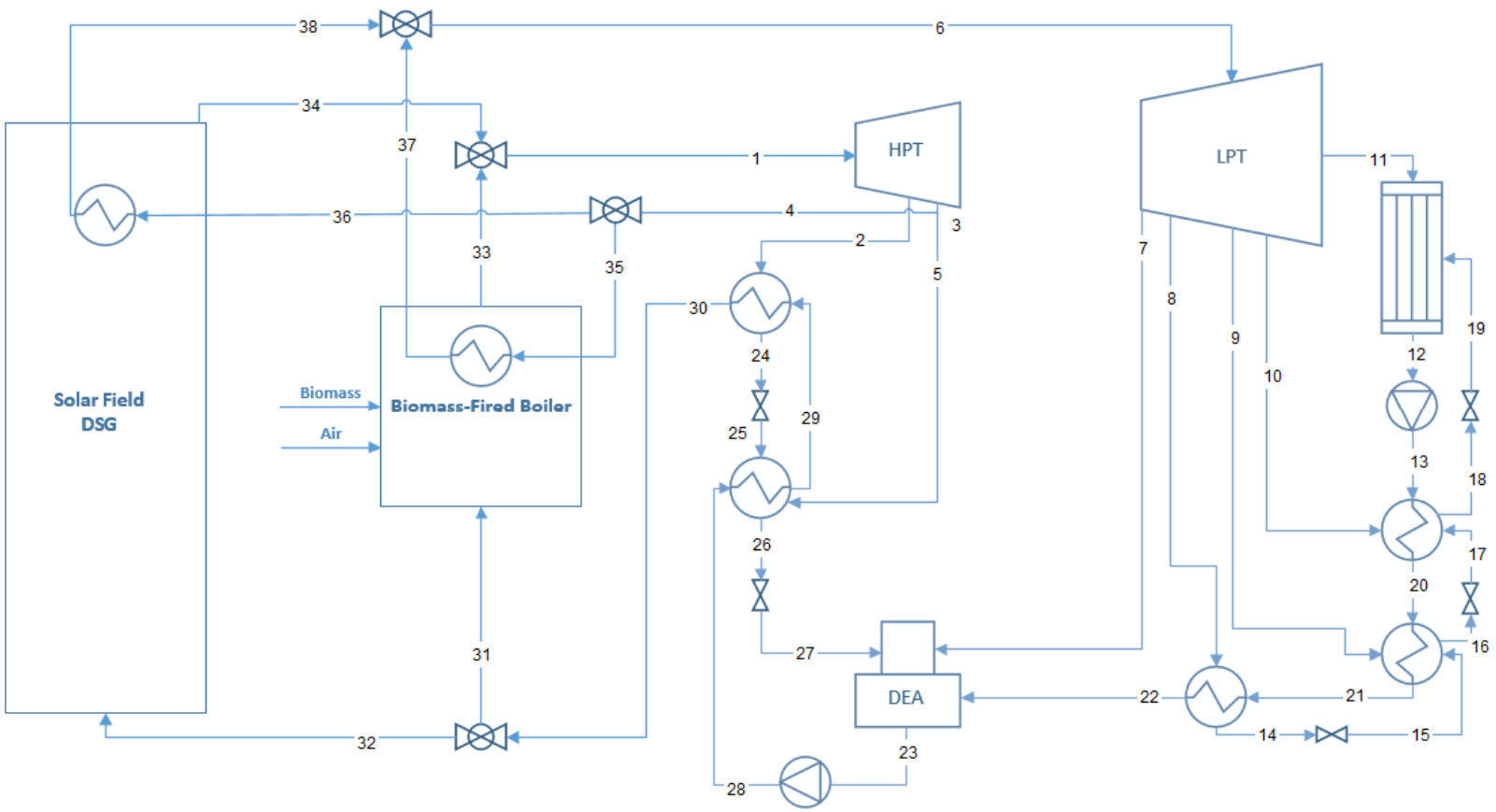

Figure 3.9: Direct Steam Generation in Parabolic Trough Power Plant Hybridized with a biomass boiler

Chapter 4: Analyses of the Proposed Solar-Biomass Energy Systems

In this chapter, the analyses performed for each subsystem is summarized in detail. For all systems, energy and exergy analyses were conducted. In the first section, the analysis of the solar PTC field is listed where the losses were identified and calculated. In the second section, various biomass fuels including the group shown in Table 3.1 are analyzed, and their heating values were calculated to help further analyze the overall system.

4.1 Solar Field Analysis

As mentioned earlier, the collectors considered for the proposed systems are PTCs with similar characteristics to those of the Andasol's collectors. The analysis of the solar field is presented in this section. The first section presents the general formulas used to analyze PTC fields. The second section presents a simplified model to expect the thermal losses of the used absorber tube.

4.1.1 Parabolic Trough Collector Analysis

PTCs transfer direct radiation from the sun into useful heat by reflecting the solar beam onto the absorber tube where the working fluid passes through. Useful heat produced by a solar collector/field can be described as the heat gained in the working fluid circulating inside. The formulations presented for the PTC field are adopted and modified from previous studies [44, 76, 97].

$$Q_{solar} = m_f . (C_{p,o}\ T_o - C_{p,i}\ T_i), \quad (4.1)$$

where m_f is the mass of the fluid circulating inside the field, $C_{p,O}$ and $C_{p,i}$ are specific heat capacity of the fluid at the outlet and the inlet of the solar field respectively.

Another way of describing the useful heat supplied by the collectors is:

$$Q_{solar} = A_{ap} \cdot DNI \cdot Cos\theta \cdot \boldsymbol{\eta}_{collector}, \quad (4.2)$$

where A_{ap} is the collector aperture area, DNI is sun's direct normal irradiance, θ is the incidence angle, and $\boldsymbol{\eta}_{collector}$ is the total efficiency of the collector. The efficiency of the collector is mainly described by its optical characteristics.

$$\boldsymbol{\eta} = \rho_m \cdot \tau \cdot \alpha \cdot \Upsilon \cdot K_\theta, \quad (4.3)$$

where ρ_m, τ, α, Υ, and K_θ are the reflectance of the mirror, transmittance of the glass cover, the absorptance of the absorber tube, intercept factor, and incidence angle modifier, respectively. Another way to model the energy efficiency of a PTC is:

$$\boldsymbol{\eta} = \boldsymbol{\eta}_{optical} - a_1 \frac{(T_m - T_{amb})}{DNI * Cos\theta} - a_2 \frac{(T_m - T_{amb})^2}{DNI * Cos\theta}, \quad (4.4)$$

where a_1 and a_2 are the first order and the second order coefficients of the collector efficiency, and T_m is the mean temperature difference of the working fluid. Generally, the optical efficiency of today's PTCs ranges from 0.6 to 0.75 [76].

4.1.2 Parabolic Trough Collectors Thermal Losses

Generally, losses from the solar field are divided into two main categories; optical losses and thermal losses. Optical losses are related to the characteristics of the equipment used to construct the solar field, and are usually easy to predict based on those specifications. Thermal losses, on the other hand, are related to the temperature difference

between the absorber temperature and the ambient temperature. The main drivers for thermal losses for PTR70 are radiative thermal losses, followed by convective heat losses. However, conductive heat losses are minimal due to the presence of the vacuum between the tube and the glass envelope, and thus such losses can be neglected. A simple heat losses model can be presented where the main losses are taken into consideration as follows:

$$\text{Absorber Thermal Losses} = \text{Radiation Losses} + \text{Convection Losses}, \quad (4.5)$$

$$\text{Radiation loss}: \dot{Q}_{rad} = \varepsilon * \sigma * \text{AAbsorber} * (\text{Tamb}^4 - \text{TAbsorber}^4), \quad (4.6)$$

$$\text{Convection Loss}: \dot{Q}_{conv} = \text{h} * \text{A} * \Delta\text{T}, \quad (4.7)$$

$$\text{Convective Heat Transfer Coefficient}: \text{h} = \text{Nu} * \frac{\text{k}}{\text{D}}, \quad (4.8)$$

where ε, σ, and Nu are the absorber emittance, Stefan-Boltzman constant and Nusslet number respectively.

4.2 Biomass Subsystem Analysis

Biomass fuels are combusted with excess air to ensure complete combustion and avoid CO emissions. The combustion process occurs according to the following reaction.

$$C_xH_yO_z + \lambda\,(O_2 + 3.76N_2) \rightarrow aCO_2 + bH_2O + cN_2$$

A full biomass combustion analysis was conducted for the various biomass fuels considered in the study. Biomass fuels are combusted with 50% excess air. The combustion model is adopted and modified from [98].

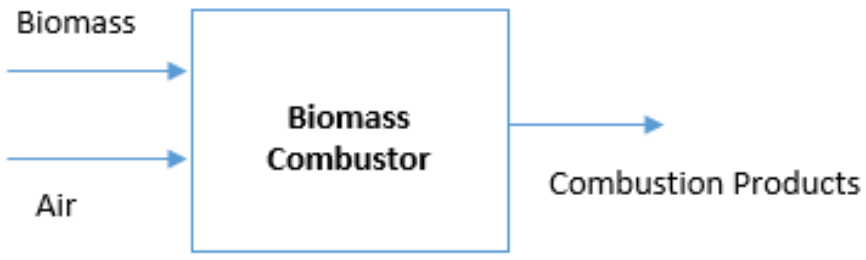

Figure 4.1: Biomass combustor

4.2.1 Biomass Combustion and Combustion Gases Analysis

Biomass combustion formulas used in this analysis are presented below. The atmospheric air mixed with the fuel contains oxygen and nitrogen, and they can be calculated as follows:

Amount of O_2 in Air:

$$m_{O_2}\left[\frac{kgO_2}{kg\ fuel}\right] = \left[X_c\frac{M_{O_2}}{M_C} + \frac{X_H}{4}\frac{M_{O_2}}{M_H} + X_S\frac{M_{O_2}}{M_S} - X_O\right] * \left(1 - X_{H_2O}\right)\gamma \quad (4.9)$$

X_i : Mass of fraction i

M_i: Molar mass of i

γ: Air to fuel ration

Amount of N_2 in Air:

$$m_{N_2}\left[\frac{kgN_2}{kg\ fuel}\right] = m_{O_2}\frac{Y_{N_2}}{Y_{O_2}}\frac{M_{N_2}}{M_{O_2}} \quad (4.10)$$

Y_i: Fraction of i in the air; 0.79 for O_2, 0.21 for N_2

$$Air(\frac{kg\ air}{kg\ fuel}) = m_{O_2} + m_{N_2} \quad (4.11)$$

The flue gas produced during the combustion process contains multiple gasses, the mass content of each gas in the overall mixture can be calculated as follows:

Flue gas species mass:

$$Flue\ Gas(\frac{kg\ flue\ gas}{kg\ fuel}) = Air + 1 \quad (4.12)$$

$$m_{CO_2}(\frac{kg\ CO_2}{kg\ fuel}) = X_c\frac{M_{CO_2}}{M_C} * (1 - X_{H_2O}) \quad (4.13)$$

$$m_{H_2O}\left(\frac{kg\ H_2O}{kg\ fuel}\right) = X_H\frac{M_{H2O}}{M_{H_2}} * \left(1 - X_{H_2O}\right) + X_{H_2O} \quad (4.14)$$

$$m_{SO_2}\left(\frac{kg\ SO_2}{kg\ fuel}\right) = X_S\frac{M_{SO_2}}{M_S} * \left(1 - X_{H_2O}\right) \quad (4.15)$$

$$m_{N_2}\left(\frac{kg\ N_2}{kg\ fuel}\right) = m_{N_2} + X_N\left(1 - X_{H_2O}\right) \quad (4.16)$$

$$m_{O_2}\left(\frac{kg\ O_2}{kg\ fuel}\right) = \frac{m_{O_2}}{\gamma}(\gamma - 1) \quad (4.17)$$

4.2.2 Heating Value Calculations

One of the most descriptive parameters of fuel quality is its heating value. A fuel heating value represents the amount of energy released when the fuel is burned. Higher heating value (HHV) is the amount of energy released taking in consideration latent heat of vaporization of water in the combustion products. However, biomass fuels contain water and other volatile materials which require energy to vaporize this water. To account for moisture in the fuel, lower heating value (LHV) is calculated. The moisture content of biomass in this study is considered to be 5.5% as recommended [98]. HHV and LHV are calculated using the model provided by [98], where the mass percentage of each element is taken into consideration.

$$HHV\left(\frac{MJ}{kg}\right) = 0.3491X_c + 1.1783X_H + 0.1005X_s - 0.0151X_N - 0.01034X_O \quad (4.18)$$

X_i: Content of i (%) in dry basis samples

$$LHV = HHV * (1 - w) - (2.44w) * \left(8.396(1 - w)\right) \quad (4.19)$$

w: Moisture content on mass basis

4.3 Thermodynamic Analysis

A thermodynamic analysis is mainly divided into two main categories; energy and exergy. The energy analysis is mainly based on the first law thermodynamics, and the exergy analysis is based on the second law of thermodynamics. For the analysis, mass, energy, entropy, and exergy balance equation are considered for each component. The analysis neglects changes in potential and kinetic energies, and pressure losses in heat

exchangers and pipes, as those changes are minimal compared to thermal changes in the system. In addition, it is assumed that the turbines and pumps are adiabatic.

4.3.1 Energy Analysis

The overall energy efficiencies of the proposed cycles are the ratios of useful work output to total energy input.

$$\eta_{\text{overall}} = \frac{\dot{W}_{net}}{\dot{Q}_{in}} \tag{4.20}$$

The heat input for the cycle is not the same for all cases. The input to the first system shown in Figure 3.6 is supplied by the solar field through the heat exchanger and the biomass boiler. In the second systems shown in Figure 3.7, the input to the system is fully supplied by the solar field, so the energy input is the heat supplied through the HRSG. For the last two systems in Figures 3.8 and 3.9, the energy supplied to the cycle comes from the solar field and the biomass boiler. The energy supplied by the boiler depends on the fuel used and the mass flow rate of the fuel. For the DSG, energy from the solar field is directly supplied to the working fluid, whereas for the indirect steam generation, the HRSG is used to transfer the energy from the solar field to the working fluid.

The heat supplied by the biomass boiler is calculated as follows:

$$\dot{Q}_{Biomass} = \dot{m}_f * LHV, \tag{4.21}$$

where $\dot{m}_f$ is the mass flow rate of the fuel

4.3.2 Exergy Analysis

Exergy can be defined as the maximum amount of work that can be obtained from the system with respect to ambient conditions.

Based on the second law of thermodynamics, the exergy balance for a control volume is:

$$\dot{E}x^{Q} + \sum_i \dot{m}_i \dot{ex}_i = \sum_o \dot{m}_o \dot{ex}_o + \dot{E}x_w + \dot{E}x_D, \quad (4.22)$$

where i and o denotes the inlet and the outlet of the system respectively. $\dot{ex}, \dot{E}x^{Q}, \dot{E}x_w, and\ \dot{E}x_D$ are; exergy of the fluid, heat exergy, work exergy, and exergy destruction respectively.

$$\text{ex}\left(\frac{\text{kJ}}{\text{kg}}\right) = (\text{h} - \text{h}_\text{a}) - \text{T}_\text{a}(\text{s} - \text{s}_\text{a}), \quad (4.23)$$

where h, s, and T are enthalpy, entropy, and temperature, respectively, and the subscript "a" refers to the ambient conditions.

$$\dot{E}x^{Q} = \dot{Q}(1 - \frac{T_a}{T}), \quad (4.24)$$

$$\dot{E}x_w = \dot{W} \quad (4.25)$$

As the role of exergy is to identify the maximum useful work that can be produced by a system, calculating exergy destruction emerge is a useful tool to find the locations of most irreversible losses in the system, which helps to understand the performance of the systems and locating components where most development is needed [99]. Fundamentally, exergy destruction can be calculated as:

$$\dot{E}x_d = T_o \dot{S}_{gen}, \quad (4.26)$$

where $\dot{E}x_d$ and $\dot{S}_{gen}$ are the rate of exergy destruction and entropy generation, respectively. Exergy destruction can also be calculated from the exergy balance equation of each component. For instance, the exergy destruction of the high pressure turbine in Figure 3.7 can be calculated as:

$$\dot{E}x_{D,HPT} = \dot{m}_1 e\dot{x}_1 - \dot{m}_2 e\dot{x}_2 - \dot{m}_3 e\dot{x}_3 - \dot{W}_{HPT}, \quad (4.27)$$

where $\dot{W}_{HPT}$ is the work output of the high pressure turbine.

The exergy supplied by the solar system can be calculated as follows[100]:

$$\dot{E}x_{solar} = \dot{Q}_{solar}(1 - \frac{4}{3}\frac{T_o}{T_{sun}}(1 - 0.28ln f_{dill})) , \quad (4.28)$$

where f_{dill} is the dilution factor and given as $1.3x10^{-5}$

The exergetic efficiency of the system can be defined as the useful power output to the total exergy input.

$$\eta_{ex} = \frac{\dot{W}_{net}}{\dot{E}x_{in}}, \quad (4.29)$$

Finally, the exergetic efficiency of each component is defined as the ratio of the exergy output of the component to the exergy input of the component.

$$\eta_{ex,Component} = \frac{ex_{out}}{ex_{in}} \quad (4.30)$$

4.4 First and Second Law Analyses

Mass, energy, entropy, and exergy balance equations are written for each component of the proposed systems. Since Systems 2-4 are fundamentally similar, the balance equations of the shared components will be presented once for System 2 and will not be repeated for Systems 3 and 4.

4.4.1 System 1 Analysis: Basic Arrangement of Indirect Steam Generation in PTC Hybridized with a Biomass Boiler

The balance equations for System 1 shown in Figure 3.6 are summarized below.

Solar Field Balance

The mass flow rate balance equation for the solar field can be written as:

$$\dot{m}_{oil,in} = \dot{m}_{oil,out} \tag{4.31}$$

The energy balance equation for the solar field can be written as:

$$\dot{m}_{oil,in} h_{oil,in} + \dot{Q}_{solar} = \dot{m}_{oil,out} h_{oil,out}, \tag{4.32}$$

where $\dot{Q}_{solar}$ is the energy supplied by the solar collectors to the flowing oil

The entropy balance equation for the solar field can be written as:

$$\dot{m}oil_{,in}\, s_{oil,in} + \dot{S}_g + \frac{\dot{Q}}{T_a} = \dot{m}_{oil,out} s_{oil,out} \tag{4.33}$$

The exergy balance equation for the solar field can be written as:

$$\dot{m}_{oil,in} ex_{oil,in} + \dot{E}x^{Q} = \dot{m}_{oil,out} ex_{oil,out} + \dot{E}x_{D} \tag{4.34}$$

Heat Exchanger I

The mass flow rate balance equation for the heat Exchanger I can be written as:

$$\dot{m}_{oil,in} = \dot{m}_{oil,out} \; ; \; \dot{m}_3 = \dot{m}_4 \tag{4.35}$$

The energy balance equation for the heat Exchanger I can be written as:

$$\dot{m}_{oil,out} h_{oil,out} + \dot{m}_3 h_3 = \; \dot{m}_4 h_4 + \dot{m}_{in,oil} h_{in,oil} \tag{4.36}$$

The entropy balance equation for the solar field can be written as:

$$\dot{m}_{oil,out} s_{oil,out} + \dot{m}_3 s_3 + \dot{S}_g = \; \dot{m}_{oil,in} s_{oil,in} + \dot{m}_4 s_4 \tag{4.37}$$

The exergy balance equation for the solar field can be written as:

$$\dot{m}_{oil,out} ex_{oil,out} + \dot{m}_3 ex_3 = \; \dot{m}_{oil,in} ex_{oil,in} + \dot{m}_4 ex_4 + \dot{E}x_D \tag{4.38}$$

Biomass Combustion Chamber

The mass flow rate balance equation for the biomass combustion chamber can be written as:

$$\dot{m}_8 = \dot{m}_9 \tag{4.39}$$

The energy balance equation for the biomass combustion chamber can be written as:

$$\dot{m}_8 h_8 + \dot{Q}_{Biomass} = \; \dot{m}_9 h_9 \tag{4.40}$$

where $\dot{Q}_{Biomass}$ is the energy supplied by biomass to the water

The entropy balance equation for the biomass combustion chamber can be written as:

$$\dot{m}_8 s_8 + \dot{S}_g + \frac{\dot{Q}}{T_a} = \; \dot{m}_9 s_9 \tag{4.41}$$

The exergy balance equation for the biomass combustion chamber can be written as:

$$\dot{m}_8 ex_8 + \dot{E}x^Q = \; \dot{m}_9 ex_9 + \dot{E}x_D \tag{4.42}$$

Mixing Chamber

The mass flow rate balance equation for the mixing chamber can be written as:

$$\dot{m}_9 + \dot{m}_4 = \dot{m}_5 \tag{4.43}$$

The energy balance equation for the mixing chamber can be written as:

$$\dot{m}_9 h_9 + \dot{m}_4 h_4 = \dot{m}_5 h_5 \tag{4.44}$$

The entropy balance equation for the mixing chamber can be written as:

$$\dot{m}_9 s_9 + \dot{S}_g + \dot{m}_4 s_4 = \dot{m}_5 s_5 \tag{4.45}$$

The exergy balance equation for the mixing chamber can be written as:

$$\dot{m}_9 ex_9 + \dot{m}_4 ex_4 = \dot{m}_5 ex_5 + \dot{E}x_D \tag{4.46}$$

Steam Turbine

The mass flow rate balance equation for the steam turbine can be written as:

$$\dot{m}_5 = \dot{m}_6 \tag{4.47}$$

The energy balance equation for the steam turbine can be written as:

$$\dot{m}_5 h_5 = \dot{m}_6 h_6 + \dot{W}_T \tag{4.48}$$

where $\dot{W}_T$ is the work output of the steam turbine

The entropy balance equation for the steam turbine can be written as:

$$\dot{m}_5 s_5 + \dot{S}_g = \dot{m}_6 s_6 \tag{4.49}$$

The exergy balance equation for the steam turbine can be written as:

$$\dot{m}_5 ex_5 = \dot{m}_6 ex_6 + \dot{E}x_D + \dot{W}_T \quad (4.50)$$

Condenser

The mass flow rate balance equation for the condenser can be written as:

$$\dot{m}_6 = \dot{m}_1 \quad (4.51)$$

The energy balance equation for the condenser can be written as:

$$\dot{m}_6 h_6 = \dot{m}_1 h_1 + \dot{Q}_C \quad (4.52)$$

where $\dot{Q}_C$ is the heat rejected by the condenser to the environment

The entropy balance equation for the condenser can be written as:

$$\dot{m}_6 s_6 + \dot{S}_g = \dot{m}_1 s_1 + \frac{\dot{Q}_C}{T_a} \quad (4.53)$$

The exergy balance equation for the condenser can be written as:

$$\dot{m}_6 ex_6 = \dot{m}_1 ex_1 + \dot{E}x^{Q_C} + \dot{E}x_D \quad (4.54)$$

Pump

The mass flow rate balance equation for the pump can be written as:

$$\dot{m}_1 = \dot{m}_2 \quad (4.55)$$

The energy balance equation for the pump can be written as:

$$\dot{m}_1 h_1 + \dot{W}_p = \dot{m}_2 h_2 \quad (4.56)$$

where $\dot{W}_p$ is the work needed to operate the pump

The entropy balance equation for the pump can be written as:

$$\dot{m}_1 s_1 + \dot{S}_g = \dot{m}_2 s_2 \quad (4.57)$$

The exergy balance equation for the pump can be written as:

$$\dot{m}_1 ex_1 + \dot{W}_p = \dot{m}_2 ex_2 + \dot{E}x_D \quad (4.58)$$

Heat Exchanger II

The mass flow rate balance equations for Heat Exchanger II can be written as:

$$\dot{m}_2 = \dot{m}_3 + \dot{m}_8, \quad (4.59)$$

$$\dot{m}_7 = \dot{m}_{exhaust} \quad (4.60)$$

The energy balance equation for Heat Exchanger II can be written as:

$$\dot{m}_2 h_2 + \dot{m}_7 h_7 = \dot{m}_3 h_3 + \dot{m}_8 h_8 + \dot{m}_{exhaust} h_{exhaust} \quad (4.61)$$

The entropy balance equation for Heat Exchanger II can be written as:

$$\dot{m}_2 s_2 + \dot{m}_7 s_7 + \dot{S}_g = \dot{m}_3 s_3 + \dot{m}_8 s_8 + \dot{m}_{exhasut} s_{exhasut} \quad (4.62)$$

The exergy balance equation for heat Exchanger II can be written as:

$$\dot{m}_2 ex_2 + \dot{m}_7 ex_7 = \dot{m}_3 ex_3 + \dot{m}_8 ex_8 + \dot{m}_{exhaust} ex_{exhaust} + \dot{E}x_D \quad (4.63)$$

4.4.2 System 2 Analysis: Indirect Steam Generation in PTC Power Plant

The balance equations for System 2 shown in Figure 3.7 are summarized below.

High-Pressure Turbine

The mass flow rate balance equations for the high-pressure turbine can be written as:

$$\dot{m}_1 = \dot{m}_2 + \dot{m}_3 \quad (4.64)$$

The energy balance equation for high-pressure turbine can be written as:

$$\dot{m}_1 h_1 = \dot{m}_2 h_2 + \dot{m}_3 h_3 + \dot{W}_{T1} \tag{4.65}$$

The entropy balance equation for high-pressure turbine can be written as:

$$\dot{m}_1 s_1 + \dot{S}_g = \dot{m}_2 s_2 + \dot{m}_3 s_3 \tag{4.66}$$

The exergy balance equation for high-pressure turbine can be written as:

$$\dot{m}_1 ex_1 = \dot{m}_2 ex_2 + \dot{m}_3 ex_3 + \dot{W}_{T1} + \dot{Ex}_D \tag{4.67}$$

Low-Pressure Turbine

The mass flow rate balance equations for the low-pressure turbine can be written as:

$$\dot{m}_6 = \dot{m}_7 + \dot{m}_8 + \dot{m}_9 + \dot{m}_{10} + \dot{m}_{11} \tag{4.68}$$

The energy balance equation for low-pressure turbine can be written as:

$$\dot{m}_6 h_6 = \dot{m}_7 h_7 + \dot{m}_8 h_8 + \dot{m}_9 h_9 + \dot{m}_{10} h_{10} + \dot{m}_{11} h_{11} + \dot{W}_{T2} \tag{4.69}$$

The entropy balance equation for low-pressure turbine can be written as:

$$\dot{m}_6 s_6 + \dot{S}_g = \dot{m}_7 s_7 + \dot{m}_8 s_8 + \dot{m}_9 s_9 + \dot{m}_{10} s_{10} + \dot{m}_{11} s_{11} \tag{4.70}$$

The exergy balance equation for low-pressure turbine can be written as:

$$\dot{m}_6 ex_6 = \dot{m}_7 ex_7 + \dot{m}_8 ex_8 + \dot{m}_9 ex_9 + \dot{m}_{10} ex_{10} + \dot{m}_{11} ex_{11} + \dot{W}_{T2} + \dot{Ex}_D \tag{4.71}$$

Condenser

The mass flow rate balance equation for the condenser can be written as follows:

$$\dot{m}_{11} + \dot{m}_{19} = \dot{m}_{12} \tag{4.72}$$

The energy balance equation for the condenser can be written as follows:

$$\dot{m_{11}}h_{11} + \dot{m_{19}}h_{19} = \dot{m_{12}}h_{12} + \dot{Q_C} \quad (4.73)$$

The entropy balance equation for the condenser can be written as follows:

$$\dot{m_{11}}s_{11} + \dot{m_{19}}s_{19} + \dot{S_g} = \dot{m_{12}}s_{12} + \frac{\dot{Q_C}}{T} \quad (4.74)$$

The exergy balance equation for the condenser can be written as:

$$\dot{m_{11}}ex_{11} + \dot{m_{19}}ex_{19} = \dot{m_{12}}ex_{12} + \dot{Ex_D} + \dot{Ex_Q} \quad (4.75)$$

Pump I

The mass flow rate balance equation for Pump I can be written as:

$$\dot{m_{12}} = \dot{m_{13}} \quad (4.76)$$

The energy balance equation for Pump I can be written as:

$$\dot{m_{12}}h_{12} + \dot{W_{PI}} = \dot{m_{13}}h_{13} \quad (4.78)$$

The entropy balance equation for Pump I can be written as:

$$\dot{m_{12}}s_{12} + \dot{S_g} = \dot{m_{13}}s_{13} \quad (4.79)$$

The exergy balance equation for Pump I can be written as:

$$\dot{m_{12}}ex_{12} + \dot{W_{PI}} = \dot{m_{13}}ex_{13} + \dot{Ex_D} \quad (4.80)$$

Feedwater Heater I

The mass flow rate balance equation for feedwater Heater I can be written as:

$$\dot{m_{10}} + \dot{m_{17}} = \dot{m_{18}}\ ,\ \dot{m_{13}} = \dot{m_{20}} \quad (4.81)$$

The energy balance equation for Feedwater Heater I can be written as:

$$\dot{m_{13}}h_{13} + \dot{m_{10}}h_{10} + \dot{m_{17}}h_{17} = \dot{m_{18}}h_{18} + \dot{m_{20}}h_{20} \quad (4.82)$$

The entropy balance equation for Feedwater Heater I can be written as:

$$\dot{m}_{13}s_{13} + \dot{m}_{10}s_{10} + \dot{m}_{17}s_{17} + \dot{S}_g = \dot{m}_{18}s_{18} + \dot{m}_{20}s_{20} \quad (4.83)$$

The exergy balance equation for Feedwater Heater I can be written as:

$$\dot{m}_{13}ex_{13} + \dot{m}_{10}ex_{10} + \dot{m}_{17}ex_{17} = \dot{m}_{18}ex_{18} + \dot{m}_{20}ex_{20} + \dot{E}x_D \quad (4.84)$$

Feedwater heater II

The mass flow rate balance equation for Feedwater Heater II can be written as:

$$\dot{m}_9 + \dot{m}_{15} = \dot{m}_{16}\ ,\ \dot{m}_{20} = \dot{m}_{21} \quad (4.85)$$

The energy balance equation for Feedwater Heater II can be written as:

$$\dot{m}_{20}h_{20} + \dot{m}_9h_9 + \dot{m}_{15}h_{15} = \dot{m}_{16}h_{16} + \dot{m}_{21}h_{21} \quad (4.86)$$

The entropy balance equation for Feedwater Heater II can be written as:

$$\dot{m}_{20}s_{20} + \dot{m}_9s_9 + \dot{m}_{15}s_{15} + \dot{S}_g = \dot{m}_{16}s_{16} + \dot{m}_{21}s_{21} \quad (4.87)$$

The exergy balance equation for feedwater Heater II can be written as:

$$\dot{m}_{20}ex_{20} + \dot{m}_9ex_9 + \dot{m}_{15}ex_{15} = \dot{m}_{16}ex_{16} + \dot{m}_{21}ex_{21} + \dot{E}x_D \quad (4.88)$$

Feedwater Heater III

The mass flow rate balance equation for Feedwater Heater III can be written as:

$$\dot{m}_8 = \dot{m}_{14}\ ,\ \dot{m}_{21} = \dot{m}_{22} \quad (4.89)$$

The energy balance equation for Feedwater Heater III can be written as:

$$\dot{m}_{21}h_{21} + \dot{m}_8h_8 = \dot{m}_{14}h_{14} + \dot{m}_{22}h_{22} \quad (4.90)$$

The entropy balance equation for Feedwater Heater III can be written as:

$$\dot{m}_{21}s_{21} + \dot{m}_8 s_8 + \dot{S}_g = \dot{m}_{14}s_{14} + \dot{m}_{22}s_{22} \quad (4.91)$$

The exergy balance equation for Feedwater Heater III can be written as:

$$\dot{m}_{21}ex_{21} + \dot{m}_8 ex_8 = \dot{m}_{14}ex_{14} + \dot{m}_{22}ex_{22} + \dot{Ex}_D \quad (4.92)$$

Deaerator

The mass flow rate balance equation for the deaerator can be written as:

$$\dot{m}_7 + \dot{m}_{22} + \dot{m}_{27} = \dot{m}_{23} \quad (4.93)$$

The energy balance equation for the deaerator can be written as:

$$\dot{m}_7 h_7 + \dot{m}_{22}h_{22} + \dot{m}_{27}h_{27} = \dot{m}_{23}h_{23} \quad (4.94)$$

The entropy balance equation for the deaerator can be written as:

$$\dot{m}_7 s_7 + \dot{m}_{22}s_{22} + \dot{m}_{27}s_{27} + \dot{S}_g = \dot{m}_{23}s_{23} \quad (4.95)$$

The exergy balance equation for the deaerator can be written as:

$$\dot{m}_7 ex_7 + \dot{m}_{22}ex_{22} + \dot{m}_{27}ex_{27} = \dot{m}_{23}ex_{23} + \dot{Ex}_D \quad (4.96)$$

Pump II

The mass flow rate balance equation for Pump II can be written as:

$$\dot{m}_{23} = \dot{m}_{28} \quad (4.97)$$

The energy balance equation for Pump II can be written as:

$$\dot{m}_{23}h_{23} + \dot{W}_{PII} = \dot{m}_{28}h_{28} \quad (4.98)$$

The entropy balance equation for Pump II can be written as:

$$\dot{m}_{23}s_{23} + \dot{S}_g = \dot{m}_{28}s_{28} \quad (4.99)$$

The exergy balance equation for Pump II can be written as:

$$\dot{m}_{23}ex_{23} + \dot{W}_{PII} = \dot{m}_{28}ex_{28} + \dot{Ex}_D \quad (4.100)$$

Feedwater Heater IV

The mass flow rate balance equation for Feedwater Heater IV can be written as:

$$\dot{m_5} + \dot{m_{25}} = \dot{m_{26}} \, , \dot{m_{28}} = \dot{m_{29}} \tag{4.101}$$

The energy balance equation for Feedwater Heater IV can be written as:

$$\dot{m_5} h_5 + \dot{m_{28}} h_{28} + \dot{m_{25}} h_{25} = \dot{m_{26}} h_{26} + \dot{m_{29}} h_{29} \tag{4.102}$$

The entropy balance equation for Feedwater Heater IV can be written as:

$$\dot{m_5} s_5 + \dot{m_{28}} s_{28} + \dot{m_{25}} s_{25} + \dot{S_g} = \dot{m_{26}} s_{26} + \dot{m_{29}} s_{29} \tag{4.103}$$

The exergy balance equation for Feedwater Heater IV can be written as:

$$\dot{m_5} ex_5 + \dot{m_{28}} ex_{28} + \dot{m_{25}} ex_{25} = \dot{m_{26}} ex_{26} + \dot{m_{29}} ex_{29} + \dot{Ex_D} \tag{4.104}$$

Feedwater heater V

The mass flow rate balance equation for Feedwater Heater V can be written as:

$$\dot{m_2} = \dot{m_{24}} \, , \dot{m_{29}} = \dot{m_{30}} \tag{4.105}$$

The energy balance equation for Feedwater Heater V can be written as:

$$\dot{m_2} h_2 + \dot{m_{29}} h_{29} = \dot{m_{24}} h_{24} + \dot{m_{30}} h_{30} \tag{4.106}$$

The entropy balance equation for Feedwater Heater V can be written as:

$$\dot{m_2} s_2 + \dot{m_{29}} s_{29} + \dot{S_g} = \dot{m_{24}} s_{24} + \dot{m_{30}} s_{30} \tag{4.107}$$

The exergy balance equation for Feedwater Heater V can be written as:

$$\dot{m_2} ex_2 + \dot{m_{29}} ex_{29} = \dot{m_{24}} ex_{24} + \dot{m_{30}} ex_{30} + \dot{Ex_D} \tag{4.108}$$

Heat Recovery Steam Generator

The energy balance equation for the heat recovery steam generator can be written as:

$$\dot{m_{30}} = \dot{m}_1 \, , \dot{m}_4 = \dot{m}_6, \dot{m}_{oil,in} = \dot{m}_{oil,out} \quad (4.109)$$

The energy balance equation for the heat recovery steam generator can be written as:

$$\dot{m}_{oil,in} h_{oil,in} + \dot{m_{30}} h_{30} + \dot{m}_4 h_4 = \dot{m_{oil,out}} h_{oil,out} + \dot{m}_1 h_1 + \dot{m}_6 h_6 \quad (4.110)$$

The entropy balance equation for the heat recovery steam generator can be written as:

$$\dot{m}_{oil,in} s_{oil,in} + \dot{m_{30}} s_{30} + \dot{m}_4 s_4 + \dot{S}_g = \dot{m_{oil,out}} s_{oil,out} + \dot{m}_1 s_1 + \dot{m}_6 s_6 \quad (4.111)$$

The exergy balance equation for the heat recovery steam generator can be written as:

$$\dot{m}_{oil,in} ex_{oil,in} + \dot{m_{30}} ex_{30} + \dot{m}_4 ex_4 = \dot{m_{oil,out}} ex_{oil,out} + \dot{m}_1 ex_1 + \dot{m}_6 ex_6 + \dot{E x}_D \quad (4.112)$$

4.4.3 System 3 Analysis: Indirect Steam Generation in PTC Power Plant Hybridized with a Biomass Boiler

System 3 shown in Figure 3.8 is very similar in principle to System 2 in Figure 3.7. The main difference between the two system is the biomass boiler added to System 3. In System 3, the feedwater will be split between the biomass boiler and the solar field instead of just flowing through the solar field as for System 2. The balance equations for the biomass boiler are listed below.

Biomass Boiler

The mass flow rate balance equation for the biomass boiler can be written as:

$$\dot{m}_{31} = \dot{m}_{33}; \; \dot{m}_{35} = \dot{m}_{37} \quad (4.113)$$

The energy balance equation for the biomass boiler can be written as:

$$\dot{m}_{31}h_{31} + \dot{m}_{35}h_{35} + \dot{Q}_{Biomass} = \dot{m}_{33}h_{33} + \dot{m}_{37}h_{37} \quad (4.114)$$

where $\dot{Q}_{Biomass}$ is the energy supplied by the biomass boiler to the water

The entropy balance equation for the biomass boiler can be written as:

$$\dot{m}_{31}s_{31} + \dot{m}_{35}s_{35} + \frac{\dot{Q}_{Biomass}}{T_a} + \dot{S}_g = \dot{m}_{33}s_{33} + \dot{m}_{37}s_{37} \quad (4.115)$$

The exergy balance equation for the biomass boiler can be written as:

$$\dot{m}_{31}ex_{31} + \dot{m}_{35}ex_{35} + \dot{E}x_Q = \dot{m}_{33}ex_{33} + \dot{m}_{37}ex_{37} + \dot{E}x_D \quad (4.116)$$

4.4.4 System 4 Analysis: Direct Steam Generation in PTC Power Plant Hybridized with a Biomass Boiler

The components of System 4 shown in Figure 3.9 are all the same as of system's 3 with one major difference which is the solar field. In the DSG field of System 4, there is no heat exchanger as for Systems 2 and 3. The solar field balance equations for System 4 are listed below.

Solar Field

The mass flow rate balance equations for the solar field can be written as:

$$\dot{m}_{32} = \dot{m}_{34};\ \dot{m}_{36} = \dot{m}_{38} \quad (4.117)$$

The energy balance equation for the solar field can be written as:

$$\dot{m}_{32}h_{32} + \dot{m}_{36}h_{36} + \dot{Q}_{Solar} = \dot{m}_{34}h_{34} + \dot{m}_{38}h_{38} \quad (4.118)$$

where $\dot{Q}_{Solar}$ is the energy supplied by the solar field to the water

The entropy balance equation for the solar field can be written as:

$$\dot{m}_{32}s_{32} + \dot{m}_{36}s_{36} + \frac{\dot{Q}_{Solar}}{T_a} + \dot{S}_g = \dot{m}_{34}s_{34} + \dot{m}_{38}s_{38} \quad (4.119)$$

The exergy balance equation for the biomass boiler can be written as:

$$\dot{m}_{32}ex_{32} + \dot{m}_{36}ex_{36} + \dot{E}x_Q = \dot{m}_{34}ex_{34} + \dot{m}_{38}ex_{38} + \dot{E}x_D \quad (4.120)$$

4.5 Method of Analysis

All cycles were modeled using Engineering Equation Solver (EES), where all states were identified and simulated. Engineering Equation Solver is widely used in thermodynamic analyses, as it includes physical properties and thermodynamic relations of various working fluids under a wide range of operating conditions. The analyses neglected changes in potential and kinetic energies, and pressure losses in heat exchangers and pipes, as those changes are minimal compared to thermal changes in the system [101, 102]. In addition, it is assumed that the turbines and pumps are adiabatic. Biomass fuels are combusted with 50% excess air. The air enters the combustion chamber at 20 °C and 1 atm. The results shown below are for a biomass fuel with a LHV of 17.8 MJ/kg.

Chapter 5: Results and Discussion

In this chapter, the results of all subsystems are presented and validated. In the first section, the results of the analyses conducted on the various biomass fuels shown in Table 3.1 and in Appendix A are reported. The second section presents the validation of the thermal losses of the absorber tube. Sections 5.3-5.6 present the results of the energy and exergy analyses of the proposed cycles separately.

5.1 Biomass Subsystem

Biomass fuels presented in Table 3.1 and Appendix A were analyzed to understand the behavior of the biomass subsystem further. Elemental analysis is carried out to observe the average elemental content in the various biomass fuels studied. Figure 5.1 shows the average elemental content of the various biomass fuels. Generally, on a dry mass basis, 50% of biomass weight is carbon. The next major content in biomass is oxygen with about 40%. The remaining 10% is distributed between nitrogen, hydrogen, and Sulphur. In the proposed work, biomass fuels are directly combusted with 50% excess air and the combustion gasses produced are used to heat up the working fluid the power block. It is assumed that the moisture content of the fuels is 5.5% as recommended by [98].

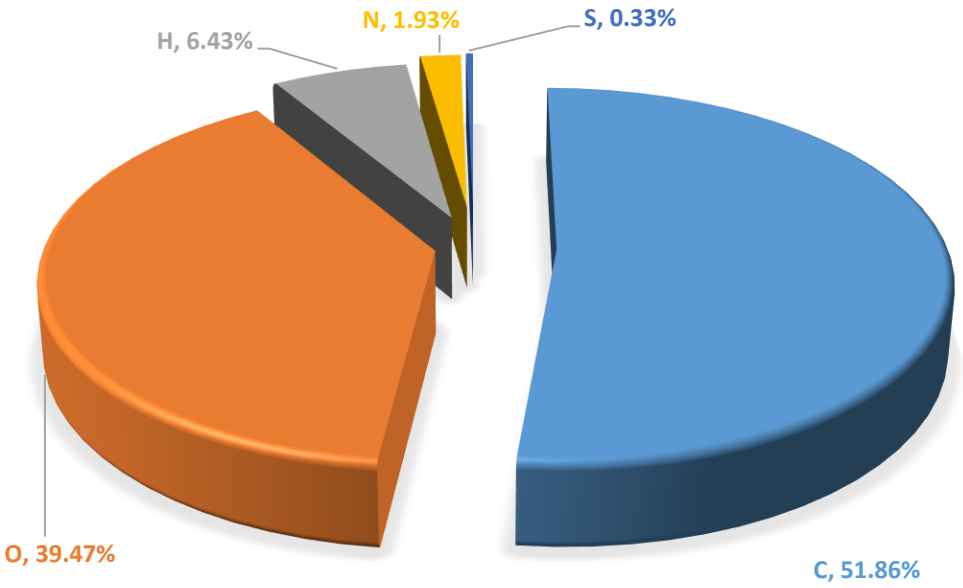

Figure 5.1: Average elemental content of analyzed biomass fuels

5.1.1 Heating Value Calculations and Validation

Based on the heating value formulation provided in Section 4.2.2., the heating values of various biomass fuels were calculated using their ultimate elemental content. In order to validate the heating values calculated, experimental data was collected, analyzed and compared to the model presented earlier. Table 5.1 shows some of the experimental data of multiple biomass fuels and their heating values [103]. In a previous study available in the literature, those experimental values were used to develop another mathematical model to approximate the heating value based on the ultimate composition content of any fuel. To facilitate comparison and validation accuracy, the same fuels used for the experiments were also used to calculate the HHV using the model presented in the present work and the model available in the literature. Table 5.2 shows the different heating values of the biomass fuels, where the model presented in this work and the model developed in

the literature were compared to the experimental results. Generally, both formulas have shown an acceptable agreement with the experimental results, with a percent difference of below 9% for all biomass fuels except waste fuel. This relatively high error can be justified by the low carbon content in waste fuel as heating value mathematical models consider the carbon content average in biomass fuels and waste fuel is below this average. Figure 5.2 shows the three sets of data, where the error bars are shown for the two mathematical models with respect to the experimental data to show the agreement between all the results. The three models are in very good agreement and the model presented in this work in Section 4.2.2 is used as it is simple and accurate enough for this study.

Table 5.1: Experimental data of biomass fuels HHV and their elemental composition [103]

Biomass	Exp. HHV(kJ/kg)	C%	H%	N%	S%	Cl%	O%
Grass miscanthusa	19135	48.3	5.5	0.6	0.1	0.2	41.5
Energy grass,	18035	45.0	5.3	2.1	0.2	0.5	37.6
Wood material	19578	49.0	5.7	0.4	0.1	0.1	41.9
Wood waste	18467	49.7	6.0	1.7	0.0	0.1	41.0
Cereals	18610	46.5	6.1	1.2	0.1	0.2	42.0
Millet	18165	45.9	5.3	0.9	0.1	0.3	41.1
Sunflower	20263	50.5	5.9	1.3	0.1	0.4	34.9
Hemp	18036	45.7	6.3	0.6	0.0	0.1	44.1
Waste	15974	42.6	5.7	3.4	0.4	0.1	32.2
Plant material	19790	49.4	5.9	0.8	0.1	0.2	38.8

After validating the model presented in this work, HHV and LHV are calculated for all the fuels considered earlier. The results of HHV and LHV calculations for wood and woody biomass are presented in Table 5.3 and the rest of the calculated HHV and LHV for other fuels are available in Appendix B. The average HHV and LHV for the fuels analyzed are 21.4 MJ/kg and 18.7 MJ respectively.

Table 5.2: HHV comparison between experimental and analytical results

Biomass	Exp. HHV (kJ/kg)	HHV Analytical (kJ/kg)	% Error	Present HHV (kJ/kg)	% Error
Grass miscanthusa	19135	19091	0.230	18972	0.852
Energy grass,	18035	18016	0.105	17859	0.977
Wood material	19578	19397	0.924	19433	0.743
Wood waste	18467	19949	8.025	20123	8.969
Cereals	18610	18565	0.241	18988	2.029
Millet	18165	18185	0.108	17878	1.579
Sunflower	20263	20206	0.283	20818	2.737
Hemp	18036	18182	0.811	18741	3.907
Waste	15974	17326	8.464	17920	12.184
Plant material	19790	19673	0.591	20080	1.466

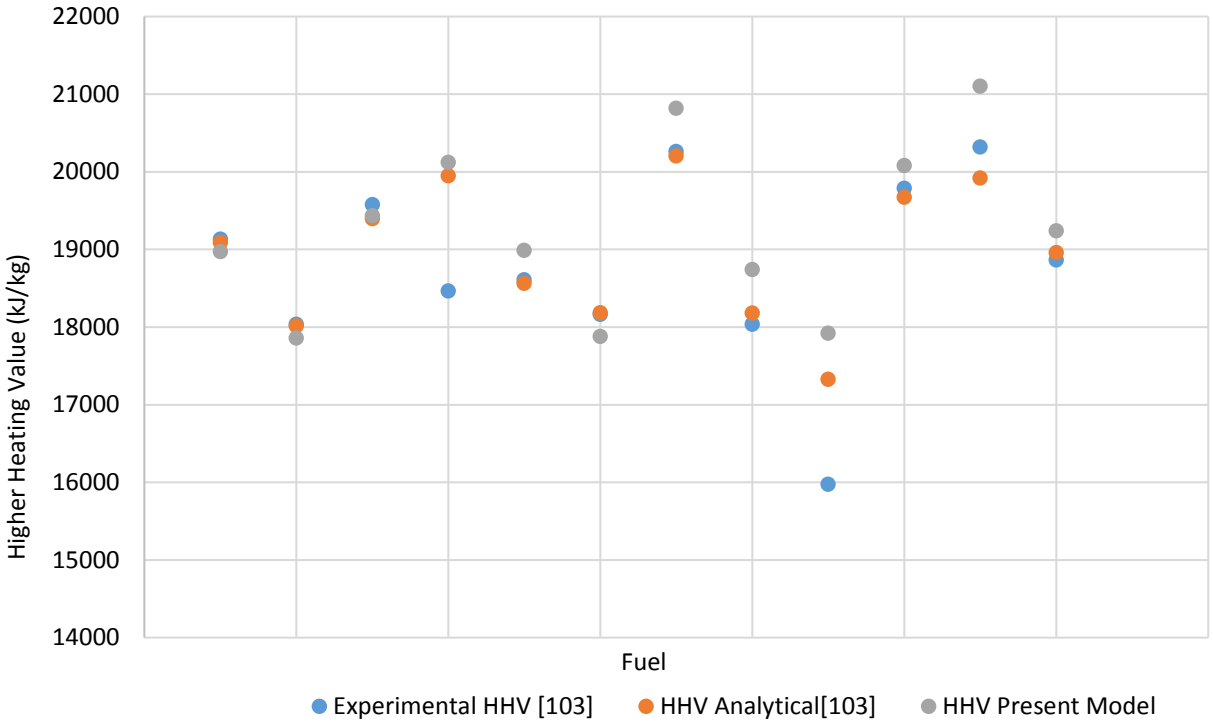

Figure 5.2: Heating value comparison between analytical and experimental results

To observe the effect of the moisture content on the HHV and LHV, the moisture content of one of the analyzed fuels (Olive wood) is varied from 0% to 30% and the results are plotted in Figure 5.3. It is clear that the moisture content does not affect the HHV as

the latent heat of vaporization of water is taken into account in the HHV. On the other hand, the LHV has an inversely proportional relationship with the moisture content as it assumes that part of the energy content released by the fuels during the combusting process is required to vaporize the water content at the given pressure and temperature.

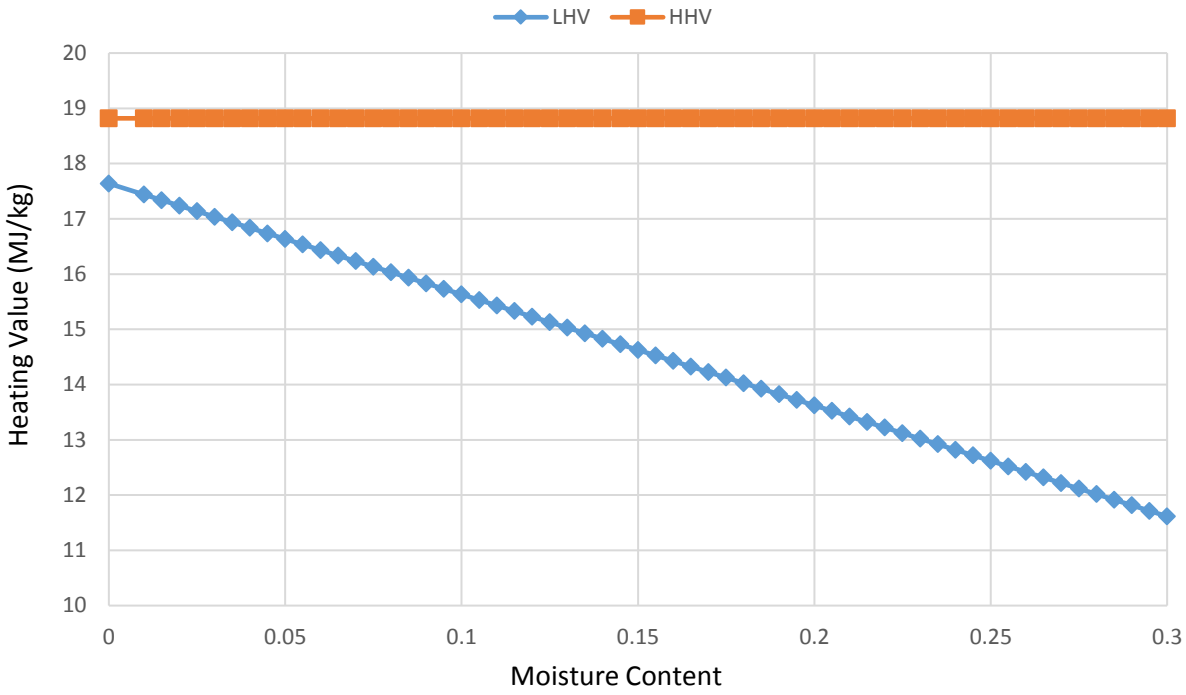

Figure 5.3: Higher and lower heating values of olive wood as a function of moisture content

Table 5.3: HHV and LHV of various biomass fuels analyzed

Fuel Type/Group	**Heating Value (MJ/kg)**	
Wood and woody biomass (WWB)	**HHV**	**LHV**
Alder-fir sawdust	21.60	19.02
Balsam bark	22.08	19.45
Beech bark	20.69	18.18
Birch bark	24.10	21.26
Christmas trees	22.01	19.45
Elm bark	20.21	17.77
Eucalyptus bark	19.03	16.68
Fir mill residue	20.62	18.11
Forest Residue	20.51	18.13
Hemlock bark	22.15	19.58
Land clearing wood	20.34	17.85
Maple bark	21.19	18.61
Oak sawdust	19.90	17.46
Oak wood	20.42	17.91
Olive wood	18.82	16.53
Pine bark	21.61	19.07
Pine chips	21.43	18.86
Pine pruning	21.26	18.66
Pine sawdust	20.44	17.94
Poplar	20.88	18.34
Poplar bark	22.55	19.79
sawdust	19.93	17.46
Spruce bark	21.89	19.27
Spruce wood	21.19	18.63
Tamarack bark	28.61	24.80
Willow	20.08	17.58
Wood	19.95	17.46
Wood residue	20.80	18.26
Mean	21.24	18.65
Minimum	20.05	17.70
Maximum	27.26	23.53

5.1.2 Combustion Gas Composition

Based on the combustion model presented in Section 4.2.1, a combustion gasses analysis is conducted for the biomass fuels shown in Table 3.1 and Appendix A, and the results are summarized in Table 5.4 and Appendix C. Figure 5.4 shows the average gas content in the combustion gasses produced from biomass fuels. The main gas present in the combustion gasses is N_2, owing to the fact that 76% of the atmospheric air that is added to the fuel during the combustion process is N_2. The second major content in the combustion gasses mixture is CO_2. The high percentage of CO_2 in the combustion gasses can be justified by the high carbon content in biomass fuels as discussed earlier and shown in Figure 5.1. Generally, CO_2 produced during biomass combustion is largely balanced by the CO_2 consumed during its growth. Nonetheless, the CO_2 produced when biomass fuels are combusted is noticeably less than the amount produced when conventional fuels are combusted. One of the main advantages of using biomass fuels over conventional fuels such as coal is its low sulfur content. The SO_2 produced during fuel combustion is a major contributor to many environmental issues such as acid rain and global warming. On average, biomass fuels contain about 0.33% Sulfur while some coal types contain up to 5% [104]. As illustrated in Figure 5.4, on average, only 0.04% of the combustion gasses produced during biomass combustion is SO_2.

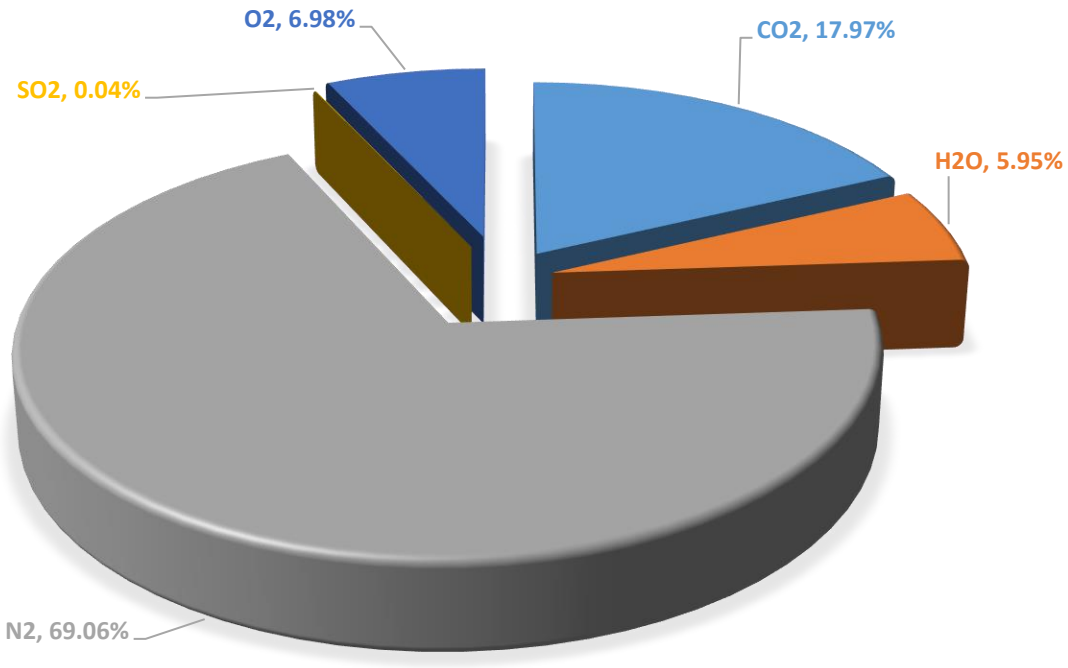

Figure 5.4: Average gasses content in biomass combustion gas mixture

Among all biomass fuels analyzed, animal biomass has shown the highest heating value along with the highest CO_2 in the combustion gasses. The high heating value would be attributed to the high carbon content in the raw fuels and the combustion gasses. This observation, to an extent, justifies the high heating value of coal and other conventional fuels as they generally have higher carbon content. Figure 5.5 shows the content of combustion gasses of various fuels analyzed. Generally, the lowest CO_2 emission rate has been seen for herbaceous and agricultural biomass (HAB), particularly the grass group has the lowest CO_2 rate with a value of around 1.7 kg CO_2/kg fuel.

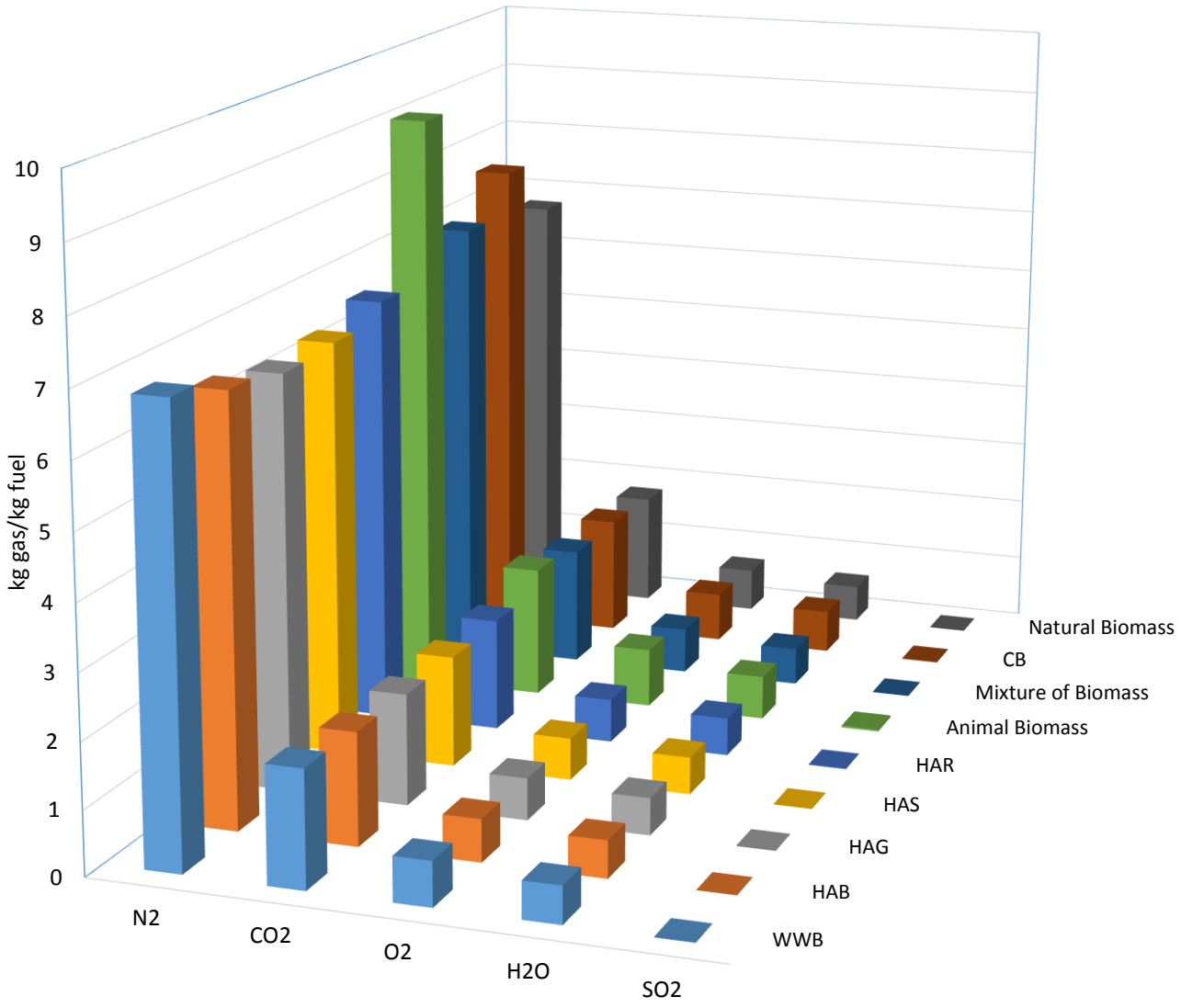

Figure 5.5: Gas content of combustion gasses mixture for various biomass fuels

Table 5.4: Gas content in combustion gas mixture for wood and woody biomass fuels

Fuel group	**Gas content in combustion gas mixture (kg gas/kg fuel)**				
Wood and woody biomass (WWB)	**CO_2**	**H_2O**	**SO_2**	**N_2**	**O_2**
Alder-fir sawdust	1.8421	0.5701	0.0008	7.0064	0.7087
Balsam bark	1.8698	0.5786	0.0019	7.1756	0.7261
Beech bark	1.7798	0.5617	0.0021	6.6759	0.6750
Birch bark	1.9737	0.6208	0.0019	7.9142	0.8005
Christmas trees	1.8871	0.5533	0.0079	7.1817	0.7264
Elm bark	1.7624	0.5448	0.0021	6.5070	0.6579
Eucalyptus bark	1.6863	0.5364	0.0009	6.0590	0.6130
Fir mill residue	1.7798	0.5617	0.0006	6.6339	0.6713
Forest Residue	1.8248	0.5110	0.0019	6.6475	0.6722
Hemlock bark	1.9044	0.5533	0.0019	7.2215	0.7307
Land clearing wood	1.7555	0.5617	0.0013	6.5375	0.6613
Maple bark	1.8005	0.5786	0.0021	6.8452	0.6924
Oak sawdust	1.7347	0.5533	0.0002	6.3688	0.6445
Oak wood	1.7521	0.5701	0.0019	6.5579	0.6635
Olive wood	1.6967	0.5110	0.0006	6.0067	0.6073
Pine bark	1.8629	0.5533	0.0013	7.0204	0.7103
Pine chips	1.8282	0.5701	0.0017	6.9450	0.7024
Pine pruning	1.7971	0.5870	0.0002	6.8661	0.6945
Pine sawdust	1.7659	0.5617	0.0002	6.5645	0.6643
Poplar	1.7867	0.5701	0.0004	6.7374	0.6813
Poplar bark	1.8559	0.6208	0.0019	7.3214	0.7407
sawdust	1.7244	0.5617	0.0004	6.3822	0.6455
Spruce bark	1.8559	0.5786	0.0019	7.1015	0.7187
Spruce wood	1.8109	0.5701	0.0019	6.8487	0.6929
Tamarack bark	1.9737	0.9164	0.0021	9.3860	0.9493
Willow	1.7244	0.5701	0.0011	6.4360	0.6508
Wood	1.7174	0.5701	0.0011	6.3738	0.6450
Wood residue	1.7798	0.5701	0.0015	6.7050	0.6782
Mean	1.8040	0.5786	0.0015	6.8609	0.6940
Minimum	1.6863	0.5110	0.0002	6.5650	0.6644
Maximum	1.9737	0.9164	0.0079	8.7796	0.8879

5.2 Solar Collector

Thermal losses were calculated for the PTR70 absorber using the specifications collected and the formulas in Section 4.1.2 and at an ambient temperature of 293 K. The results were validated using experimental results obtained from National Renewable Energy Laboratory (NREL) for the same absorber under various temperature ranges [105]. Table 5.5 shows the losses calculated at different absorber temperatures. Figure 5.6 shows the results of the NREL experiments and the current study model. It is clearly observed from the graph that the calculations are mostly within an acceptable margin of error with respect to the experimental results. In spite of the simplicity of the model used, the results have shown an agreement with the experiments conducted on the same absorber tube. In the calculations conducted, the emissivity of the absorber is taken as a constant, which is not the case in real life. At high temperatures, the emissivity of metals tends to increase, which would increase the radiative heat transfer, hence the diversion between the experimental data and the calculations after 450°C temperature difference between the absorber surface and ambient temperature. Although there is a deviation between the presented calculations and the experimental data, the model is still acceptable for this system as PTCs work in a temperature range around 400°C where the two models are in good agreement.

Table 5.5: Total thermal losses for PTR70 absorber

Temperature (K)	Total heat loss (W/m)	Temperature (K)	Total heat loss (W/m)
370.0	15.3	616.0	164.4
423.0	31.1	659.0	217.5
483.0	57.8	686.0	256.6
515.0	76.7	723.0	318.2
586.0	133.3	727.0	325.5

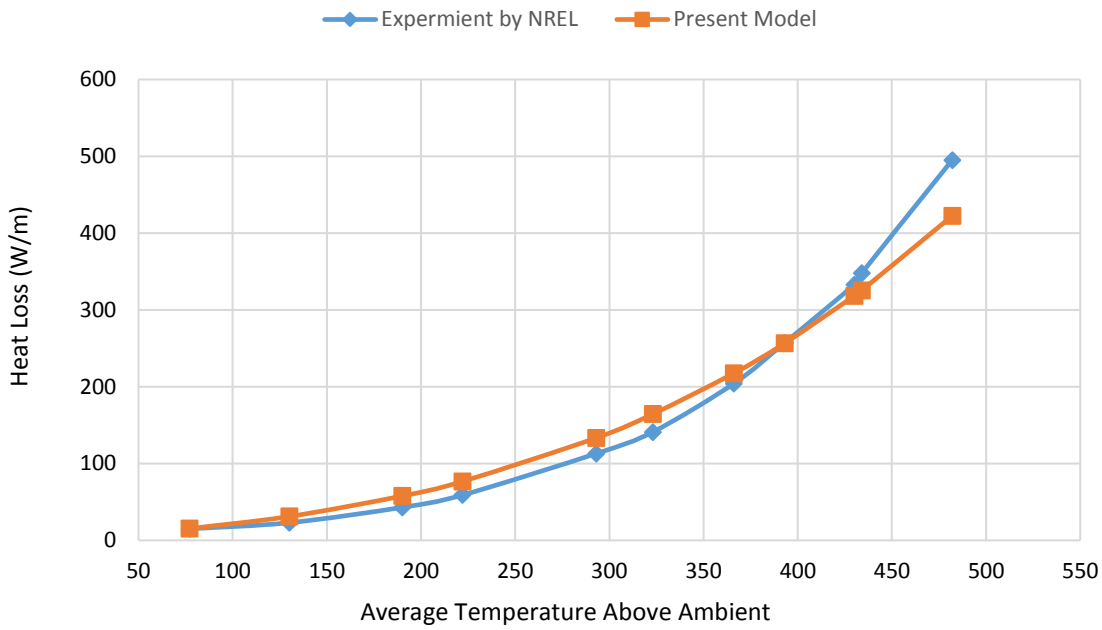

Figure 5.6: Thermal losses for the PTR70 absorber at different temperatures in comparison with experimental data

5.3 System 1 Results: Basic Arrangement of Indirect Steam Generation in PTC Hybridized with a Biomass Boiler

This section presents the results for System 1 shown in Figure 3.6. The steam is supplied to the turbine at 370 °C and 100 bar. Two-thirds of the steam is supplied by the biomass subsystem, and the remaining third is supplied by the solar field. The fuel considered for the analysis has a LHV of 17.8 MJ/kg and enters the combustion chamber at 20°C and is combusted with 50% excess air. The flue gas of the combustion process has a temperature of about 1600°C. The energy content of the flue gas is calculated based on the composition of the gas at the specified temperature. The flue gas in the boiler is used to heat the working fluid of the cycle before entering the turbine. The steam turbine work output has been set to 50 MW to ensure reasonable comparison with benchmark projects like Andasol, the mass flow rate of the steam was then calculated based on the turbine

boundary conditions. Table 5.6 shows the temperature, energy content, pressure, and entropy at each state. The steam leaving the solar field heat exchanger has the same characteristics as the steam passing through the biomass subsystem, and the two streams are mixed prior to entering the turbine. The overall energy efficiency of the system is found to have a peak value 30.7% and an average of 27.0%. Those efficiencies are slightly higher than the overall efficiency of the Andasol thermal plant which has 28% overall peak efficiency. Moreover, the performance of this system has not been optimized, as a simple Rankine cycle is utilized to demonstrate the work, however, multistage expansion turbines and multiple feedwater heaters would definitely enhance the performance of the system. The net solar collector aperture area required for this project for an average solar irradiance value of 800 W/m^2 would be around 93,900 m^2, which imposes a significant area and initial cost savings when compared to 510,000 m^2 collector area required by Andasol. The reduction in the total initial investment cost and total area needed will lead to a lower levelized cost of electricity as both the operating and total investment costs are reduced. The results of this system demonstrate the potential of combining solar and biomass in one system to avoid using TES while maintaining a sustainable power supply.

Table 5.6: System 1 state points

State	Flow Rate [kg/s]	Temperature [°C]	Pressure [bar]	Enthalpy [kJ/kg]	Entropy [kJ/kgK]
1	62.1	81.3	0.5	340.5	1.1
2	62.1	82.2	100.0	351.9	1.1
3	20.7	269.8	100.0	1182.0	3.0
4	20.7	370.0	100.0	2997.0	6.1
5	62.1	370.0	100.0	2997.0	6.1
6	62.1	81.3	0.5	2192.0	6.3
7	57.0	753.4	1.0	1282.0	8.7
8	41.4	269.8	100.0	1182.0	3.0
9	41.4	370.0	100.0	2997.0	6.1

5.4 System 2 Results: Indirect Steam Generation in PTC Power Plant

Energy and exergy analyses are conducted for System 2 shown in Figure 3.7. The performance of the system considered is evaluated at 70% efficiency value of the solar field, which is the efficiency reported by Andasol power plants. The characteristics of the flow at each state are summarized in Table 5.7. and the main results of the cycle are summarized in Table 5.8. As the energy input for this cycle is fixed from the solar field, the efficiency of the overall system is constant. The steam mass flow rates supplied to the turbine and the feedwater heaters were calculated based on a net power output of 50 MWe and the design parameters of the cycle are shown in Table 3.2. The efficiency of the power block is 39.3 % which is in good agreement with the 40 % efficiency reported for the power block of the Andasol plants [43]. This system has a fixed value energy efficiency of 27.5 %, as the system was running solely on solar energy. Energy losses in the indirect steam generation power plant are mainly found in the steam generator where the heat is transferred from the HTF of the solar field to the working fluid of the power block. Losses are also found in the pipes, pumps, and turbines. To identify the locations where most irreversible losses occur, exergy destruction values were calculated for each component. The exergy destruction values for the main components of System 2 are shown in Figure 5.7. As seen in Figure 5.7, it is clear that the solar field has the highest exergy destruction rate, presenting about 92% of the total destruction rate in the system. The high exergy destruction value found in the solar field is mainly justified by the process of converting high-quality solar irradiance to a relatively lower quality temperature of the working fluid. The overall exergy efficiency of the cycle is found to be 29%.

Table 5.7: Input and calculated process data for PTC-only power plant

State	$\dot{m}_f \left(\frac{kg}{s}\right)$	Temperature (°C)	Pressure (bar)	Enthalpy (kJ/kg)	Exergy (kJ/kg)	Entropy (kJ/kgK)
0	-	30.0	1.00	125.8	-	0.44
1	52.57	370.0	100.00	2997.0	1167.0	6.06
2	2.76	233.9	30.00	2778.0	925.2	6.14
3	49.81	212.4	20.00	2712.0	851.7	6.16
4	46.66	212.4	20.00	2712.0	851.7	6.16
5	3.15	212.4	20.00	2712.0	851.7	6.16
6	46.66	370.0	20.00	3181.8	1059.0	7.03
7	4.94	284.0	10.00	3016.0	883.2	7.06
8	1.54	126.3	1.98	2720.0	555.5	7.16
9	1.26	100.0	1.01	2619.0	443.1	7.20
10	2.45	79.8	0.47	2514.0	324.0	7.25
11	36.45	41.5	0.08	2301.0	79.7	7.35
12	41.72	41.5	0.08	173.9	0.82	0.59
13	41.72	41.6	10.00	175.2	1.8	0.59
14	1.54	102.0	1.98	427.5	31.3	1.33
15	1.54	100.0	1.01	427.5	31.2	1.33
16	2.80	81.8	1.01	342.5	16.8	1.10
17	2.80	79.8	0.47	342.5	16.7	1.10
18	5.27	46.6	0.47	195.3	1.8	0.66
19	5.27	41.5	0.08	195.3	1.6	0.66
20	41.72	76.8	10.00	322.3	14.7	1.04
21	41.72	97.0	10.00	407.1	28.1	1.28
22	41.72	117.0	10.00	491.6	45.3	1.50
23	52.57	179.9	10.00	762.9	121.3	2.14
24	2.76	214.4	30.00	918.1	178.0	2.46
25	2.76	212.4	20.00	918.1	177.3	2.47
26	5.92	187.0	20.00	794.4	132.7	2.20
27	5.92	179.9	10.00	794.4	131.8	2.21
28	52.57	182.0	100.00	776.4	132.6	2.15
29	52.57	209.4	100.00	898.0	175.5	2.41
30	52.57	230.9	100.00	995.7	213.2	2.60

Table 5.8: System 2 main results

Parameter	Value
Gross work output (MW)	50.0
Steam mass flow rate (kg/s)	52.6
HPT work output (MW)	14.8
LPT work output (MW)	35.9
Power block efficiency (%)	39.3
Cycle energy efficiency (%)	27.5
Cycle exergy efficiency (%)	29.0

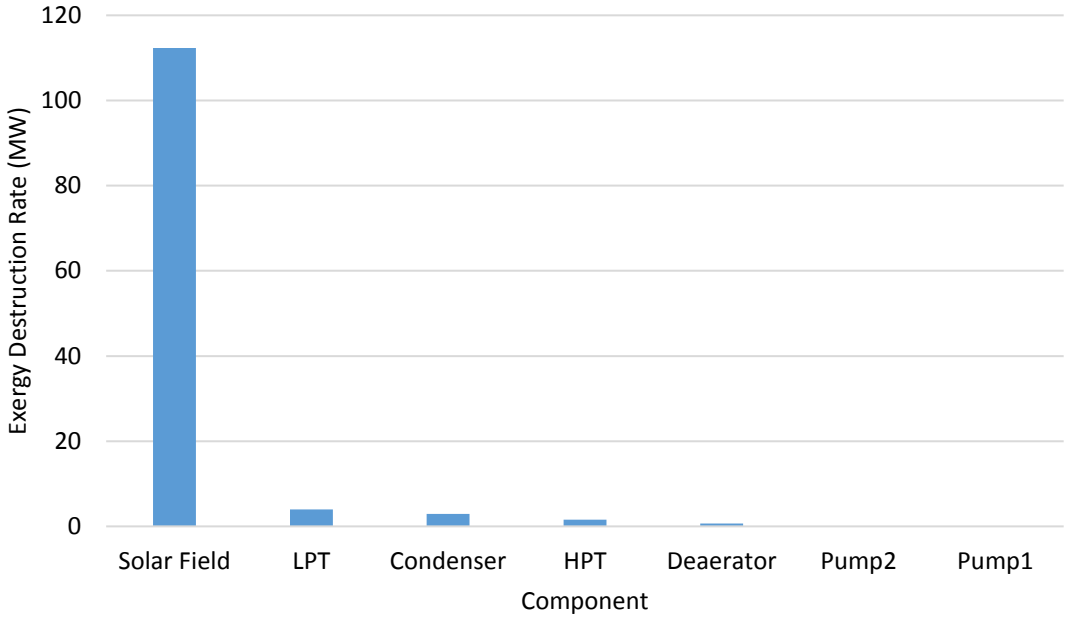

Figure 5.7: System 2 exergy destruction rates in the main components

5.5 System 3 Results: Indirect Steam Generation in PTC Power Plant Hybridized with a Biomass Boiler

As mentioned earlier, the power blocks for Systems 2-4 are identical. The only difference between the systems is the energy input. As System 2 is solely running on solar energy, Systems 3 and 4 are supplied by the solar field and the biomass boiler concurrently. Energy and exergy analyses are conducted while varying the share of each energy input in order to consider various cases during the operation of those plants. The different modes are; solar only, solar and biomass while varying the share, and biomass only. The characteristics of the working fluid at each state in System 3 is the same as those of System 2 shown in Table 5.7, as the additional component in this system is the biomass boiler which supplies a stream with the same characteristics of the stream supplied by the solar field HRSG. Although the quality of biomass is not as high as that of fossil fuels, biomass

still represents a high-quality solution to boost the performance of solar-based power plants. The integration of biomass with the PTC solar field which is illustrated in Figures 3.8 and 3.9, improves the gross efficiency of the overall system. The analysis results showed a positive correlation between the share of the biomass and overall energy and efficiencies. Table 5.9 shows the main results of System 3 with a biomass share of 50% of the total energy input. Compared to the solar-only arrangement illustrated in System 2, the overall energy efficiency has increased to 30.2% which imposes practical performance enhancements. While increasing the share of biomass fuel, the energy efficiency of the system reaches a maximum value 33.2% at a biomass share of 100%. Figure 5.8 shows the energy and exergy efficiency of System 2 as a function of the biomass share.

Table5.9: System 3 main results

Parameter	Value
Gross work output (MW)	50.0
Steam mass flow rate (kg/s)	52.6
HPT work output (MW)	14.8
LPT work output (MW)	35.9
Power block efficiency (%)	39.3
Cycle energy efficiency (%)	30.2
Cycle exergy efficiency (%)	33.5

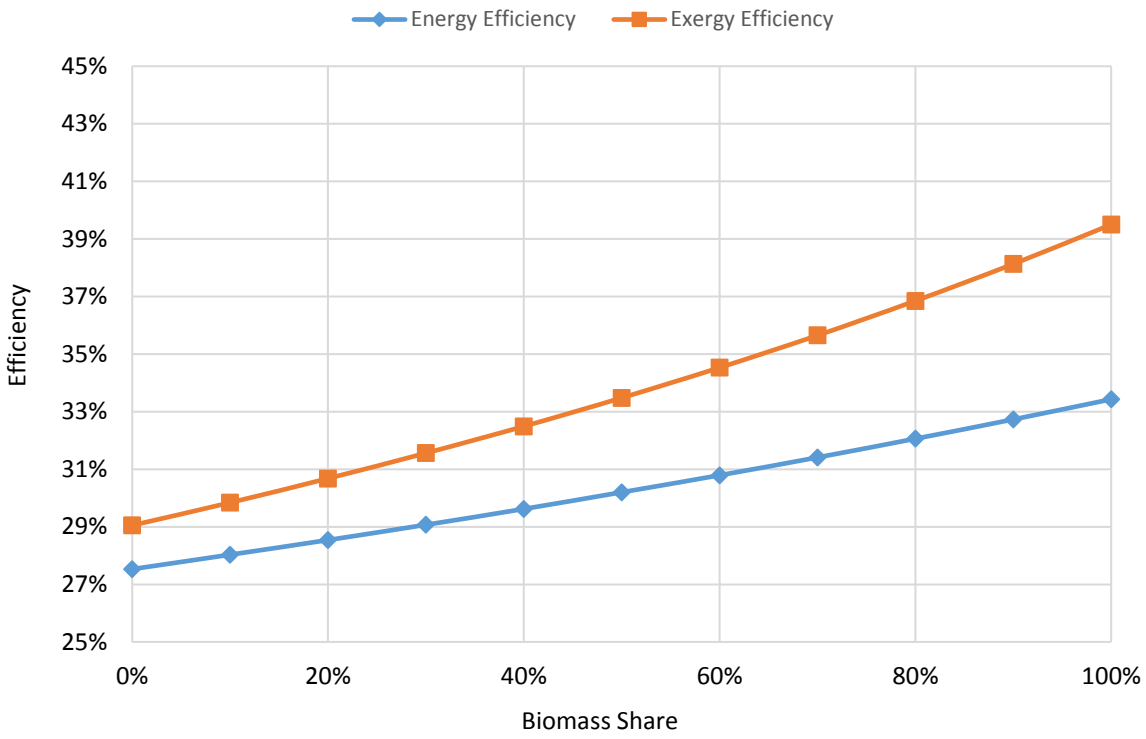

Figure 5.8: System 3 energy and exergy efficiencies as a function of the biomass share

As seen in Figure 5.8, the exergy efficiency increases as the biomass share is increased as well, reaching a maximum value of 39.5%. The increase in the efficiency compared to the PTC-only power plant is not the only advantage of integrating biomass with the main system. The other advantage is the higher reliability of the integrated system. When biomass fuels are available, the system can constantly produce power without a TES, which further reduces the cost and the technical complexity of the system.

The exergy destruction rates for all components of System 3 are calculated at a biomass share of 50%, and the main values are shown in Figure 5.9. Similar to System 2, the solar field has the highest exergy destruction followed by the biomass boiler. The reason that most of the exergy destruction occurring in the solar field and the biomass boiler is that these two subsystems are responsible for transferring the high exergy content of the solar irradiance and the biomass fuels to a lower exergy content in the steam

supplied. Although both subsystems deliver identical shares of the exergy input to the system, the exergy destruction rate is higher in the solar field as the temperature of the exergy source, being the sun, is higher than the temperature produced when biomass fuels are combusted. The exergy destruction rates for Systems 2 and 3 are compared in Figure 5.10 and Table 5.10. Figure 5.10 shows the exergy destruction rates for each component in oil PTC cycles. The *y*-axis is shown on a logarithmic scale to clearly show all destruction values, as some of the destruction values were very minimal since it was assumed that there are no heat losses from those components. Only the exergy destruction values of the indirect steam generation plants are compared in Table 5.10, as they operated at the same temperature levels.

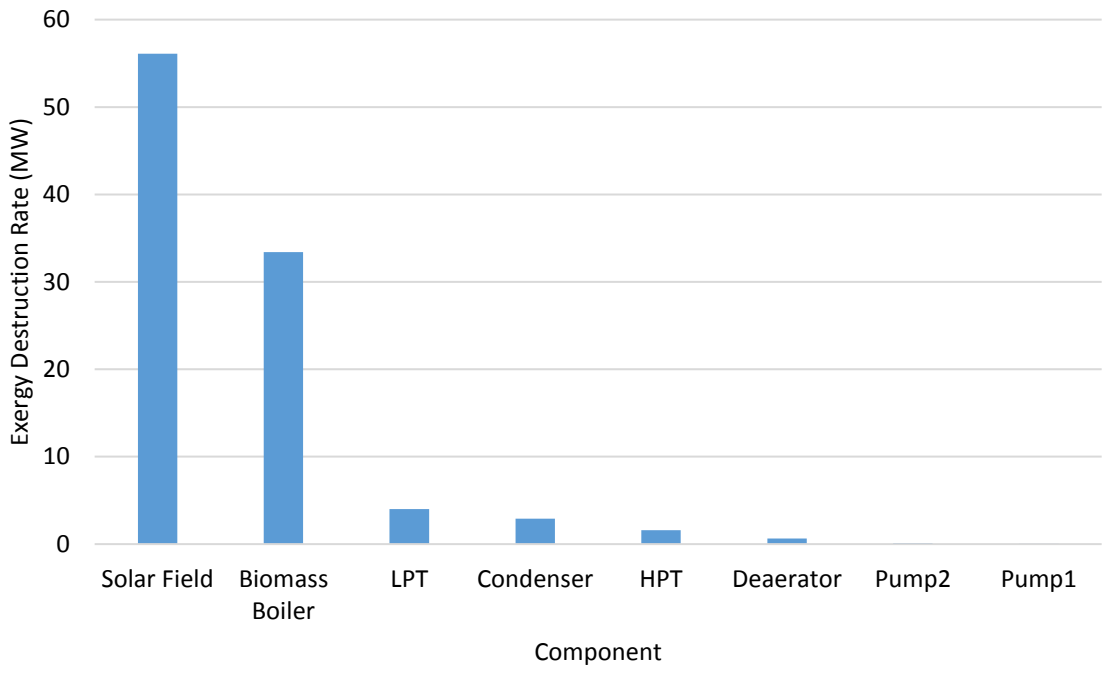

Figure 5.9: System 3 exergy destruction rates in the main components

Table 5.10: Exergy destruction results for oil PTC and oil PTC-biomass

Component	Oil PTC		Oil PTC Biomass	
	$\dot{E}x_D$ (KW)	$\dot{X}_D(\%)$	$\dot{E}x_D$ (KW)	$\dot{X}_D(\%)$
SF	112268	91.997	56134.0	56.511
BB	0	0	33387.0	33.611
HPT	1566	1.283	1566.0	1.577
LPT	3927	3.218	3972.0	3.999
CP	13.4	0.011	13.4	0.013
BP	119.4	0.098	119.4	0.120
WH 1	300	0.246	300.0	0.302
WH 2	1.69	0.001	1.7	0.002
WH 3	91.54	0.075	91.5	0.092
WH 4	131.6	0.108	131.6	0.132
WH 5	82.73	0.068	82.7	0.083
DEA	652.8	0.535	652.8	0.657
COND	2880	2.360	2880.0	2.899
Overall	122034.16	100	99332.1	100.0

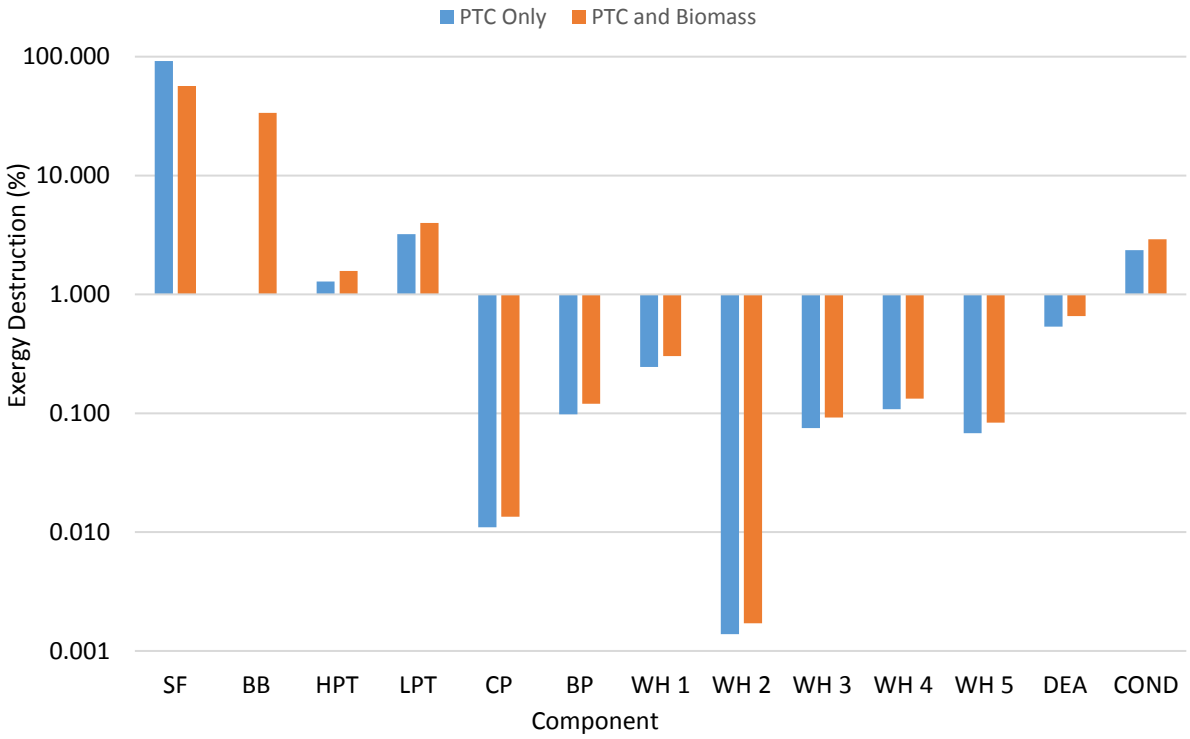

Figure 5.10: Exergy destruction (XD%) in each component

5.6 System 4 Results: Direct Steam Generation in PTC Power Plant Hybridized with a Biomass Boiler

Increasing the efficiency of PTC-only power plants is challenging due to the limited HTF temperature allowable. Generally, synthetic oils used in solar fields are thermally unstable beyond 400 °C [106], which limits the temperature of the power block working fluid to lower the values further due to losses during the transfer process. This challenge limits the efficiency of the power block, as the quality of the steam entering the system is limited. The use of DSG in PTC presents a feasible solution to this issue. By avoiding the use of synthetic oils, high-temperature levels can be achieved in the collectors. The system shown in Figure 3.9 has the integration of a DSG field with a biomass-fueled boiler. The major difference between this system and Systems 2 and 3 shown in Figures 3.7 and 3.8 is that the steam temperature at the turbine inlet is 500 °C compared to only 370 °C. Similar to the work done for System 3, the biomass share is varied from 0% to 100% to account for different operating conditions. The results of the DSG system combined with a biomass boiler are shown in Table 5.11 for a biomass share of 50 % at a 0% biomass share, the increase in the steam temperature at the turbine inlet increased the energy efficiency of the overall cycle to 30.3%.

Table 5.11: System 4 main results

Parameter	Value
Gross work output (MW)	50.0
Steam mass flow rate (kg/s)	46.2
HPT work output (MW)	18.7
LPT work output (MW)	31.9
Power block efficiency (%)	39.3
Cycle energy efficiency (%)	33.2
Cycle exergy efficiency (%)	36.8

The relationship between the biomass share and the energy and exergy efficiencies of the DSG system is demonstrated in Figure 5.11. The DSG-based plant has a minimum energy efficiency of 30.3%. The minimum exergy efficiency of the DSG system is 32% at a biomass share of 0%. When the biomass share reaches a maximum value of 100%, energy and exergy efficiencies of the system reach up to 37% and 43% respectively. The reason that System 4 efficiencies are noticeably higher than Systems 2 and 3 even at a 100% biomass share is due to the higher allowable temperature in the power block reaching up to 500 °C. The exergy destruction rates for System 4 are calculated and presented in Figure 5.12 at a biomass share of 50% as well, and the results are presented in Figure 5.11. Compared to Systems 2 and 3 which run on indirect steam generation, the destruction rates for System 4 are noticeably lower. In System 4 the solar field has a destruction rate of 49 MW compared to 56 MW for System 3, while the biomass boiler of System 4 has a destruction rate of 28.4 MW compared to 33.4 for System 3. System 4 has shown considerable exergy destruction reduction with a total of 86MW compared to 99MW for System 3. This reduction is due to the fact that the quality of the working fluid in the power block is considerably higher for the DSG field than it is in the oil field, leading to lower destruction values. A previous study evaluated the exergy destruction for a DSG field at a temperature of 400 °C [95]. The solar field exergy destruction share for the former study is 86%. Compared to the results of the present study, where the steam temperature considered is 500 °C, the losses are comparable with exergy destruction of around 92%.

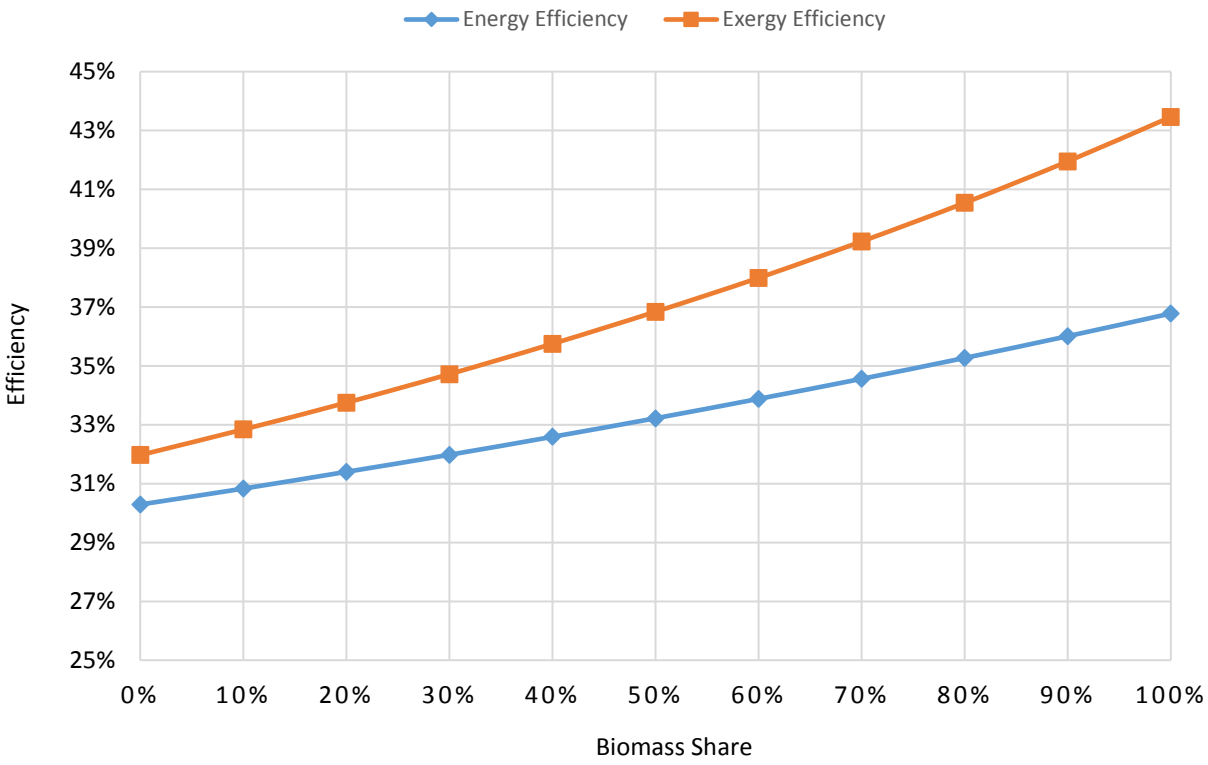

Figure 5.11: System 4 energy and exergy efficiencies as a function of the biomass share

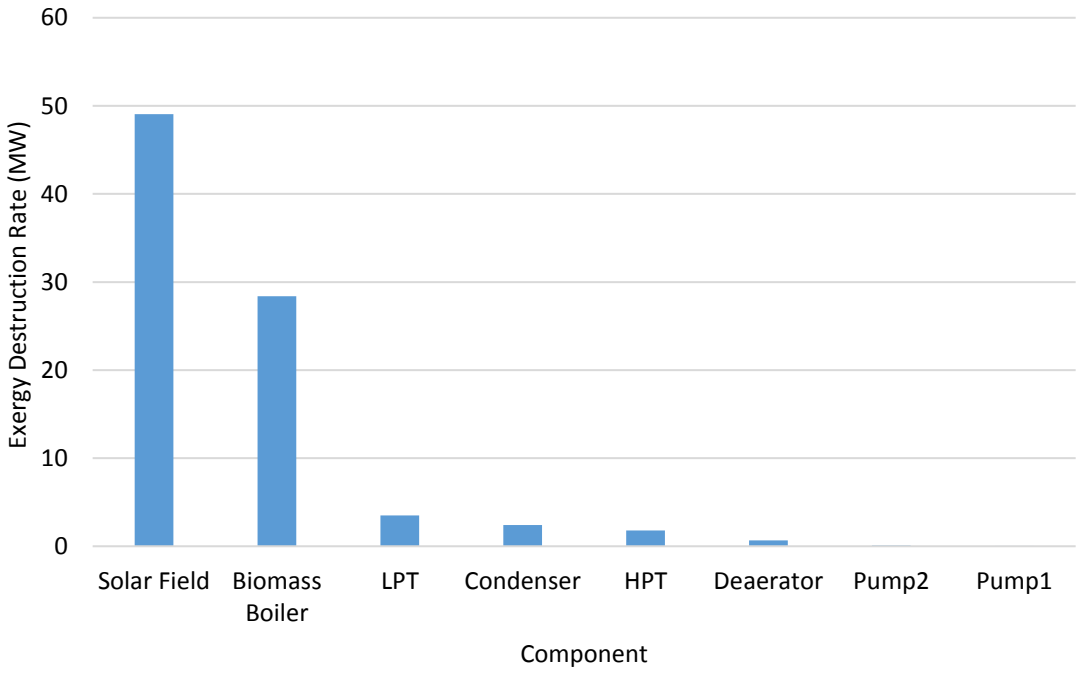

Figure 5.12: System 4 exergy destruction rates in the main component

To facilitate a reasonable comparison between Systems 2-4, which is one of the main objectives of the present work, the energy and exergy efficiencies for Systems 2-3 are plotted in Figure 5.13 as a function of the biomass share. System 2 has constant efficiencies as it is a standalone solar system and it does not have a biomass boiler. System 4 which is supplied by the DSG field and the biomass boiler has shown the highest efficiency both energetically and exergetically due to the fact that it is running at higher temperature levels. System 3, which runs on an indirect steam generation and a biomass boiler have lower efficiencies than the DSG plant, but it still performs better than the PTC-only system which had the lowest efficiencies. Figure 5.14 shows the energy and exergy efficiencies of all the mentioned systems at a biomass share of 50%.

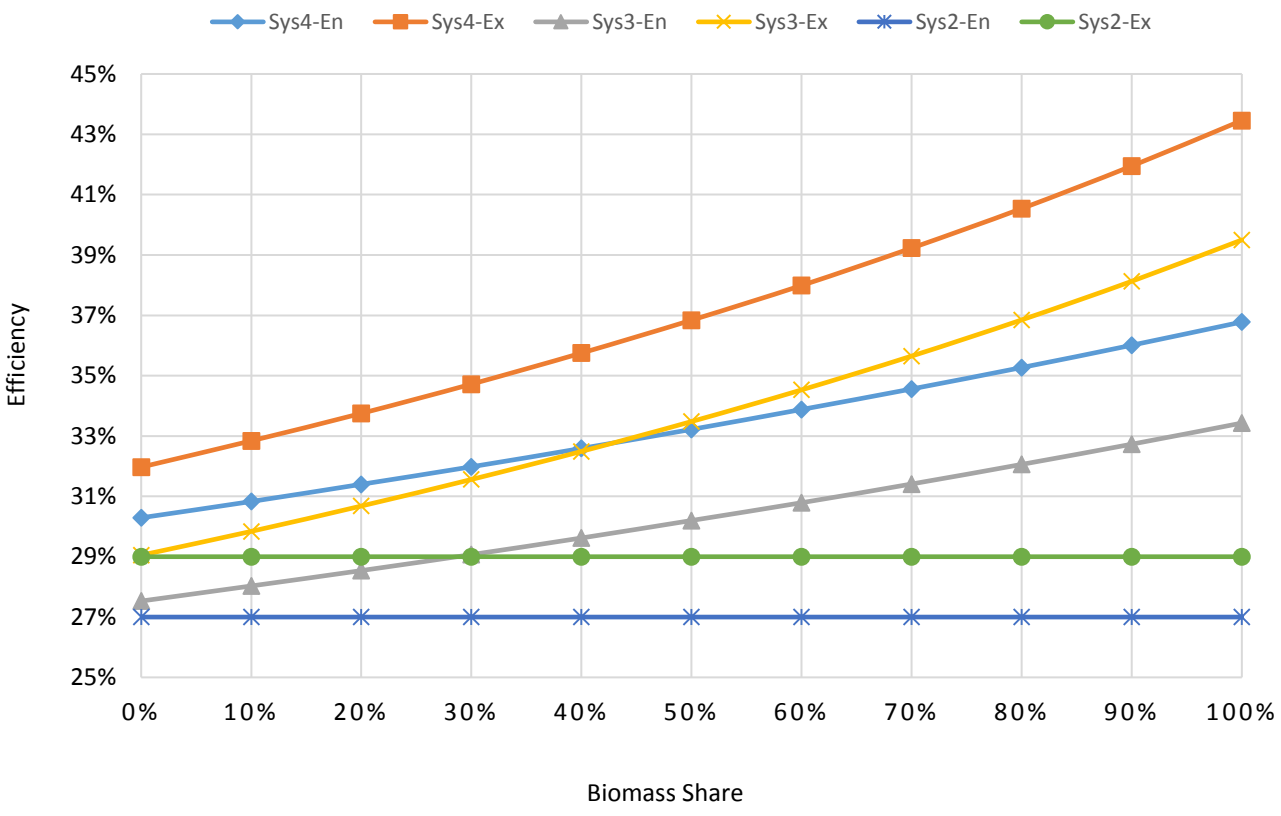

Figure 5.13: Energy and exergy efficiencies of analyzed systems as a function of the biomass share

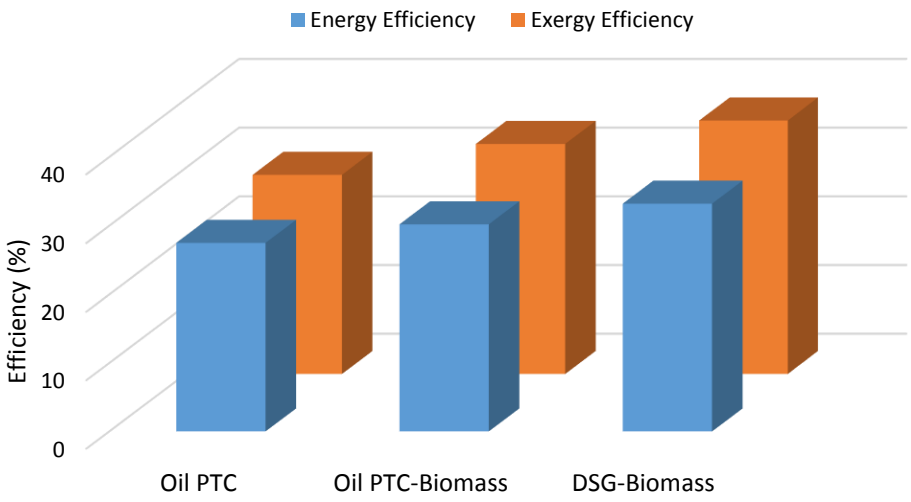

Figure 5.14: Energy and exergy efficiencies of analyzed systems at a biomass share of 50%

Chapter 6: Concluding Remarks

6.1 Conclusions

The potential of combining more than one renewable energy source in one system is demonstrated in this thesis. The two sources considered are solar energy and biomass fuels. The collector type suggested for the solar subsystem is a PTC. However, instead of utilizing an indirect steam generation technique that requires an intermediate heat exchanger which imposes further losses and costs, direct steam generation is proposed in the PTC field. To further understand the biomass subsystem that is integrated with the solar field, multiple biomass fuels are analyzed in the present work. Heating values for all fuels employed for this study are calculated based on their elemental content. The model used to calculate the heating values was validated using experimental data collected from the literature. Moreover, combustion analysis for all fuels is presented along with their flue gas composition. Four different systems were presented and analyzed. The first system shows the potential of the hybridization without DSG by comparing it to standalone PTC power plants. The system presents competitive efficiency values when compared to the Andasol plants, although a simple power block is utilized where no reheating or regeneration is considered. The second system is a detailed arrangement of a standalone PTC power plant which is similar to the Andasol arrangement. The objective of this system is to serve as the benchmark for the comparison. In the third system, a biomass boiler has been added to the standalone arrangement, in an attempt to enhance the dispatchability of the plant and increase the efficiency. The last system is the DSG system with the biomass boiler. To

account for various operation modes of the hybridized plants, the share of biomass fuels is varied from 0% to 100% and the results are reported accordingly.

Energy and exergy analyses are conducted for all presented systems, to draw a reasonable comparison. The results showed that;

- The standalone PTC plant has the lowest energy and exergy efficiencies with values of 27.5% and 29.0%, respectively.
- The addition of the biomass boiler to the indirect steam generation has not only improved the dispatchability but has improved the overall efficiencies as well. At a biomass share of 50%, the hybridized system has energy and exergy efficiencies of 30.2% and 33.5 %, respectively.
- The hybridization of solar and biomass with DSG in the solar field has shown the best results. At a biomass share of 50%, the energy and exergy efficiencies of the DSG arrangement are 33.2% and 36.8%, respectively.
- Exergy destruction results have shown that for all analyzed systems, the solar field has the highest exergy destruction rate, followed by the biomass boiler in the hybridized arrangements. However, the DSG plant has shown the lowest total exergy destruction values.

The present work has shown the potential of combining PTC solar plants with biomass boilers to avoid using TES. Moreover, it is demonstrated that DSG in PTC plants has shown a noticeable improvement compared to current indirect steam generation plants, which achieves the objective of developing a sustainable arrangement for power production. The proposed system presents a critical improvement in the field of renewable energy systems, which will help in faster deployment of such systems.

6.2 Contribution of Thesis

The contribution of the presented work is in the novelty of the proposed system and the improvements this system offers compared to existing systems, where the proposed DSG plant hybridized with a biomass-fired boiler is the first of its kind in the open literature. Moreover, the proposed cycle is capable of supplying a continuous feed of electrical power without utilizing TES by adjusting the share of biomass input to the cycle. Avoiding TES use can reduce the cost of the overall system, as TES represents one of the highest cost components of solar energy systems in general and DSG in particular. This research work has shown the potential of DSG in the PTC field to increase the overall efficiency of the system, which further lowers the cost of energy and enhances the reliability of those systems. In addition, in the proposed DSG-biomass arrangement, multiple fuels can be utilized to run the biomass boiler, presenting a flexible solution to overcome the challenge of the limited supply of biomass fuels

6.3 Recommendations for Future Work

Based on the present work, multiple research areas have been identified as future work opportunities. First, the proposed DSG arrangement can be considered for multi-generation which would further improve the efficiency of the system, and provide more commodities. Life cycle assessment of the proposed system can also be conducted, as it presents a useful tool to assess systems' performance. Economic and exergoeconomic analyses are also needed to present reliable and accurate details with regards to the cost of the energy produced by the system, which is necessary to decision making. Lastly, as the combination of more than one system is a complex process in terms of operation and

control, work is required to develop efficient and reliable control systems to smoothly run the hybridized power plants.

References

[1] G. Luft and A. Korin, *Energy security challenges for the 21st century: a reference handbook*. Santa Barbara, California: Greenwood publishing group, 2009.

[2] A. Shah. (2011, Sep, 08). *Energy security*. Available: http://www.globalissues.org/article/595/energy-security

[3] J. P. Doriana, H. T. Franssen, D. R. Simbeck, and MD, "Global challenges in energy," *Energy Policy*, vol. 34, pp. 1984-1991, 2006.

[4] B. Prasartkaew and S. Kumar, "Experimental study on the performance of a solar-biomass hybrid air-conditioning system," *Renewable energy*, vol. 57, pp. 86-93, 2013.

[5] M. Hoel and S. Kverndokk, "Depletion of fossil fuels and the impacts of global warming," *Resource and Energy Economics*, vol. 18, pp. 115-136, 1996.

[6] IEA, "Key World Energy Statistics," ed, 2015.

[7] S. A. Kalogirou, "Solar thermal collectors and applications," *Progress in energy and combustion science*, vol. 30, pp. 231-295, 2004.

[8] H. O. Pörtner, M. Langenbuch, and A. Reipschläger, "Biological impact of elevated ocean CO2 concentrations: lessons from animal physiology and earth history," *Journal of Oceanography*, vol. 60, pp. 705-718, 2004.

[9] Y. Desjardins, F. Laforge, C. Lussier, and A. Gosselin, "Effect of CO2 enrichment and high photosynthetic photon flux on the development of autotrophy and growth of tissue-cultured strawberry, raspberry and asparagus plants," in *Symposium on High Technology in Protected Cultivation 230*, 1988, pp. 45-54.

[10] D. Ø. Hjermann, A. Melsom, G. E. Dingsør, J. M. Durant, A. M. Eikeset, L. P. Røed, *et al.*, "Fish and oil in the Lofoten–Barents Sea system: synoptic review of the effect of oil spills on fish populations," *Marine Ecology Progress Series*, 2007.

[11] G. S. Alemán-Nava, V. H. Casiano-Flores, D. L. Cárdenas-Chávez, R. Díaz-Chavez, N. Scarlat, J. Mahlknecht, *et al.*, "Renewable energy research progress in Mexico: A review," *Renewable and Sustainable Energy Reviews*, vol. 32, pp. 140-153, 2014.

[12] M. Tingem and M. Rivington, "Adaptation for crop agriculture to climate change in Cameroon: turning on the heat," *Mitigation and Adaptation Strategies for Global Change*, vol. 14, pp. 153-168, 2009.

[13] I. C. Change, "Mitigation of climate change," *Contribution of working group III to the fourth assessment report of the Intergovernmental Panel on Climate Change*, 2007.

[14] I. B. Fridleifsson, "Geothermal energy for the benefit of the people," *Renewable and sustainable energy reviews*, vol. 5, pp. 299-312, 2001.

[15] N. L. Panwar, S. C. Kaushik, and S. Kothari, "Role of renewable energy sources in environmental protection: a review," *Renewable and Sustainable Energy Reviews*, vol. 15, pp. 1513-1524, 2011.

[16] R. A. Zakhidov, "Central Asian countries energy system and role of renewable energy sources," *Applied Solar Energy*, vol. 44, pp. 218-223, 2008.

[17] O. Ellabbana, H. Abu-Rub, and F. Blaabjerg, "Renewable energy resources: Current status, future prospects and their enabling technology," *Renewable and Sustainable Energy Reviews,* vol. 39, pp. 748-764, 2014.
[18] IEA, "World Energy Outlook 2012," 2012.
[19] J. L. Sawin, E. Martinot, V. Brien, A. McCrone, J. Roussell, D. Barnes, *et al.*, "Renewables 2010-Global status report," 2010.
[20] P. Ren, "Renewables 2015- Global status report," 2015.
[21] C. LINS, "Renewables 2014- Global status report," 2014.
[22] A. Zervos, "Renewables 2013- Global status report," 2013.
[23] E. Martinot and J. L. Sawin, "Renewables 2012- Global status report," 2012.
[24] J. L. Sawin, E. Martinot, D. Barnes, A. McCrone, J. Roussell, R. Sims, *et al.*, "Renewables 2011-Global status report," ed: REN21 Secretariat: Paris, France, 2011.
[25] I. S. Bortnikov, N. Lidorenko, G. Muchnik, S. Riabikov, and D. Strebkov, "Solar-energy perspectives," *Akademiia Nauk SSSR Izvestiia Mekhanika Zhidkosti i Gaza,* vol. 17, pp. 3-12, 1981.
[26] H.-Y. Chan, S. B. Riffat, and J. Zhu, "Review of passive solar heating and cooling technologies," *Renewable and Sustainable Energy Reviews,* vol. 14, pp. 781-789, 2010.
[27] G. Knier, "How do photovoltaics work?," *Science@ NASA,* 2002.
[28] G. Masson, J. I. Briano, and M. J. Baez, "Review and Analysis of PV Self-consumption Policies," 2016.
[29] A. Sherwani and J. Usmani, "Life cycle assessment of solar PV based electricity generation systems: A review," *Renewable and Sustainable Energy Reviews,* vol. 14, pp. 540-544, 2010.
[30] X. Zhang, X. Zhao, S. Smith, J. Xu, and X. Yu, "Review of R&D progress and practical application of the solar photovoltaic/thermal (PV/T) technologies," *Renewable and Sustainable Energy Reviews,* vol. 16, pp. 599-617, 2012.
[31] D. Barlev, R. Vidu, and P. Stroeve, "Innovation in concentrated solar power," *Solar Energy Materials and Solar Cells,* vol. 95, pp. 2703-2725, 2011.
[32] H. L. Zhang, J. Baeyens, J. Degrève, and G. Cacères, "Concentrated solar power plants: review and design methodology," *Renewable and Sustainable Energy Reviews,* vol. 22, pp. 466-481, 2013.
[33] M. Günther, M. Joemann, and S. Csambor, "Parabolic Trough Technologyy. In: Advanced CSP teaching materials," enerMENA2011.
[34] Y. Li and Y. Yang, "Impacts of solar multiples on the performance of integrated solar combined cycle systems with two direct steam generation fields," *Applied Energy,* vol. 160, pp. 673-680, 2015.
[35] T. E. Boukelia, O. Arslanb, and M. S. Mecibah, "ANN-based optimization of a parabolic trough solar thermal power plant," *Applied Thermal Engineering,* vol. 107, pp. 1210-1218, 2016.
[36] L.Guzman, A. Henao, and R.Vasquez, "Simulation and optimization of a parabolic trough solar power plant in the city of Barranquilla by using system advisor model (SAM) " *Energy Procedia,* vol. 57, pp. 497-506, 2014.

[37] V. S. Reddy, S. C. Kaushik, and S. K. Tyagi, "Exergetic analysis and performance evaluation of parabolic trough concentrating solar thermal power plant (PTCSTPP)," *Energy,* vol. 39, pp. 258-273, 2012.
[38] V. Jebasingh and G. J. Herbert, "A review of solar parabolic trough collector," *Renewable and Sustainable Energy Reviews,* vol. 54, pp. 1085-1091, 2016.
[39] N. B. Desai and S. Bandyopadhyay, "Optimization of concentrating solar thermal power plant based on parabolic trough collector," *Journal of Cleaner Production,* vol. 89, pp. 262-271, 2015.
[40] T. E. Boukelia, M. S. Mecibah, B. N. Kumar, and K. S. Reddy, "Optimization, selection and feasibility study of solar parabolic trough power plants for Algerian conditions," *Energy conversion and Management,* vol. 101, pp. 450-459, 2015.
[41] R. Silva, M. Berenguel, M. Pérez, and A. Fernández-Garcia, "Thermo-economic design optimization of parabolic trough solar plants for industrial process heat applications with memetic algorithms," *Applied Energy,* vol. 113, pp. 603-614, 2014.
[42] F. Dinter and D. M. Gonzalez, "Operability, reliability and economic benefits of CSP with thermal energy storage: first year of operation of ANDASOL 3," *Energy Procedia,* vol. 49, pp. 2472-2481, 2014.
[43] S. Millennium, "The parabolic trough power plants Andasol 1 to 3:The largest solar power plants in the world – Technology premiere in Europe," 2008.
[44] G. Mittelman and M. Epstein, "A novel power block for CSP systems," *Solar Energy,* vol. 84, pp. 1761-1771, 2010.
[45] T. E. Boukelia, M. S. Mecibah, B. N. Kumar, and K. S. Reddy, "Investigation of solar parabolic trough power plants with and without integrated TES (thermal energy storage) and FBS (fuel backup system)using thermic oil and solar salt," *Energy,* vol. 88, pp. 292-303, 2015.
[46] I. L. Garcı´a, J. L. Alvarez, and D. Blanco, "Performance model for parabolic trough solar thermal power plants with thermal storage: Comparison to operating plant data," *Solar Energy,* vol. 85, pp. 2443-2460, 2011.
[47] D. Laing, W. D. Steinmann, P. Viebahn, F. Gräter, and C. Bahl, "Economic analysis and life cycle assessment of concrete thermal energy storage for parabolic trough power plants," *Journal of Solar Energy Engineering,* vol. 132, p. 041013, 2010.
[48] S. Kuravi, J. Trahan, D. Y. Goswami, M. M. Rahman, and E. K. Stefanakos, "Thermal energy storage technologies and systems for concentrating solar power plants," *Progress in Energy and Combustion Science,* vol. 39, pp. 285-319, 2013.
[49] N. Fraidenraich, C. Oliveira, A. F. V. d. Cunha, J. M. Gordon, and O. C. Vilela, "Analytical modeling of direct steam generation solar power plants," *Solar Enegy,* vol. 98, pp. 511-522, 2013.
[50] E. Zarza, L. Valenzuela, J. Leo´n, K. Hennecke, M. Eck, H.-D. Weyers, *et al.*, "Direct steam generation in parabolic troughs: Final results and conclusions of the DISS project," *Energy,* vol. 29, pp. 635-644, 2004.
[51] J. F. Feldhoff, K. Schmitz, M. Eck, L. Schnatbaum-Laumann, D. Laing, F. Ortiz-Vives, *et al.*, "Comparative system analysis of direct steam generation and synthetic oil parabolic trough power plants with integrated thermal storage," *Solar Energy,* vol. 86, pp. 520-530, 2012.

[52] H. Price, E. Lu¨pfert, D. Kearney, E. Zarza, G. Cohen, R. Gee, *et al.*, "Advances in Parabolic Trough Solar Power Technology," *Journal of Solar Energy Engineering,* vol. 124, pp. 109-125, 2002.
[53] J. F. Feldhoff, D. Benitez, M. Eck, and K.-J. Riffelmann, "Economic Potential of Solar Thermal Power Plants With Direct Steam Generation Compared With HTF Plants," *Journal of Solar Energy Engineering,* vol. 132, pp. 041001-041009, 2010.
[54] M. J. Montes, A. Rovira, M. Muñoz, and J. M. Martínez-Val, "Performance analysis of an Integrated Solar Combined Cycle using Direct Steam Generation in parabolic trough collectors," *Applied Energy,* vol. 88, pp. 3228-8238, 2011.
[55] T. Larraı´n, R. Escobar, and J. Vergara, "Performance model to assist solar thermal power plant siting in northern Chile based on backup fuel consumption," *Renewable Energy,* vol. 35, pp. 1632-1643, 2010.
[56] M. J. Montes, A. Aba'nades, and J. M. Martínes-Val, "Performance of a direct steam generation solar thermal power plant for electricity production as a function of the solar multiple," *Solar Energy,* vol. 83, pp. 679-689, 2009.
[57] I. Niknia and M. Yaghoubi, "Transient simulation for developing a combined solar thermal power plant," *Applied Thermal Engineering,* vol. 37, pp. 196-207, 2012.
[58] A. Baghernejad and M. Yaghoubi, "thermodynamic methodology for analysis and optimization of a hybrid solar thermal power plant," *International Journal of Green Energy,* vol. 10, pp. 588-609, 2013.
[59] R. Saidur, E. A. Abdelaziz, A. Demirbas, M. S. Hossain, and S. Mekhilef, "A review on biomass as a fuel for boilers," *Renewable and Sustainable Energy Reviews,* vol. 15, pp. 2262-2289, 2011.
[60] E. Agbor, X. Zhang, and A. Kumar, "A review of biomass co-firing in North America," *Renewable and Sustainable Energy Reviews,* vol. 40, pp. 930-943, 2014.
[61] F. Tabet and I. Gökalp, "Review on CFD based models for co-firing coal and biomass," *Renewable and Sustainable Energy Reviews,* vol. 51, pp. 1101-1114, 2015.
[62] B. E. Centre. (April, 24). *Gasification*. Available: http://www.biomassenergycentre.org.uk/portal/page?_pageid=75,17504&_dad=portal&_schema=PORTAL
[63] A. Molino, S. Chianese, and D. Musmarra, "Biomass gasification technology: The state of the art overview," *Journal of Energy Chemistry,* 2015.
[64] C. F. McDonlad, "A Hybrid solar closed-cycle gas turbine combined heat and power plant concept to meet the continuous total energy need of a small community," *Hear Recovery Systems,* vol. 6, pp. 399-419, 1986.
[65] A. Cot, A. Amettler, J. Vall-Llovera, J. Aguilo, and J. M. Arque, "Termosolar Borges: a thermosolar hybrid plant with biomass," in *Third international symposium on energy from biomass and waste*, 2010.
[66] U. H. Juergen H. Peterseim, Amir Tadros, Stuart White, "Hybridisation optimization of concentrating solar thermal and biomass power generation facilities," *SOLAR ENERGY,* vol. 99, pp. 203-214, 2014.

[67] P. K. D. J.D. Nixon, P.A. Davies "The feasibility of hybrid solar-biomass power plants in India," *Energy,* vol. 46, pp. 541-554, 2012.
[68] J.-P. Rafael Soria n, Alexandre Szklo, Rodrigo Milani, Roberto Schaeffer, "Hybrid concentrated solar power (CSP)–biomass plants in a semiarid region: A strategy for CSP deployment in Brazil," *Energy Policy,* vol. 86, pp. 57-72, 2015.
[69] A. Colmenar-Santos, José-Luis, Bonilla-Gómez, D. Borge-Diez, and M. Castro-Gil, "Hybridization of concentrated solar power plants with biogas production systems as an alternative to premiums: The case of Spain," *Renewable and Sustainable Energy Reviews,* vol. 47, pp. 186-197, 2015.
[70] J. H. Peterseim, A. Tadros, U. Hellwig, and S. White, "Increasing the efficiency of parabolic trough plants using thermal oil through external superheating with biomass," *Energy Conversion and Management,* vol. 77, pp. 784-793, 2014.
[71] J. H. Peterseim, A. Tadros, S. White, U. Hellwig, J. Landler, and K. Galang, "Solar tower-biomass hybrid plants – maximizing plant performance," *Energy Procedia,* vol. 49, pp. 1197-1206, 2014.
[72] H. HongJuan, Y. YongPing, H. Eric, S. JiFeng, D. ChangQing, and M. Jian, "Evaluation of solar aided biomass power generation systems with parabolic trough field," *Science China,* vol. 54, 2011.
[73] A.Amoresano, G.Langella, and S.Sabino, "Optimization of solar integration in biomass fuelled steam plants," in *69th Conference of the Italian Thermal Engineering Association*, Naples, Italy, 2015.
[74] T.Srinivas and B.V.Reddy, "Hybrid solar–biomass power plant without energy storage," *Case Studies in Thermal Engineering,* vol. 2, pp. 75-81, 2014.
[75] S. Kibaara, S. Chowdhury, and S. Chowdhury, "A thermal analysis of parabolic trough CSP and biomass hybrid power system," in *Transmission and Distribution Conference and Exposition (T&D), 2012 IEEE PES*, 2012, pp. 1-6.
[76] U.Sahoo, R.Kumar, P.C.Pant, and R.Chaudhury, "Scope and sustainability of hybrid solar–biomass power plant with cooling, desalination in polygeneration process in India," *Renewable and Sustainable Energy Reviews,* vol. 51, pp. 304-316, 2015.
[77] S. Karellas and K. Braimakis, "Energy–exergy analysis and economic investigation of a cogeneration and trigeneration ORC–VCC hybrid system utilizing biomass fuel and solar power," *Energy Conversion and Management*, vol. 107, pp. 103-113, 2016.
[78] S. P. Mupparapu and K. K. Khatri, "Modelling and Simulation of Solar-Biomass Hybrid Trigeneration using ORC-VCC," *International Journal of Mechanical Engineer*ng and Computer Applications vol. 2, pp. 111-117, 2014.
[79] F. Khalid, I. Dincer, and M. A. Rosen, "Energy and exergy analyses of a solar-biomass integrated cycle for multigeneration," *Solar Energy,* vol. 112, pp. 290-299, 2015.
[80] A. Mishra, M. Chakravarty, and N. Kaushika, "Thermal optimization of solar biomass hybrid cogeneration plants," *JOURNAL OF SCIENTIFIC AND INDUSTRIAL RESEARCH,* vol. 65, p. 355, 2006.
[81] D. Borello, A. Corsini, F. Rispoli, and E. Tortora, "A co-powered biomass and concentrated solar power rankine cycle concept for small size combined heat and power generation," *Energies,* vol. 6, pp. 1478-1496, 2013.

[82] M. Jradi and S. Riffat, "Modelling and testing of a hybrid solar-biomass ORC-based micro-CHP system," *International Journal of Energy Research*, vol. 38, pp. 1039-1052, 2014.
[83] R. Sterrer, S. Schidler, O. Schwandt, P. Franz, and A. Hammerschmid, "Theoretical Analysis of the Combination of CSP with a Biomass CHP-plant Using ORC-technology in Central Europe," *Energy Procedia*, vol. 49, pp. 1218-1227, 2014.
[84] G. Angrisani, K. Bizon, R. Chirone, G. Continillo, G. Fusco, S. Lombardi, *et al.*, "Development of a new concept solar-biomass cogeneration system," *Energy Conversion and Management*, vol. 75, pp. 552-560, 2013.
[85] National.Renewable.Energy.Laboratory. Concentrated Solar Power Projects: Andasol 3 [Online]. Available: http://www.nrel.gov/csp/solarpaces/project_detail.cfm/projectID=117
[86] S. S. C. GmbH, "SCHOTT PTR ® 70 receiver the 4 th generation," 2013.
[87] S. V. Vassilev, D. Baxter, L. K. Andersen, and C. G. Vassileva, "An overview of the chemical composition of biomass," *Fuel*, vol. 89, pp. 913-933, 2010.
[88] K. S. Reddy and K. R. Kumar, "Solar collector field design and viability analysis of stand-alone parabolic trough power plants for Indian conditions," *Energy for Sustainable Development*, vol. 16, pp. 456-470, 2012.
[89] J. Garcı´a-Barberena, P. Garcia, M. Sanchez, M. J. Blanco, C. Lasheras, A. P. s, *et al.*, "Analysis of the influence of operational strategies in plant performance using SimulCET, simulation software for parabolic trough power plants," *Solar Energy*, vol. 86, 2012.
[90] W. A. K. Al-Maliki, F. Alobaid, R. Starkloff, V. Kez, and B. Epple, "Investigation on the dynamic behaviour of a parabolic trough power plant during strongly cloudy days," *Applied Thermal Engineering*, vol. 99, pp. 114-132, 2016.
[91] M. J. Montes, A. Aba´nades, J. M. Martı´nez-Val, and M. Valde´s, "Solar multiple optimization for a solar-only thermal power plant, using oil as heat transfer fluid in the parabolic trough collectors," *Solar Energy*, vol. 83, pp. 2165-2176, 2009.
[92] H. Price, "A Parabolic Trough Solar Power Plant Simulation Model " in *2003 International Solar Energy Conference* Hawaii, USA, 2003.
[93] C. Turchi, "Parabolic Trough Reference Plant for Cost Modeling with the Solar Advisor Model (SAM)," 2010.
[94] Solutia. (June 20). *THERMINOL VP-1 HEAT TRANSFER FLUID*. Available: http://twt.mpei.ac.ru/tthb/hedh/htf-vp1.pdf
[95] A. M. Elsafi, "Exergy and exergoeconomic analysis of sustainable direct steam generation solar power plants," *Energy conversion and Management*, vol. 103, pp. 338-347, 2015.
[96] M. Eck, N. Benz, J.-F. Feldhoff, Y. Gilon, Z. Hacker, T. Müller, *et al.*, "The Potential of direct steam Generation in Parabolic Troughs - Results of the German Project DIVA," in *14th International Symposium on Concentrated Solar Power and Chemical Energy Technologies*, Las Vegas (USA), 2008.
[97] F. A. Al-Sulaiman, F. Hamdullahpur, and I. Dincer, "Performance assessment of a novel system using parabolic trough solar collectors for combined cooling, heating, and power production," *Renewable Energy*, vol. 48, pp. 161-172, 2012.

[98] J. Koppejan and S. V. Loo, *The handbook of biomass combustion and co-firing*: Routledge, 2012.
[99] Y. A. Cengel and M. A. Boles, *Thermodynamics: an engineering approach*, 7th ed. New York: McGraw-Hill, 2011.
[100] E. Hu, Y. Yang, A. Nishimura, F. Yilmaz, and A. Kouzani, "Solar thermal aided power generation," *Applied Energy*, vol. 87, pp. 2881-2885, 2010.
[101] F. Khalid, I. Dincer, and M. A. Rosen, "Techno-economic assessment of a renewable energy based integrated multigeneration system for green buildings," *Applied Thermal Engineering*, vol. 99, pp. 1286-1294, 2016.
[102] F. Khalid, I. Dincer, and M. A. Rosen, "Analysis and Assessment of a Gas Turbine-Modular Helium Reactor for Nuclear Desalination," *Journal of Nuclear Engineering and Radiation Science*, vol. 2, p. 031014, 2016.
[103] A. Friedl, E. Padouvas, H. Rotter, and K. Varmuza, "Prediction of heating values of biomass fuel from elemental composition," *Analytica Chimica Acta*, vol. 544, pp. 191-198, 2005.
[104] S. S. Seyitoglu, I. Dincer, and A. Kilicarslan, "Assessment of an IGCC based trigeneration system for power, hydrogen and synthesis fuel production," *Hydrogen Energy*, vol. 41, pp. 8168-8175, 2016.
[105] F. Burkholder and C. Kutscher, "Heat loss testing of Schott's 2008 PTR70 Parabolic trough receiver," 2009.
[106] J. E. Pacheco, S. K. Showalter, and W. J. Kolb, "Development of a Molten-Salt Thermocline Thermal Storage System for Parabolic Trough Plants," *Solar Enegy Engineering*, vol. 124, pp. 153-159, 2002.

Appendix A

Table 5.12: Additional biomass fuels considered in the analysis

Herbaceous and agricultural biomass (HAB)	**C**	**O**	**H**	**N**	**S**
Mean	49.9	42.6	6.2	1.2	0.15
Minimum	42.2	34.2	3.2	0.1	0.01
Maximum	58.4	49	9.2	3.4	0.6
Arundo grass	48.7	44.5	6.1	0.6	0.13
Bamboo whole	52	42.5	5.1	0.4	0.04
Bana grass	50.1	42.9	6	0.9	0.13
Buffalo ground grass	46.1	44.5	6.5	2.6	0.27
Kenaf grass	48.4	44.5	6	1	0.15
Miscanthus grass	49.2	44.2	6	0.4	0.15
Reed canary grass	49.4	42.7	6.3	1.5	0.15
Sorghastrum grass	49.4	44	6.3	0.3	0.05
Sweet sorghum grass	49.7	43.7	6.1	0.4	0.09
Switchgrass	49.7	43.4	6.1	0.7	0.11
Mean	49.2	43.7	6.1	0.9	0.13
Minimum	46.1	42.5	5.1	0.3	0.04
Maximum	52	44.5	6.5	2.6	0.27
Straws (HAS)	**C**	**O**	**H**	**N**	**S**
Alfalfa straw	49.9	40.8	6.3	2.8	0.21
Barley straw	49.4	43.6	6.2	0.7	0.13
Corn straw	48.7	44.1	6.4	0.7	0.08
Mint straw	50.6	40.1	6.2	2.8	0.28
Oat straw	48.8	44.6	6	0.5	0.08
Rape straw	48.5	44.5	6.4	0.5	0.1
Rice straw	50.1	43	5.7	1	0.16
Straw	48.8	44.5	5.6	1	0.13
Wheat straw	49.4	43.6	6.1	0.7	0.17
Mean	49.4	43.2	6.1	1.2	0.15
Minimum	48.5	40.1	5.6	0.5	0.08
Maximum	50.6	44.6	6.4	2.8	0.28
Other residues (HAR)	**C**	**O**	**H**	**N**	**S**
Almond hulls	50.6	41.7	6.4	1.2	0.07
Almond shells	50.3	42.5	6.2	1	0.05
Coconut shells	51.1	43.1	5.6	0.1	0.1
Coffee husks	45.4	48.3	4.9	1.1	0.35
Cotton husks	50.4	39.8	8.4	1.4	0.01
Grape marc	54	37.4	6.1	2.4	0.15

Groundnut shells	50.9	40.4	7.5	1.2	0.02
Hazelnut shells	51.5	41.6	5.5	1.4	0.04
Mustard husks	45.8	44.4	9.2	0.4	0.2
Olive husks	50	42.1	6.2	1.6	0.05
Olive pits	52.8	39.4	6.6	1.1	0.07
Olive residue	58.4	34.2	5.8	1.4	0.23
Palm fibres-husks	51.5	40.1	6.6	1.5	0.3
Palm kernels	51	39.5	6.5	2.7	0.27
Pepper plant	42.2	49	5	3.2	0.57
Pepper residue	45.7	47.1	3.2	3.4	0.6
Pistachio shells	50.9	41.8	6.4	0.7	0.22
Plum pits	49.9	42.4	6.7	0.9	0.08
Rice husks	49.3	43.7	6.1	0.8	0.08
Soya husks	45.4	46.9	6.7	0.9	0.1
Sugar cane bagasse	49.8	43.9	6	0.2	0.06
Sunflower husks	50.4	43	5.5	1.1	0.03
Walnut blows	54.9	36.9	6.7	1.4	0.11
Walnut hulls and blows	55.1	36.5	6.7	1.6	0.12
Walnut shells	49.9	42.4	6.2	1.4	0.09
Mean	50.2	41.9	6.3	1.4	0.16
Minimum	42.2	34.2	3.2	0.1	0.01
Maximum	58.4	49	9.2	3.4	0.6
Animal Biomass	**C**	**O**	**H**	**N**	**S**
Chicken litter	60.5	25.3	6.8	6.2	1.2
Meat-bone meal	57.3	20.8	8	12.2	1.69
Mean	58.9	23.1	7.4	9.2	1.45
Mixture of Biomass	**C**	**O**	**H**	**N**	**S**
Biomass mixture	56.7	33.1	6.6	2.7	0.85
Wood-agricultural residue	52.4	41.2	6	0.4	0.04
Wood-almond residue	50.9	42.5	5.9	0.6	0.08
Wood-straw residue	51.7	41.5	6.3	0.4	0.13
Mean	52.9	39.6	6.2	1	0.28
Minimum	50.9	33.1	5.9	0.4	0.04
Maximum	56.7	42.5	6.6	2.7	0.85
Contaminated biomass (CB)	**C**	**O**	**H**	**N**	**S**
Currency shredded	45.4	46.1	6.3	1.9	0.32
Demolition wood	51.7	40.7	6.4	1.1	0.09
Furniture waste	51.8	41.8	6.1	0.3	0.04
Mixed waste paper	52.3	40.2	7.2	0.2	0.08
Greenhouse-plastic waste	70.9	16.4	11.2	1.5	0.01
Refuse-derived fuel	53.8	36.8	7.8	1.1	0.47

Sewage sludge	50.9	33.4	7.3	6.1	2.33
Wood yard waste	52.2	40.4	6	1.1	0.3
Mean	53.6	37	7.3	1.7	0.46
Minimum	45.4	16.4	6	0.2	0.01
Maximum	70.9	46.1	11.2	6.1	2.33
All variety of Biomass	**C**	**O**	**H**	**N**	**S**
Mean	51.3	41	6.3	1.2	0.19
Minimum	42.2	16.4	3.2	0.1	0.01
Maximum	70.9	49	11.2	12.2	2.33
Natural Biomass	**C**	**O**	**H**	**N**	**S**
Mean	51.1	41.4	6.2	1.1	0.2
Minimum	42.2	20.8	3.2	0.1	0.01
Maximum	60.5	49	10.2	12.2	1.69

Appendix B

Table 5.13: HHV and LHV of various biomass fuels

Herbaceous and agricultural biomass (HAB)	**HHV**	**LHV**
Mean	20.32	17.79
Minimum	14.97	13.35
Maximum	26.17	22.70
Grasses(HAG)	**HHV**	**LHV**
Arundo grass	19.59	17.12
Bamboo whole	19.77	17.49
Bana grass	20.12	17.64
Buffalo ground grass	19.14	16.61
Kenaf grass	19.36	16.93
Miscanthus grass	19.68	17.23
Reed canary grass	20.25	17.70
Sorghastrum grass	20.12	17.58
Sweet sorghum grass	20.02	17.53
Switchgrass	20.05	17.55
Mean	19.84	17.36
Minimum	17.71	15.55
Maximum	21.20	18.56
Straws (HAS)	**HHV**	**LHV**
Alfalfa straw	20.60	18.04
Barley straw	20.05	17.53
Corn straw	19.98	17.43
Mint straw	20.81	18.25
Oat straw	19.49	17.05
Rape straw	19.87	17.33
Rice straw	19.76	17.36
Straw	19.03	16.69
Wheat straw	19.93	17.44
Mean	19.96	17.47
Minimum	19.38	17.03
Maximum	20.58	17.99
Other residues (HAR)	**HHV**	**LHV**
Almond hulls	20.88	18.28
Almond shells	20.46	17.92
Coconut shells	19.99	17.60

Coffee husks	16.65	14.59
Cotton husks	23.36	20.20
Grape marc	22.15	19.54
Groundnut shells	22.41	19.50
Hazelnut shells	20.14	17.76
Mustard husks	22.25	19.00
Olive husks	20.39	17.85
Olive pits	22.13	19.41
Olive residue	23.69	21.05
Palm fibres-husks	21.62	18.93
Palm kernels	21.37	18.71
Pepper plant	15.57	13.54
Pepper residue	14.86	13.25
Pistachio shells	21.00	18.39
Plum pits	20.92	18.26
Rice husks	19.88	17.39
Soya husks	18.89	16.33
Sugar cane bagasse	19.92	17.45
Sunflower husks	19.62	17.27
Walnut blows	23.23	20.44
Walnut hulls and blows	23.34	20.54
Walnut shells	20.33	17.80
Mean	20.61	18.04
Minimum	14.97	13.35
Maximum	26.17	22.70
Animal Biomass	**HHV**	**LHV**
Chicken litter	26.54	23.55
Meat-bone meal	27.26	23.98
Mean	26.90	23.76
Mixture of Biomass	**HHV**	**LHV**
Biomass mixture	24.19	21.37
Wood-agricultural residue	21.10	18.57
Wood-almond residue	20.33	17.86
Wood-straw residue	21.19	18.59
Mean	21.69	19.08
Minimum	21.30	18.77
Maximum	23.22	20.45
Contaminated biomass (CB)	**HHV**	**LHV**
Currency shredded	18.51	16.06

Demolition wood	21.37	18.74
Furniture waste	20.95	18.40
Mixed waste paper	22.59	19.73
Greenhouse-plastic waste	36.23	31.79
Refuse-derived fuel	24.20	21.12
Sewage sludge	23.06	20.15
Wood yard waste	21.13	18.59
Mean	23.51	20.57
Minimum	21.22	18.68
Maximum	33.32	29.04
All variety of Biomass	**HHV**	**LHV**
Mean	21.09	18.50
Minimum	16.81	15.09
Maximum	32.93	28.67
Natural Biomass	**HHV**	**LHV**
Mean	20.87	18.31
Minimum	16.35	14.66
Maximum	28.06	24.28

Appendix C

Table 5.14: Gas content in combustion gas mixture for various biomass fuels

Herbaceous and agricultural biomass (HAB)	**CO_2**	**H_2O**	**SO_2**	**N_2**	**O_2**
Mean	1.7278	0.5786	0.0028	6.5327	0.6600
Minimum	1.4612	0.3252	0.0002	4.8388	0.4897
Maximum	2.0221	0.8319	0.0113	8.4443	0.8514
Grasses(HAG)	**CO_2**	**H_2O**	**SO_2**	**N_2**	**O_2**
Arundo grass	1.6863	0.5701	0.0025	6.2511	0.6321
Bamboo whole	1.8005	0.4857	0.0008	6.3783	0.6452
Bana grass	1.7347	0.5617	0.0025	6.4657	0.6536
Buffalo ground grass	1.5962	0.6039	0.0051	6.1014	0.6151
Kenaf grass	1.6759	0.5617	0.0028	6.1815	0.6247
Miscanthus grass	1.7036	0.5617	0.0028	6.2893	0.6362
Reed canary grass	1.7105	0.5870	0.0028	6.5058	0.6570
Sorghastrum grass	1.7105	0.5870	0.0009	6.4291	0.6504
Sweet sorghum grass	1.7209	0.5701	0.0017	6.4091	0.6483
Switchgrass	1.7209	0.5701	0.0021	6.4269	0.6498
Mean	1.7036	0.5701	0.0025	6.3535	0.6422
Minimum	1.5962	0.4857	0.0008	5.6436	0.5709
Maximum	1.8005	0.6039	0.0051	6.8352	0.6893
Straws (HAS)	**CO_2**	**H_2O**	**SO_2**	**N_2**	**O_2**
Alfalfa straw	1.7278	0.5870	0.0040	6.6717	0.6726
Barley straw	1.7105	0.5786	0.0025	6.4182	0.6489
Corn straw	1.6863	0.5955	0.0015	6.3796	0.6450
Mint straw	1.7521	0.5786	0.0053	6.7577	0.6813
Oat straw	1.6897	0.5617	0.0015	6.2186	0.6289
Rape straw	1.6793	0.5955	0.0019	6.3351	0.6407
Rice straw	1.7347	0.5364	0.0030	6.3523	0.6420
Straw	1.6897	0.5279	0.0025	6.0821	0.6146
Wheat straw	1.7105	0.5701	0.0032	6.3830	0.6454
Mean	1.7105	0.5701	0.0028	6.4055	0.6472
Minimum	1.6793	0.5279	0.0015	6.2431	0.6314
Maximum	1.7521	0.5955	0.0053	6.6217	0.6675
Other residues (HAR)	**CO_2**	**H_2O**	**SO_2**	**N_2**	**O_2**
Almond hulls	1.7521	0.5955	0.0013	6.7322	0.6802
Almond shells	1.7417	0.5786	0.0009	6.5806	0.6651
Coconut shells	1.7694	0.5279	0.0019	6.4236	0.6501

Coffee husks	1.5720	0.4688	0.0066	5.2337	0.5287
Cotton husks	1.7451	0.7644	0.0002	7.5361	0.7614
Grape marc	1.8698	0.5701	0.0028	7.2597	0.7325
Groundnut shells	1.7624	0.6884	0.0004	7.2354	0.7312
Hazelnut shells	1.7832	0.5195	0.0008	6.5158	0.6582
Mustard husks	1.5859	0.8319	0.0038	7.0451	0.7127
Olive husks	1.7313	0.5786	0.0009	6.5676	0.6632
Olive pits	1.8282	0.6124	0.0013	7.1863	0.7263
Olive residue	2.0221	0.5448	0.0043	7.8394	0.7921
Palm fibres-husks	1.7832	0.6124	0.0057	7.0065	0.7077
Palm kernels	1.7659	0.6039	0.0051	6.9452	0.7004
Pepper plant	1.4612	0.4772	0.0108	4.8702	0.4899
Pepper residue	1.5824	0.3252	0.0113	4.7306	0.4755
Pistachio shells	1.7624	0.5955	0.0042	6.7671	0.6843
Plum pits	1.7278	0.6208	0.0015	6.7212	0.6794
Rice husks	1.7070	0.5701	0.0015	6.3627	0.6432
Soya husks	1.5720	0.6208	0.0019	5.9524	0.6016
Sugar cane bagasse	1.7244	0.5617	0.0011	6.3719	0.6447
Sunflower husks	1.7451	0.5195	0.0006	6.3104	0.6376
Walnut blows	1.9009	0.6208	0.0021	7.6059	0.7685
Walnut hulls and blows	1.9079	0.6208	0.0023	7.6519	0.7729
Walnut shells	1.7278	0.5786	0.0017	6.5412	0.6607
Mean	1.7382	0.5870	0.0030	6.6421	0.6709
Minimum	1.4612	0.3252	0.0002	4.8388	0.4897
Maximum	2.0221	0.8319	0.0113	8.4443	0.8514
Animal Biomass	**CO_2**	**H_2O**	**SO_2**	**N_2**	**O_2**
Chicken litter	2.0949	0.6293	0.0227	8.9771	0.9027
Meat-bone meal	1.9841	0.7306	0.0319	9.3134	0.9310
Mean	2.0395	0.6799	0.0274	9.1431	0.9166
Mixture of Biomass	**CO_2**	**H_2O**	**SO_2**	**N_2**	**O_2**
Biomass mixture	1.9633	0.6124	0.0160	8.0169	0.8088
Wood-agricultural residue	1.8144	0.5617	0.0008	6.8222	0.6901
Wood-almond residue	1.7624	0.5533	0.0015	6.5417	0.6615
Wood-straw residue	1.7901	0.5870	0.0025	6.8365	0.6916
Mean	1.8317	0.5786	0.0053	7.0501	0.7126
Minimum	1.7624	0.5533	0.0008	6.9768	0.7058
Maximum	1.9633	0.6124	0.0160	7.5781	0.7644
Contaminated biomass (CB)	**CO_2**	**H_2O**	**SO_2**	**N_2**	**O_2**
Currency shredded	1.5720	0.5870	0.0060	5.8613	0.5914
Demolition wood	1.7901	0.5955	0.0017	6.9157	0.6989

Furniture waste	1.7936	0.5701	0.0008	6.7557	0.6835
Mixed waste paper	1.8109	0.6630	0.0015	7.3010	0.7388
Greenhouse-plastic waste	2.4550	1.0008	0.0002	12.2164	1.2350
Refuse-derived fuel	1.8629	0.7137	0.0089	7.8953	0.7981
Sewage sludge	1.7624	0.6715	0.0440	7.6420	0.7676
Wood yard waste	1.8075	0.5617	0.0057	6.8534	0.6926
Mean	1.8559	0.6715	0.0087	7.6810	0.7758
Minimum	1.5720	0.5617	0.0002	7.1061	0.7190
Maximum	2.4550	1.0008	0.0440	10.9815	1.1056
All variety of Biomass	**CO_2**	**H_2O**	**SO_2**	**N_2**	**O_2**
Mean	1.7763	0.5870	0.0036	6.8205	0.6892
Minimum	1.4612	0.3252	0.0002	5.6698	0.5738
Maximum	2.4550	1.0008	0.0440	10.9037	1.0919
Natural Biomass	**CO_2**	**H_2O**	**SO_2**	**N_2**	**O_2**
Mean	1.7694	0.5786	0.0038	6.7394	0.6811
Minimum	1.4612	0.3252	0.0002	5.4644	0.5530
Maximum	2.0949	0.9164	0.0319	9.2100	0.9205